

Analysis of postural stability of the human body during the  
execution of standing industrial hand tasks

by

Fabrice LATOUR

THESIS PRESENTED TO ÉCOLE DE TECHNOLOGIE SUPÉRIEURE  
IN PARTIAL FULFILLMENT FOR A MASTER'S DEGREE WITH  
THESIS IN HEALTHCARE TECHNOLOGY ENGINEERING  
M.A.Sc.

MONTREAL, OCTOBER 7, 2020

ÉCOLE DE TECHNOLOGIE SUPÉRIEURE  
UNIVERSITÉ DU QUÉBEC

Copyright © 2020, Fabrice Latour All rights reserved

© Copyright reserved

It is forbidden to reproduce, save, or share the content of this document either in whole or in parts. The reader who wishes to print or save this document on any media must first get the permission of the author.

**PRESENTATION OF THE BOARD OF EXAMINERS**

THIS THESIS HAS BEEN EVALUATED

BY THE FOLLOWING BOARD OF EXAMINERS

Mr. Rachid Aissaoui, Thesis Supervisor  
Department of Systems Engineering, École de technologie supérieure

Ms. Nicola Hagemeister, Thesis Co-supervisor  
Department of Systems Engineering, École de technologie supérieure

Mr. Mustapha Ouhimmou, President of the Board of Examiners  
Department of Systems Engineering, École de technologie supérieure

Mr. Carlos Vázquez, Member of the jury  
Department of Software and Information Technology Engineering, École de technologie supérieure

THIS THESIS WAS PRESENTED AND DEFENDED

IN THE PRESENCE OF A BOARD OF EXAMINERS AND PUBLIC

ON SEPTEMBER 30, 2020

AT ÉCOLE DE TECHNOLOGIE SUPÉRIEURE



## ACKNOWLEDGMENTS

To Mamie Pauline, Lynda, Marie-France & Catherine

These last two years have been filled with ups and downs. But like a roller coaster, when the whole process comes to an end and you finally get a second to catch your breath, you realize it was worth it. The process of completing a Master's degree was much more than just an educational one, it was also learning about myself, what I'm able to accomplish, and how to balance uncontrollable situations. In life, just like with this thesis, when everything seems to be going sideways, composure, determination, and not derailing off course helped me ensure that all ended well. Although the unthinkable events of 2020 impacted the course and the outcome of this thesis, the learning experience became even more valuable.

Unfortunately, I wasn't able to conduct experimental trials on all my planned participants. At first, I was frustrated by the turn of events, but my two directors, Rachid and Nicola reassured me that my project was not a failure and provided me guidance that I had sufficient material to complete the project. This whole learning process would not have been possible without them and I am forever grateful that they have given me this opportunity of completing this thrilling project. They have challenged me on many occasions, gave me constructive feedback, and acknowledged when good work was accomplished. Thank you Rachid and Nicola for this professional and personal enrichment experience.

I would also like to thank Julie Charland and the whole team at Dassault Systèmes for their help and support during this project.

I thank my father who has supported me through this journey by giving me his advice from his own doctoral dissertation experience. I also thank my father and mother in law who were extremely generous with their time when it came to guiding me and allowing me to fabricate most of the experimental test bench in their garage. My dear friends, I thank you for supporting me throughout these years and understanding my absence on occasion.

It's hard to think that at first, I didn't want to continue my education after high school and that I wanted to become a heavy truck mechanic. This is why I would like to dedicate this master's degree to the four most important women in my life.

Mamie Pauline my grandmother, who has always been there for me with generous amounts of meals, always has a reassuring hug and taught me that when you smile, others will smile back in your presence. Lynda my mother, always had faith that I could succeed whatever I put my mind to. You and Michel supported me throughout my studies and always made sure that I had what I needed. You taught me so much about life, to be generous with others, and my knowledge of how to become autodidactic, qualities that I am forever grateful to have. Marie-France, my caring sister. You taught me to be rigorous and meticulous as paying attention to detail counts, but above all to live, laugh, and have exceptional food, because life is all about enjoying the little things, just like a Hershey's chipits. I am grateful to have had your guidance during my childhood and to have you as a friend for life today. At last, Catherine my loving fiancé, without who this thesis would not have been possible. Countless moments of proofreading my work, your patience during those infinite times of me asking you questions regarding the phrasing of sentences. I am so grateful to have your encouragement, support, and trust in me. Now that both of our Masters are accomplished, it's time to focus on our life dreams.

Although going back on this ride, as a researcher, might seem tempting, I have decided not to return on the same ride, but instead try a new one.

*"Tuition is very valuable,  
but you know what's invaluable? Intuition."*

-Michael Scott

# **Analyse de la stabilité posturale du corps humain lors d'exécution de tâches industrielles debout avec les mains**

Fabrice LATOUR

## **RÉSUMÉ**

**Introduction:** Le positionnement des pieds a un impact significatif sur le contrôle de la stabilité du corps humain lors de la réalisation d'une tâche industrielle. Dans les modèles de simulation de la posture humaine actuels (DHM: *Digital Human Model*), l'utilisation de stratégies de pas pour générer des postures stables repose sur des modèles simplistes, qui localisent généralement le centre de masse (COM) du DHM à mi-distance entre le contact des pieds ou limitent seulement la projection d'un point nommé ZMP (*Zero Moment Point*) dans le polygone de sustentation nommé couramment BOS (*Base of Support*). Les données expérimentales assurant la coordination des mouvements humains pendant des tâches industrielles, qui peuvent être utilisées pour simuler et valider ces modèles DHM, sont rares.

**Objectif:** L'objectif de cette étude est de développer un banc d'essai expérimental représentant des conditions industrielles et de réaliser des expériences pour fournir à ces modèles DHM des paramètres de stabilité posturale.

**Méthodologie:** Un sujet pilote a effectué quatre conditions de travail debout à une main, c'est-à-dire: atteindre une cible, pousser et tirer une poignée, ainsi qu'utiliser un tournevis. Chaque condition fut réalisée dans deux positions différentes de cibles. Un obstacle transversal a été utilisé pour une des positions afin d'imposer des contraintes spatiales. La cinématique 3D de cinquante marqueurs réfléchissants, apposés sur des repères anatomiques, avec trois marqueurs auxiliaires sur le tournevis a été acquise à 200 Hz avec un système de capture de mouvement (VICON). Les forces et moments de réaction au sol sous chaque pied et à la cible ont été mesurés simultanément par trois plateformes de force (AMTI) à 1000 Hz. Les paramètres de stabilité posturale évalués pour cette étude étaient la longueur de support, qui est une variation de la longueur de pas, et la position du ZMP par rapport au BOS.

**Résultats:** Les expériences ont montré que les exigences de la tâche varient le placement et l'orientation des pieds lorsqu'un obstacle est présent ou non, ce qui était conséquent pour tous les essais avec l'obstacle transversal, où la jambe controlatérale se déplaçait vers l'arrière. La moyenne de la longueur de support semblait plus petite pour les essais avec l'obstacle transversalement, ce qui indique que l'atteinte de la cible aurait pu être préférée à la stabilité.

**Conclusion:** La taille de l'échantillon est limitée ce qui restreint les conclusions. Les travaux futurs prévoient réaliser le protocole expérimental complet sur un échantillon de sujet plus grand afin de développer un modèle de régression plus précis permettant de prédire la longueur de support selon le ZMP et son orientation selon la cible et les exigences à la main.

**Mots-clés:** Posture, Stabilité, Faire un pas, Zero Moment Point



# **Analysis of postural stability of the human body during the execution of standing industrial hand tasks**

Fabrice LATOUR

## **ABSTRACT**

**Introduction:** Foot positioning has a significant impact on human body stability control when completing a manufacturing task. In current Digital Human Models (DHM), the use of stepping strategies to generate stable postures relies on simplistic models, which generally locate the DHM center of mass (COM) at half distance between feet contact or limit the zero moment point (ZMP) projection within the base of support (BOS). Experimental data providing human movement coordination during manufacturing tasks, which can be used to simulate and validate these DHM models, are very scarce.

**Objective:** The objective of this study is to develop an experimental test bench representing industrial conditions and to carry out experiments to provide these DHM models with parameters of postural stability.

**Material and Methods:** A pilot subject performed four different one-handed standing working conditions namely: reaching a target, pushing and pulling a handle, as well as using a screwdriver. Each condition was performed in two different target positions. A transverse obstacle was used to impose spatial constraints for one of the target positions. The 3D kinematics of fifty reflective markers affixed on the anatomic human body with three additional markers on the screwdriver was recorded at 200 Hz using a motion capture system (VICON). Ground reaction forces and moments beneath each foot and at the targets was measured by three force plates (AMTI) simultaneously at 1000 Hz. The assessed postural stability parameters in this study were the support length which is a variation of the step length, and the ZMP position with respect to the BOS.

**Results:** Experiments showed that task requirements vary the position and orientation of feet placement when an obstacle is present or not, which was consistent over all trials of moving the contralateral leg backward when the transverse obstacle was present. The mean support length magnitude appeared smaller for the handle location with a transverse offset which indicates hand-target reach might have been favored over stability.

**Conclusion:** It is noted that the sample size is limited, hence the conclusions remain partial. In future works, it is intended to carry out the presented experimental protocol on a larger population size to develop a more precise regression model able of predicting the support length with respect to the ZMP position and its orientation about the target and the hand load direction requirements.

**Keywords:** Posture, Stability, Stepping, Zero Moment Point



## TABLE OF CONTENTS

	Page
CHAPTER 1 INTRODUCTION.....	21
1.1 Context.....	21
1.2 Problem statement.....	23
1.3 Objectives .....	26
1.4 Research questions.....	26
1.5 Overview.....	27
CHAPTER 2 LITERATURE REVIEW.....	29
2.1 Human stability control overview.....	31
2.1.1 Description of postural strategies.....	31
2.1.2 Foot placement prediction models .....	37
2.1.3 Definition of the Zero Moment Point.....	40
2.2 Experimental human data capture systems .....	44
2.2.1 Force evaluation for industrial tasks using hand tools .....	44
2.2.2 Experimental test bench designs .....	47
2.3 Conclusion .....	50
CHAPTER 3 METHODOLOGY.....	53
3.1 Industrial task posture evaluation .....	53
3.1.1 Grouping of postures.....	55
3.1.2 Posture strategies classifications .....	57
3.1.3 Posture strategies occurrences.....	58
3.1.4 Conclusion.....	61
3.2 The conception of an experimental test bench.....	62
3.2.1 Requirements.....	62
3.2.1.1 Attributes.....	62
3.2.1.2 Constraints .....	63
3.2.1.3 Good to have .....	63
3.2.2 Design .....	64
3.3 Case study .....	70
3.3.1 Experimental methodology .....	70
3.3.1.1 Setup .....	70
3.3.1.2 Data collection equipment .....	71
3.3.1.3 Test tasks, locations, and conditions.....	74
3.3.1.4 Experimental protocol.....	78
3.3.2 Data collection protocol .....	83
3.3.2.1 Pilot subject.....	85
3.3.3 Data preparation .....	86
3.3.3.1 Evaluated parameters.....	88
3.3.3.2 Data modeling.....	89

CHAPTER 4	RESULTS & ANALYSIS.....	93
4.1	Data verification & validation .....	93
4.2	Results from experiments .....	100
4.3	ZMP projection .....	102
4.3.1	Results .....	102
4.3.2	Analysis.....	106
4.4	Feet adjustments.....	108
4.4.1	Results .....	108
4.4.2	Analysis.....	110
4.5	Postural stability control .....	111
4.5.1	Results .....	111
4.5.2	Analysis.....	113
4.6	Limitations .....	114
CONCLUSION & RECOMMENDATIONS.....		115
APPENDIX I	LITERATURE REVIEW SUMMARY TABLES.....	119
APPENDIX II	INDUSTRIAL TASK EVALUATION .....	125
LIST OF REFERENCES.....		139
BIBLIOGRAPHY.....		147

## LIST OF TABLES

		Page
Table 2.1	Definition of Net COP equation variables.....	32
Table 2.2	Definition of ZMP equation variables.....	43
Table 3.1	Automotive companies & Assembly lines assessed.....	53
Table 3.2	Task assessment examples legend.....	54
Table 3.3	Comparison of task assessments for three data sets in the automotive industry.....	56
Table 3.4	Primary Posture Strategies Definitions .....	57
Table 3.5	Secondary Posture Strategies Definitions.....	57
Table 3.6	Test location lexicon.....	75
Table 3.7	Full experimental protocol overview.....	77
Table 3.8	Body landmarks lexicon.....	81
Table 3.9	Pilot subject data collection protocol test conditions and number of trials analyzed.....	83
Table 3.10	Pilot subject characteristics .....	85
Table 3.11	Center of mass calculation points.....	88
Table 4.1	Visual repeatability representation task high centered.....	93
Table 4.2	Summary of feet positioning and parameters projection.....	99
Table 4.3	Mean normalized (and standard deviations) D <sub>2</sub> ratio, support length magnitude and lead foot occurrence across trials.....	103
Table 4.4	Mean (and standard deviations) lead foot-target distance and Support length-target orientation by condition .....	108
Table 4.5	Mean (and standard deviations) of the total postural sway by condition.....	112



## LIST OF FIGURES

		Page
Figure 2.1	The reference planes and axis representation.....	29
Figure 2.2	Subregion based stability criterion .....	33
Figure 2.3	Zero moment point representation with and without external loads when standing.....	41
Figure 2.4	Zero moment point representation with external loads when leaning.....	42
Figure 2.5	Industrial hand task with a tool .....	44
Figure 2.6	Capture system with adapter design .....	46
Figure 3.1	Task assessment examples .....	54
Figure 3.2	Distribution by grouping of postures.....	55
Figure 3.3	Distribution of Occurrences grouped by Primary Posture Strategies.....	58
Figure 3.4	Distribution of Secondary Posture Strategies in terms of Occurrence classified by Primary Posture Strategies .....	59
Figure 3.5	Distribution of Primary Posture Strategies in terms of Occurrence classified by Secondary Posture Strategies .....	60
Figure 3.6	Summary of postural evaluation tasks.....	61
Figure 3.7	Experimental test bench schematic diagram .....	64
Figure 3.8	Experimental test bench design .....	65
Figure 3.9	Screwdriver capture interface.....	66
Figure 3.10	Alternative tool interfaces .....	66
Figure 3.11	Pushing and Pulling handle capture interface.....	67
Figure 3.12	Installed experimental test bench .....	68
Figure 3.13	Task requiring a transverse obstacle.....	69
Figure 3.14	Tasks underneath an obstacle .....	69

Figure 3.15	Experimental setup .....	71
Figure 3.16	AMTI MC3A load cell .....	71
Figure 3.17	ATMI Side-By-Side Treadmill.....	72
Figure 3.18	VICON MX T20-S camera .....	73
Figure 3.19	Markers used with a tool .....	73
Figure 3.20	Designed test tasks .....	74
Figure 3.21	Tool shape effect comparison.....	76
Figure 3.22	Applied hand force monitor ( $F_z$ ).....	79
Figure 3.23	Anatomical landmarks for markers .....	80
Figure 3.24	Verification of gloves with markers .....	82
Figure 3.25	Hand marker gloves.....	82
Figure 3.26	Passive reflective marker affixed on the pilot subject.....	85
Figure 3.27	Gap filling.....	86
Figure 3.28	Three phases of a trial.....	87
Figure 3.29	Data modeling representation.....	89
Figure 3.30	ML and MR points, support length, and local coordinate system definition during quiet standing.....	90
Figure 3.31	Lead foot-target distance and support length-target orientation definition.....	91
Figure 4.1	Repeatability over 5 trials ( <i>Pushing a Centered High task</i> ).....	94
Figure 4.2	NetCOP, COP <sub>L</sub> , and COP <sub>R</sub> in the anterior-posterior direction ( <i>Quiet side-by-side standing</i> ).....	95
Figure 4.3	NetCOP, COP <sub>C</sub> , and COP <sub>V</sub> in the anterior-posterior direction ( <i>Quiet side-by-side standing</i> ).....	95
Figure 4.4	NetCOP, COP <sub>C</sub> , and COP <sub>V</sub> in the transverse direction ( <i>Quiet side-by- side standing</i> ).....	96

Figure 4.5	COG and NetCOP fluctuations in the anterior-posterior direction ( <i>Quiet side-by-side standing</i> ) .....	97
Figure 4.6	Comparison between the COG and the net COP anterior-posterior distance from the ankle joint .....	98
Figure 4.7	Quiet side-by-side standing and pushing trial feet positioning projection .....	99
Figure 4.8	COG and net COP correlation distribution .....	101
Figure 4.9	Processed trial parameters (XY plane projection) for a pushing centered trial .....	102
Figure 4.10	Scatter plot of Support length magnitude with respect to the ZMP D <sub>2</sub> ratio from the root foot grouped by conditions .....	103
Figure 4.11	Scatter plot of Support length magnitude with respect to the ZMP D <sub>2</sub> ratio from the root foot grouped by handle location. Single-factor regression fitted model displayed with confidence and prediction intervals .....	104
Figure 4.12	Plot of residuals and limits with a confidence interval of 95% .....	105
Figure 4.13	ZMP projection in yellow and COG projection blue on the support length between ML and MR. Mean normalized (and standard deviations) D <sub>2</sub> ratio, support length magnitude, and lead foot occurrence across trials. Reference quiet standing trial support length of 250.73 mm.....	109
Figure 4.14	Mean ZMP in yellow and mean COG in blue over the 5-second static trial .....	113



## LIST OF ABBREVIATIONS AND ACRONYMS

<b>BOS</b>	Base of Support
<b>COG</b>	Center of Gravity
<b>COP</b>	Center of Pressure
<b>COM</b>	Center of Mass
<b>CRCHUM</b>	Centre de Recherche du Centre Hospitalier de l'Université de Montréal
<b>DHM</b>	Digital Human Model
<b>DOF</b>	Degree of Freedom
<b>ETS</b>	École de Technologie Supérieure
<b>FSR</b>	Functional Stability Region
<b>HRF</b>	Hand Reaction Forces
<b>LIO</b>	Laboratoire de recherche en imagerie et orthopédie
<b>MOCAP</b>	Motion Capture
<b>SPE</b>	Smart Posture Engine
<b>RSME</b>	Root Squared Mean Error
<b>ZMP</b>	Zero Moment Point



## CHAPTER 1

### INTRODUCTION

#### 1.1 Context

The use of digital simulators to evaluate complex and precise phenomenon is preferred by research centers as well as by industries since they allow the analysis of multiple scenarios faster and at a lower cost, compared to full-scale physical models. Specific three-dimensional digital human models (DHM) have been developed in Computer-Aided Design programs to integrate human body representations into simulated environments. These DHMs allow for ergonomic assessment and appraisal of interactions with the environment before developing optimized work stations or manufacturing products (Chaffin, 2008; Scataglini & Paul, 2019).

At the moment there is a large variety of anthropometrical and biomechanical DHMs used for diverse purposes. JACK (Siemens, 2020), SIA & TEO (Charland, 2019; Dassault Systèmes, 2020), and SANTOS™ (Abdel-Malek et al., 2007; Santos Human inc, 2020) are commercially available DHMs that can be used for general ergonomic assessment as well as for accurate visual and physical dimension rendering of interactions between the humanoid manikin and the modeled environment. The AnyBody Modeling System™ (AnyBody Technology, 2020) allows detailed human body structure calculations in relation to the simulated environment. Other models such as SAMMIE (Marshall et al., 2010) and RAMSIS (Bubb et al., 2006; Human Solutions, 2020) have been developed to evaluate fit, reach, and line of sight for specific body positions, mostly during seated postures. IMMA developed by Hanson et al. (2012, 2014), HUMOSIM developed by Reed, Faraway, Chaffin, and Martin (2006) and the Smart Posture Engine (SPE) developed at the LIO laboratory (Lemieux, Barré, Aissaoui & Hagemester, 2020) are all research projects aiming at developing an autonomous biomechanical digital human model allowing collision-free predictions of simulated kinematics and dynamics, mostly for industrial tasks. This thesis is motivated by the SPE technology to enhance the stability control of the DHMs final postures.

A common aspect DHMs strive to improve is their autonomy to position the human manikin in a biomechanically plausible posture under specific task conditions. Currently, few models allow for semi-autonomous placement of the manikin in the simulated environment requiring manual interactions by the user to refine the final simulated postures (Berlin & Adams, 2017; Chaffin, 2008; Scataglini & Paul, 2019). Different computational methods are used by DHMs to position the manikin in the environment and ensure it is adopting a stable posture. Some models use inverse kinematics mathematical models to position the manikin's joints and segments (Chaffin, 2008). Some of these models have integrated optimization-based methods that generate plausible postures based on objective functions and constraints to predict the manikin's position when facing a defined situation (Berlin & Adams, 2017). Other models use experimental kinematic and dynamic data-bases to generate postures (Scataglini & Paul, 2019). Lastly, manual manipulations of individual joints can always be performed by the user but it is a basic and tedious method to position the humanoid manikin.

The full automation of digital human models would be a significant advancement in this field as a fully independent manikin would no longer require user inputs. For models simulating standing tasks, stability criteria are very important to ensure the generation of biomechanically plausible postures. A considerable element when evaluating the stability of the human body is foot placement with respect to the task position and load requirements (Holbein & Redfern, 1997; Winter, Patla & Frank, 1990). As specified in the works of Winter et al. (1990), during a static standing stance it is mandatory to maintain the body Center of Gravity (COG), which is the vertical projection of the Center of Mass (COM), within the Base of Support (BOS) to ensure postural stability. The BOS is an area defined by the convex hull of the feet contact points with the support plane. Moreover, Holbein and Redfern (1997) defined a functional stability region (FSR) with limits representing 60% of the Base of Support (BOS) during standing tasks while handling loads. This smaller region represents an area where small compensatory body adjustments can be made to maintain a stable posture. Postural stability adjustment strategies are classified into two predominant categories: ankle strategy and hip strategy (Horak & Nashner, 1986). Horak and Nashner (1986) defined the ankle strategy as being the restoration of stability by displacing the Center

of Mass around the ankle joints. These same researchers defined the hip strategy as being the COM movement primarily around the hips by varying moments about the knee and hip joints. When the center of mass exits the base of support and its velocity is directed away from the BOS, the ankle or hip strategies are insufficient to restore stability equilibrium, therefore stepping is prevalently required (Pai & Patton, 1997). Because the stepping strategy allows the enlargement of the base of support, it is usually preferred when accomplishing tasks that require external loads or a distant reach, as the COM will tend to move towards the functional stability region limits hence, requiring a step (Pai et al., 1998).

## **1.2 Problem statement**

In industrial conditions, the use of stepping to maintain a stable posture is frequent as workers will often reach or apply forces when accomplishing tasks (Wagner, Reed & Chaffin, 2010). Classical digital human models that utilize stepping behaviors to generate stable postures rely on simplistic models, which generally locate the DHMs center of mass at half distance between the feet contact positions (Badler, Phillips & Webber, 1993). Predictive stepping models use experimentally collected data and calculations to predict data-based feet placement. These models rely on regression equations with the task characteristics as the inputs to position the manikin's feet (Faraway, 2003; Reed & Wagner, 2007; Wagner et al., 2010). They can predict transition stepping, but pose some challenges when simulating more complex asymmetrical handling or tool manipulation tasks with task parameters different from the experimentally collected data. An alternative computed force-controlled posture model by Seitz, Recluta, Zimmermann, and Wirsching (2005) generates plausible postures that are natural representations, but that is not necessarily accurate with respect to experimental trials. Instead, it is favored to predict global whole body posture by maximizing produced joint torques while reducing joint strain. Optimization-based stepping models compute the feet position along with the posture generation through minimizing an objective function (e.g., joint torques) (Howard, Yang & Ozsoy, 2014; Marler, Knake & Johnson, 2011). The main stability criterion for these models is accomplished by limiting the calculated zero moment point (ZMP) projection to stay inside the BOS. This is a basic

formulation that respects minimal stability requirements. The ZMP represents a virtual point where the total tilting moments, generated from gravitational and external forces, applied to the manikin are zero (Vukobratović & Borovac, 2004). Although this method generates stepping according to external requirements, it has not yet been validated with suitable experimental data to verify if the feet placement is accurate. The more recent stability-based stepping model proposed, which uses the position of the ZMP with respect to the functional stability region to quantify stability, was developed as part of an improvement to the SPE (Zeighami, Lemieux, Charland, Hagemeister & Aissaoui, 2019). The SPE is a posture prediction model used to generate biomechanically plausible final postures of a DHM given the simulated environment and the task information (Lemieux, Barré, Hagemeister & Aissaoui, 2017, 2020). The main stability difference in this model is that the ZMP and the feet placement are controlled more precisely by using the functional stability region, a smaller region than the BOS situated between feet contact, allowing the manikin to recover maximum stability depending on the required target reach, height, and loads. However, no experimental data has yet been produced to validate this concept.

In the literature, the large majority of studies that have proposed feet positioning models studied general two-handed push-pull tasks (Hoffman, Reed & Chaffin, 2007a, 2010; Marler et al., 2011; Wagner et al., 2010), which is not representative of the observations found in the industrial field (Baril-Gingras & Lortie, 1995). The study conducted in industrial settings by Baril-Gingras and Lortie (1995) allowed the identification of different postural strategies used during material handling tasks. Of the 944 handling tasks that were observed one-handed tasks and two-handed asymmetrical tasks represented respectively 55.4% and 35.6% of the handlings, which accounted for more than 90% of all evaluated handlings. This indicates that one-handed and out of sagittal plane tasks should be preferred when studying industrial tasks. In this same study, horizontal pushing and pulling (48.2%) was seen almost twice as often as vertical lifting and lowering (26.6%), where tasks accomplished with horizontal and transverse components were the most frequent. When reviewing the literature, accurate stepping behavior models derived from specific industrial task experiments providing human movement coordination are very scarce. No feet prediction model assessed

tasks involving hand tools. Also, no study evaluated the effects of a transverse obstacle imposing spatial constraints and requiring subjects to execute tasks out of the sagittal plane without prescribing specific feet placement, which has been underlined by Wilkinson, Pinder, and Grieve (1995) to require further investigation. Imposing specific feet position for out of sagittal plane tasks shows a strong indication that foot placement and posture constraints may have an important effect on force exertion capability (Haslegrave, Tracy & Corlett, 1997; Warwick, Novak, Schultz & Berkson, 1980; Wilkinson et al., 1995). Granata and Bennett (2005) studied the effects of split and side-by-side stances on stability during pushing tasks, where stability was found to be significantly influenced by feet placement. For digital human models to become fully autonomous, the stepping prediction models need to be enhanced, in order to take into account the out of sagittal plane tasks.

Although bracing and other postural strategies exist in the industrial field, this study focuses on maintaining stability through the stepping strategy, while executing tasks in different hand conditions, by limiting the use of other postural strategies. In this study, the subject is free to position their feet as wanted in order to adopt a preferred posture. Moreover, the use of a transverse obstacle requires the subject to execute the conditions without aligning themselves with the direction of the applied hand force. The use of a tool while completing the same tasks allows the evaluation of its influence on feet placement when compared to typical push and pull conditions. Because no previous study evaluated a transverse obstacle, the scaling of the target position was based on other scaled parameters found in the literature (Granata & Bennett, 2005; Haslegrave et al., 1997; Jones, Reed & Chaffin, 2013).

### **1.3 Objectives**

The previous DHMs that utilize the zero moment point to maintain stability only partially control its position to stay within the base of support, which represents minimal stability requirements. The primary objective of this thesis is to develop an experimental test bench that will allow the evaluation of the required parameters to assess the zero moment point and human postural stability, such as the support length with respect to the functional stability region and the base of support. The second objective is to carry out experiments with the intent of developing a regression model that will estimate the required support length with respect to the ZMP position.

### **1.4 Research questions**

Derived from the aforementioned objectives, three research questions have been defined.

- What tasks should experimental test subjects perform to have an appropriate representation of what is observed in the industrial sector?
- How to conceive an experimental test bench that will acquire accurate and repeatable experimental data to evaluate postural stability?
- Can a regression model potentially estimate the support length from the ZMP position?

The hypothesis resides on the fact that by developing an experimental test bench capable of evaluating postural stability parameters and the ZMP position, appropriate data will be acquired enabling the development of an accurate regression model. Furthermore, it is hypothesized in support of the regression model that during either centered tasks or tasks with a transverse obstacle, the contralateral and ipsilateral legs move respectively to expand the BOS in the direction of ZMP displacement in order to maximize the stability threshold.

## 1.5 Overview

The subsequent sections will present content that answers the previously described research questions and ultimately achieves the main objectives.

Chapter 2 provides a detailed review of related works to assess previous studies that have investigated DHM postural stability by feet positioning and ZMP position, and experimental test bench evaluation.

Chapter 3 discusses the utilized methodology. The first part provides information on defining frequently encountered task postures in the industrial sector. The second part covers the development of an experimental test bench that will capture parameters of postural stability. The third and final part presents the experiments carried out on subjects with a focus to measure foot positioning and external forces.

Chapter 4 is dedicated to presenting the interpreted results acquired by the test bench and motion capture system and will lay out an analysis of these results.

Chapter 5 develops on discussion and recommendations for future works regarding postural stability evaluation when stepping.



## CHAPTER 2

### LITERATURE REVIEW

In this chapter, a review of previous works will be conducted to assess the following topics: Human stability conservation and experimental human data capture systems.

In order to facilitate the evaluation of the diversified studies retrieved from the literature, a common lexicon will be used throughout the rest of this thesis. Figure 2.1 illustrates the three reference planes and axis for a standard anatomical human position based on the works of Vaughan, Davis, and O'Connor (1999).

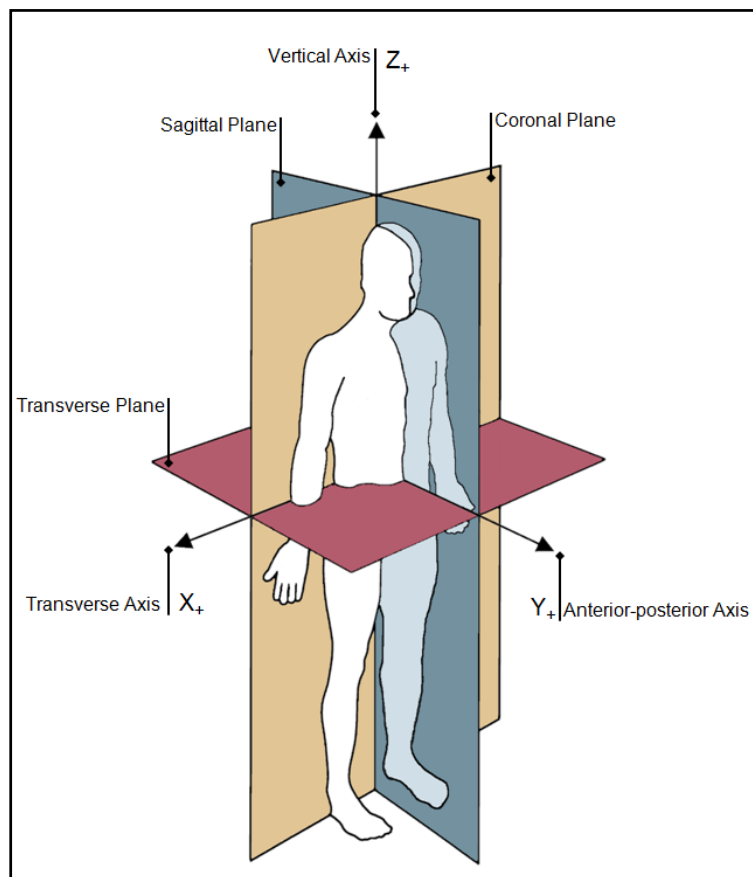


Figure 2.1 The reference planes and axis representation

- **The Base of Support (mm<sup>2</sup>):** Region defined by the points of contact between the feet with the ground;
- **Stepping:** Feet positioned in a staggered or split stance type;
- **No stepping:** Feet positioned in a side-by-side stance type;
- **Contralateral:** Opposite foot of working hand;
- **Ipsilateral:** Same side foot of working hand;
- **Step length (mm):** Distance between both heels in the anterior-posterior axis (Vaughan et al., 1999);
- **Stance (mm):** Distance between feet in a side-by-side position;
- **Support length (mm):** The support length is the line passing through the projected points ML and MR, which are virtual points obtained from the intersection of the projected longitudinal axes (straight lines connecting the Phalanx Distal II and the heel) of the feet with the balance line projected on the ground (Badler et al., 1993). The balance line is a line passing through the mean center of gravity (COG) during quiet standing and its direction is found by connecting the left and right mid malleolus (See Figure 3.30);
- **D<sub>2</sub> ratio (mm):** Ratio from the root foot (trailing leg) of the square projection of the ZMP on the support length, which is on the ground (See Figure 4.9);

## 2.1 Human stability control overview

This section will consider three notions of human stability parameters. First, the different postural strategies will be treated. Secondly, different foot placement prediction models that exist will be reviewed. Finally, the zero moment point will be described in detail.

### 2.1.1 Description of postural strategies

Postural strategies are used to maintain the human body stable when standing, as they allow repositioning of the Center of Mass (COM) in a position where the whole body will remain stable (Horak & Nashner, 1986). Table-A I-1 in APPENDIX I presents these studies.

As stated by Horak and Nashner (1986), the use of the ankle and the hip strategies allow for easier control of the body's stability when standing without requiring continuous variation in muscle structures. When standing straight without any perturbations the human body will continuously compensate for small variations, which generates a natural sway. This natural sway can be measured by assessing the COM or by evaluating the net center of pressure (net COP) derived from individual feet center of pressure. Winter, Prince, Stergiou, and Powell (1993) evaluated the effects of the natural sway on the computed net COP using the following equations (2.1), (2.2), and (2.3). Results from ten subjects displayed in the anterior-posterior direction that the left and right foot COP displacements were perceived by the net COP, but not in the transverse direction. Instead, loading and unloading of the vertical reaction forces were predominantly seen in the transverse direction to maintain balance.

$$\text{NetCOP}(t) = \text{COP}_L(t) \times \frac{\mathbf{R}_{VL}(t)}{\mathbf{R}_{VL}(t) + \mathbf{R}_{VR}(t)} + \text{COP}_R(t) \times \frac{\mathbf{R}_{VR}(t)}{\mathbf{R}_{VL}(t) + \mathbf{R}_{VR}(t)} \quad (2.1)$$

$$\text{COP}_C(t) = \frac{\text{COP}_L(t) + \text{COP}_R(t)}{2} \quad (2.2)$$

$$\text{COP}_V(t) = \text{NetCOP}(t) - \text{COP}_C(t) \quad (2.3)$$

The variables used in these equations are defined in Table 2.1.

Table 2.1 Definition of Net COP equation variables

<b>NetCOP(t)</b>	→ Net COP.
<b>t</b>	→ Time variable (s).
<b>COP<sub>L</sub>(t)</b> <b>COP<sub>R</sub>(t)</b>	→ Magnitude of Left foot COP. → Magnitude of Right foot COP. (resultant of anterior-posterior & transverse components)
<b>R<sub>VL</sub>(t)</b> <b>R<sub>VR</sub>(t)</b>	→ Vertical reaction forces of Left foot. → Vertical reaction forces of Right foot.
<b>COP<sub>C</sub>(t)</b>	→ Effect of average Left and Right foot COP.
<b>COP<sub>V</sub>(t)</b>	→ Vertical reaction forces loading/unloading contribution.

Holbein and Redfern (1997) first detailed the area where small postural strategies can be used to maintain a stable posture as the functional stability region (FSR). These researchers evaluated the COG and reported that the limits of the FSR represent 53.7% in the anterior direction, 61.5% in the posterior direction, and 62.2% in both transversal directions from the center of the Base of Support (BOS) to its limits. However, the FSR was underestimated as the transversal limit of the BOS was defined with respect to the 5<sup>th</sup> metatarsal whereas the COG displacement was calculated according to the anterior-posterior center of the BOS which is behind the 5<sup>th</sup> metatarsal, a location where the foot is slightly narrower.

During a subsequent study on this matter by Holbein-Jenny, McDermott, Shaw, and Demchak (2007) a more detailed six-sided functional stability region was established from adults aged between 23 and 73. The experimental evaluations on fifty-two subjects determined a similar anterior limit at 57.8% of the BOS limits with two additional diagonal measurements at 45 ° left and 45 ° right of 66.9% and 69% respectively. As for the other limits, posterior was evaluated at 54.7%, left transverse at 67%, and right transverse at 65.8% of the BOS limits. The FSR is significantly dependent on age. In fact, when evaluating the same data set but for the younger age groups between 20 and 39 years old, the FSR enlarges in all directions. Anterior becomes 69.2%, posterior 57.6%, 45 ° left 74.7%, 45 ° right 76.8%, transverse left 76.5% and transverse right 73.9%.

Pai, et al. (1998) evaluated the instant where stepping occurs and defined a stepping threshold. According to the results obtained from forty-nine young, old non-faller, and old faller subjects, stepping was imminent for all three perturbation conditions once the COM was within 10% of the BOS limits. Because generating a step widens the base of support, this allows the COM to return inside the BOS and therefore recover to a stable posture.

An investigation of the different subregions found inside the base of support was conducted by Popovic et al. (2000) to propose a stability criterion for quiet standing based on the location of the COP within the BOS. Three elliptical subregions normalized to the foot length and one residual region were defined as part of this study. These regions are represented in the following Figure 2.2.

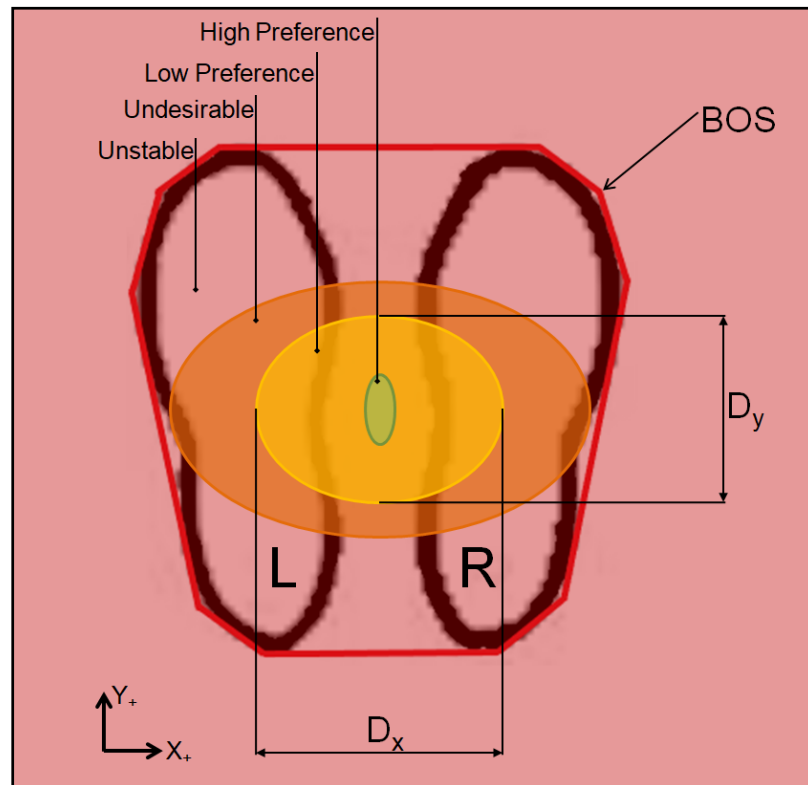


Figure 2.2 Subregion based stability criterion

The high preference region represents the zone where the COP is situated during almost the entirety of quiet standing. The low preference region is the remaining zone where the COP is situated during quiet standing. The third area is the undesirable region where the adoption of postural strategies is necessary to remain stable. The residual zone is considered the unstable region where stepping is mandatory to maintain balance. The foot length ratio parameters of each region are respectively 0.16, 0.43 & 0.59 for  $D_y$  and 0.07, 0.57 & 0.97 for  $D_x$  with all centers being in the sagittal plane and at 47% of the foot length from the heel position in the anterior-posterior axis.

Differently to what was seen in the previous studies, Stapley, Pozzo, Grishin, and Papaxanthis (2000) used both the estimated center of mass and the center of pressure to evaluate human stability when executing forward reaching. The stabilization of the COM was mainly completed by axial synergies (e.g., movement of the head and shoulders opposite from the hip displacement), limiting the required COM displacement for subjects to remain stable. As the reaching distance increased, the posterior hip displacement increased ensuring the COM stays within the BOS. The COP displacement was characterized by a three-phase trajectory sequence. The COP started by moving slightly backward as the COM moved forward. Then, it changed direction until it passed the COM. Once the terminal position achieved, the COP remained in the anterior limit of the BOS. These results are however limited to the fact that feet position was restricted. Permitting feet movement would have enabled the expansion of the BOS which in terms could have limited the required axial synergies to maintain postural control.

As mentioned earlier, stepping is important to maintain a stable posture when performing tasks that require the manipulation of loads, the application of external forces, or reaching as this strategy allows the enlargement of the base of support. In the material handling research of Wagner et al. (2010) split stance (i.e., staggered) during task pickup represented nearly 71% of all the 462 experimental trials that were evaluated. Split stance compared to side-by-side stance has a major impact on the task that can be accomplished. Larger amounts of

forces can be applied and objects do not need to be brought as close to the body when the feet are staggered.

The study by Baril-Gingras and Lortie (1995) conducted in industrial settings allowed the identification of different postural strategies used during material handling tasks. A total of 944 handling tasks were observed with on average three to four efforts per handling, representing a set of 3217 identified efforts. Several considerable results were extracted through a thirty-six variable grid covering effort type, effort direction, foot position, whole-body behavior, the position of the hands, and much more. First of all, horizontal pushing and pulling (48.2%) happens almost twice as more often than vertical lifting and lowering (26.6%). Secondly, one-handed tasks (55.4%) and two-handed asymmetrical tasks (35.6%) accounted for more than 90% of all evaluated handlings which indicates that two-handed symmetrical tasks are undoubtedly not frequent. In regards to posture, 25.4% of efforts had a form of moderate forward flexion, and 11.7% utilized the squatting strategy which was defined by knee flexion. A form of stepping was observed in 34.6% of all the handlings that required upper limb movement or exertion and a minimum of two steps, as other forms of stepping proved to not be reproducible. Lastly, 76.7% of the efforts required the exertion to have a horizontal component and 45.7% of efforts were accomplished in a single plane. Also, half of all efforts were executed towards or away from the body in the transverse axis (1582/3217, 49.2%). Despite the limited space imposed by the work environment, the predominance of asymmetry and executing tasks out of the sagittal plane were not dependent on spatial constraints of the feet, as workers could position themselves how they desired. Only 9.2% of the efforts started with the subjects' feet in line with the axis of the movement appending the fact that asymmetrical positioning is pivotal.

Wilkinson et al. (1995) evaluated posture variations for one-handed force exertion on subjects standing at a predominantly side-by-side foot position, as feet were required to be equidistant from the centerline of the target. Asymmetrical pushing and pulling were investigated, but the researchers stated that additional work needs to be conducted in order to explain the postural behaviors that support transverse force production. Forces out of the

sagittal plane require specific body strategies to ensure the maintenance of a stable posture. Moments of up to 50 Nm were seen produced in the horizontal plane about the foot center of pressure point by subjects during the study of Wilkinson et al. (1995), most likely explaining that foot base torque generation is required to overcome out of plane forces. This study was limited by the COP being calculated from the handle reaction force vector and the extreme posture assumptions made when calculating the COG from anthropometric tables, which generated positioning errors of 38 mm for the COP and 39 mm for the COG.

During the study by Haslegrave et al. (1997), one-handed force exertion was evaluated in unnatural positions requiring out of sagittal plane forces to be applied. Experiments were conducted in six directions (pull, push, upwards, downwards, across body & sideways) under four task positions (standing at shoulder height, standing twisted, standing overhead, and lying supine on floor overhead). Each task imposed a position for the right foot and had specific conditions as to subject orientation. The reference for the maximal voluntary effort was assessed from pushing a handle positioned at shoulder height while standing at maximal reach. Imposing this posture allowed the isolation of muscular effort by limiting the use of body weight to increase applied force. Results showed that task orientation and reach distance have an important impact on force exertion capability with some instances being reduced by 50%.

No study has yet explored the use of a transverse obstacle to assess the positioning of the feet. Few studies evaluated the effect of rotation for tasks out of the sagittal plane (Haslegrave et al., 1997; Warwick et al., 1980; Wilkinson et al., 1995). However, during these studies, instead of using obstacles, subjects were positioned with their feet constrained at a specific position. Moreover, comparing out of sagittal plane task results from these three studies show a strong indication that foot placement and posture constraints may have an important effect on force exertion capability.

### 2.1.2 Foot placement prediction models

Over recent years, digital human models have started to integrate more accurate foot prediction models that help to calculate and to simulate the manikins in biomechanically plausible postures. Table-A I-2 presented in APPENDIX I summarizes the five different foot placement prediction models that have been retrieved through the literature review. Some models require experimentally collected data and regression equations to generate data-based feet placement. Other models require body constraints and inverse dynamic computations before conducting an optimization process (e.g., minimizing joint torques) to generate plausible feet placement. At last, there are inverse kinematics models, that use mathematical models following biomechanical constraints and stability functions to calculate ideal static feet position.

The model proposed by Wagner, Reed, and Chaffin (2006) is based on experimental data from load manipulation transfer tasks. The predicted stepping is determined from a foot behavior matrix and regression equations arising from the task and subject descriptions, and a behavioral classification data set. Once the stepping behavior is selected, the foot placements are constrained and an inverse kinematics analysis is applied to calculate the lower limb positions. Although results from this model generate plausible postures and transition stepping, they are limited to the experimentally collected foot trajectory data, which poses some challenges when simulating more complex material handling or tool manipulation tasks (Reed & Wagner, 2007).

In terms of postures generated by optimization prediction, three models were retrieved. The main stability criteria for the models of Marler et al. (2011) and Howard et al. (2014) is accomplished by limiting the calculated zero moment point projection to staying inside a trapezoid BOS. This is a basic formulation that respects minimal stability requirements. The presented models have the same objective of minimizing an objective function (e.g., joint torques). Constraints are similar with the purpose of limiting the joint angles, the reach distance between the hand and the target as well as ensuring the stability of the manikin.

During the study of Marler et al. (2011), feet position were not fixed and after the optimization process, final feet location was calculated to simulate the most realistic posture while respecting the ZMP stability criteria. The model calculates the reach distance constraints based on anthropometric data. This specifies a boundary area on the support surfaces where hand(s) and the feet placement must remain within. These features allow the manikin to adopt a split stance position in a natural, but not necessarily accurate posture.

The model used by Howard et al. (2014) has not yet been validated with experimental data. As part of their study, results were only visually validated. Although feet were not constrained to a specific position, results don't seem to trigger any considerate stepping. Nonetheless, the model was able to predict feet position and orientation with respect to the supporting hand loads. The manikin stability for this study was such that it adhered to the minimal stability requirements. This signifies no postural adjustments, such as lowering the COG or displacing feet was accomplished to ensure the manikin was adopting the most stable posture possible. Furthermore, during the simulations researchers didn't apply any external loads at the task hand which would consequently affect the simulated posture as the ZMP calculation utilizes these forces.

In the model presented by Delfs, Bohlin, Hanson, Högberg, and Carlson (2013), which is also an optimization-based model, the objective function is defined as a comfort function. This function corresponds to joint angles, joint torques, reach distance, and interference with the environment as well as a stability parameter. Feet were free to slide on the support surface and rotate about the vertical axis, but the remaining three DOF were fixed. The balance was determined from the static equilibrium of the model, where stability was determined from the gradient of a potential function, derived from all the forces and moments, being greater than zero for all displacements. By giving more importance to the required stability in the comfort function, the manikin adopts a more stable posture (wider stance or longer step length). The model seems to produce adequate stepping but has not been validated to verify if the postures are accurate representations of what workers would do

or only generated plausible postures. The plausibility nature is due to variations in ways individuals complete tasks and prospective situations that don't physically exist to be evaluated by humans.

The stepping prediction model proposed by Zeighami et al. (2019), which is used as part of the SPE model, also uses the ZMP to generate biomechanically plausible final postures. The SPE uses an inverse kinematics solver with selective filtering and prioritized constraints similar to Baerlocher (2001) while avoiding the collision with the environment. The main stability difference in this model is that the ZMP and the feet placement are controlled more precisely with respect to the functional stability region, a smaller region than the BOS situated between feet contact. This allows the manikin to be simulated adopting the most stable posture possible depending on the required target reach, height, and loads. If the ZMP doesn't exit the functional stability region during the task, no stepping is triggered. Nonetheless, no experimental data has yet been produced to validate this concept.

### 2.1.3 Definition of the Zero Moment Point

The zero moment point (ZMP) is a concept that is widely used in the biped locomotion field. The position of this virtual point is mostly exploited for dynamic state of stability feedback in humanoid robots.

Using this concept for stability purposes is relevant as it considers the effect of external loads applied to the studied body. As stated by Winter et al. (1990), during a static posture a person is considered stable when the projected position of the center of gravity (COG) is situated inside the base of support. However, when external loads are present, this statement is no longer valid. Therefore, the ZMP can be defined as a point where the total tilting moments, generated from gravitational and external forces perceived by a studied body are zero (Vukobratović & Borovac, 2004).

As mentioned in the works of Vukobratović and Borovac (2004) if the position of the ZMP is situated within the base of support, the body is considered dynamically stable. When the ZMP approaches the edge of the BOS, the counterbalance moments created by the feet reaction forces with the support surface decrease while the tilting moments generated by gravity and external forces increase. Consequently, the body could easily fall if any perturbation would arise.

Although it is possible for the center of gravity and the zero moment point to be outside of the base of support while the studied body remains stable (Pai & Patton, 1997) in this thesis only static standing postures will be studied. Figure 2.3 and Figure 2.4 illustrate the concept of stability based on the ZMP position for four different scenarios.

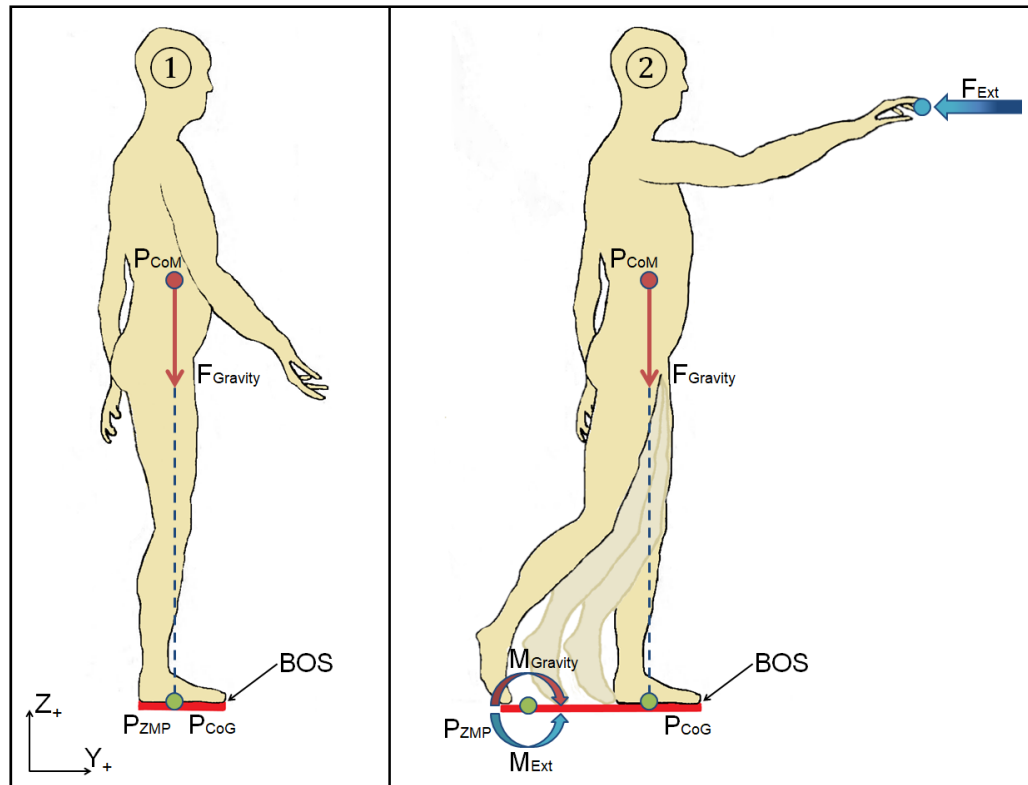


Figure 2.3 Zero moment point representation with and without external loads when standing

In the first scenario shown in Figure 2.3, no external forces are present, hence the position of the ZMP ( $P_{ZMP}$ ) and the position of the COG ( $P_{CoG}$ ) coincide, which results in no tilting moments and enabling the control of the COG inside the base of support. The ankle strategy and hip strategy are generally used to maintain a stable posture (Horak & Nashner, 1986).

In the second scenario presented in Figure 2.3, an external force ( $F_{Ext}$ ) is applied. As the external force increases, the tilting moments around the position of the ZMP increase as well. If the base of support is not large enough to compensate for the effects of the external moments, stepping is imminent to correct this unbalance trend. Thus, a foot will displace until the base of support has grown sufficiently to recover to a stable posture.

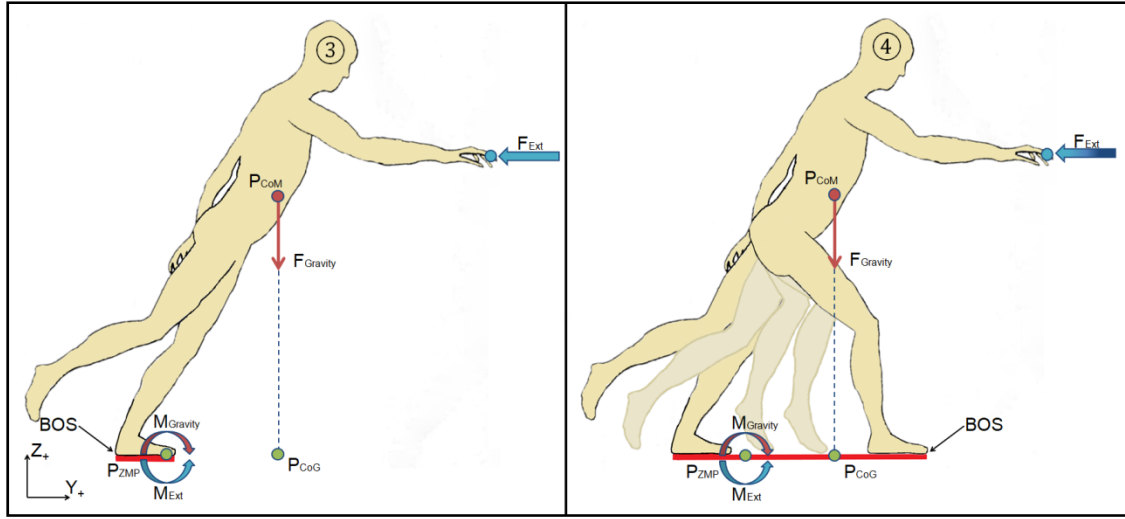


Figure 2.4 Zero moment point representation with external loads when leaning

The third scenario illustrated in Figure 2.4, shows a situation where a leaning body assessment proves to be stable. However, this is not an ideal or pragmatic representation of posture stability as if the external force ( $F_{Ext}$ ) disappears, the body would immediately fall.

The fourth scenario shown in Figure 2.4 presents a valid representation of what should occur when adopting a leaning posture. The feet should displace to enlarge the base of support and ensure that the position of the ZMP ( $P_{ZMP}$ ) and COG ( $P_{CoG}$ ) remain within the BOS as the external force increases.

For this thesis, the ZMP calculation will be accomplished with equation (2.4) which are derived from the equations presented in the works of Howard et al. (2014). As for the position of the Z component, it will be considered as being on the support surface, in other words on the ground, therefore  $ZMP_z = 0$ .

$$\begin{aligned}
 ZMP_x &= \frac{(M_{by} + f_{bx}(i) \times Z(i) - f_{bz}(i) \times X(i) + mg \times X_{CoG})}{(mg - f_{bz})} \\
 ZMP_y &= \frac{(-M_{bx} + f_{by}(i) \times Z(i) - f_{bz}(i) \times Y(i) + mg \times Y_{CoG})}{(mg - f_{bz})} \\
 ZMP_z &= 0
 \end{aligned} \tag{2.4}$$

Considering that for this thesis subjects will only complete one-handed tasks it is possible to simplify the previous equation and obtain equation (2.5).

$$\begin{aligned} ZMP_x &= \frac{(M_{by} + f_{bx} \times Z - f_{bz} \times X + mg \times X_{CoG})}{(mg - f_{bz})} \\ ZMP_y &= \frac{(-M_{bx} + f_{by} \times Z - f_{bz} \times Y + mg \times Y_{CoG})}{(mg - f_{bz})} \\ ZMP_z &= 0 \end{aligned} \quad (2.5)$$

The variables used in this equation are defined as presented in Table 2.2.

Table 2.2 Definition of ZMP equation variables

<b>ZMP<sub>x</sub></b> <b>ZMP<sub>y</sub></b> <b>ZMP<sub>z</sub></b>	<b>Coordinate of the ZMP:</b> → (X component) → (Y component) → (Z component, equal to 0)
<b>M<sub>bx</sub></b> <b>M<sub>by</sub></b>	<b>Magnitude of reaction external moments applied on the body:</b> → (X component) → (Y component)
<b>f<sub>bx</sub></b> <b>f<sub>by</sub></b> <b>f<sub>bz</sub></b>	<b>Magnitude of reaction external force applied to the working hand:</b> → (X component) → (Y component) → (Z component)
<b>X</b> <b>Y</b> <b>Z</b>	<b>Coordinates of the center of the load cell:</b> → (X component) → (Y component) → (Z component)
<b>mg</b>	→ Force applied to the body due to gravity.
<b>X<sub>CoG</sub></b> <b>Y<sub>CoG</sub></b>	<b>Position of the Center of Gravity:</b> → (X component) → (Y component)

## 2.2 Experimental human data capture systems

This section will review prior studies during which experimental data capture systems have been used or developed to evaluate human kinetics and kinematics requiring interactions with the environment. The assessment will focus on the force and moment capture systems used to evaluate applied hand loads for industrial tasks involving tools as well as the test bench structural design enabling the integration of a motion capture system.

### 2.2.1 Force evaluation for industrial tasks using hand tools

For this thesis, an industrial task with hand tools will be considered a task where a human needs to constantly hold a tool during the execution of a task. Consequently, one or more degrees of freedom may remain present between the tool effector and the target when performing the task. Figure 2.5 illustrates this definition.

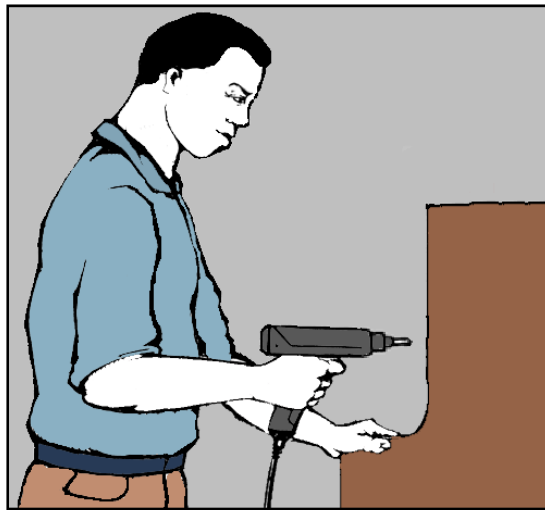


Figure 2.5 Industrial hand task with a tool

Several previous studies have attempted to evaluate the kinetic loads exerted by human hands holding tools using triaxial sensors, transducers, or load cells. Indeed, McGorry and Lin (2007) assessed the grip force on pneumatic tools as a function of the tool position and orientation.

During this study, a replica of the tool fitted with strain gauges was used to estimate the grip force of 30 subjects. Outcomes included the influences on subject grip force capability of handle height and reaching location.

Phan, Kana, and Campolo (2017) also evaluated the hand loads produced when performing industrial tasks, with a grinding wheel tool. To measure these forces and moments, an instrumented tool equipped with a load cell was developed. The results of this study included the development of different functions based on skilled worker polishing movements and contact forces applied.

A study conducted at l'Institut de recherche Robert-Sauvé en santé et en sécurité du travail (IRSST) evaluated the development of an instrumented hand-handle measuring system composed of flexible sensors for grip evaluation as well as force sensors for push and pull evaluation. The outcomes of this study by Rakheja, Marcotte, Kalra, Adewusi, and Dewangan (2016) found that using flexible resistive sensors is not only less expensive but beneficial when using tools as these sensors can easily adapt to different tool shape and size. On the other hand, flexible resistive sensors tend to drift over time, and outputs are dependent on subject hand size or tool handle size which can produce other influencing factors.

Kong, Lowe, Lee, and Krieg (2007) also used flexible resistive force sensors during their study for evaluating the effect of different screwdriver shapes on finger and phalange force application. These researches equipped subjects with a glove composed of flexible resistive sensors in conjunction with a torque transducer mounted on a workpiece to evaluate screwdriver torque. However, it was raised that flexible sensors have a shorter life as the effect of shear forces impacts the sensor's resistance which in turn may influence their performance and the produced results. The torque transducer was equipped with an adapter to permit the coupling of various screwdriver ends which allowed the evaluation of 24 different screwdrivers with one capture system. This design is represented in Figure 2.6.

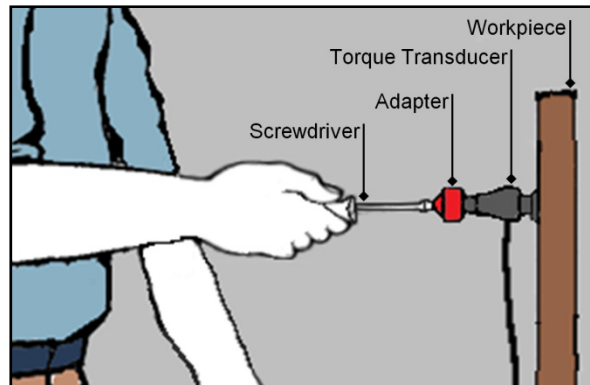


Figure 2.6 Capture system with adapter design

Other studies such as those of Ay, Sommerich, and Luscher (2013) and Singh and Khan (2010) used strain gauges combined with a rate gyro, and torque transducers to evaluate hand forces and moments. Although good results were obtained, affixing sensors directly on the tools required the development of calibration matrices to correct tool weight and geometry.

Marchand and Giguère (2012) was the only study identified that fully evaluated kinetics and kinematics of humans in industrial conditions. The purpose of this study was to assess musculoskeletal disorders related to specific automotive repair activities. Researchers used a torque transducer, strain gauges, electromyography (EMG), and light-emitting diodes (LED) to locate the human joints. Although the focus of this study was on muscle activation, contact forces and applied torques were measured when using industrial tools and a basic kinematic assessment was conducted on body segment angles to verify body ergonomics.

Table-A I-3 in APPENDIX I regroups studies that have been identified for industrial tasks using hand tools. When referring to this table, it is possible to see that few studies have simultaneously evaluated kinematics and hand loads using tools in industrial conditions. Moreover, most of these studies outfit specific tools with capture systems mounted directly on the tools, resulting in the problem that the capture system can rarely be interchangeable. Because few studies evaluated human kinematics when using tools, the next section will focus on evaluating studies that have conceived experimental test benches to evaluate simultaneously human kinetics and kinematics in various conditions.

### 2.2.2 Experimental test bench designs

The following subsection will cover studies that have developed experimental test benches to acquire human kinetics and kinematics data not specifically in industrial conditions. Summaries of these studies describing the different systems used, the methods used, and the general results obtained are presented in APPENDIX I at Table-A I-4.

A study by Wilkinson et al. (1995) evaluated the relationship between hand force in 26 directions and the adopted postures for one-handed pulling and pushing tasks. For the acquisition of data, hand forces were measured with a triaxial force sensor mounted to a fixed structure, kinematics were evaluated with 22 landmarks using biplane pictures and ground reaction forces were not assessed. The vertical plane provided researchers with information regarding the adopted posture in relation to the force magnitude, whereas the horizontal plane provided posture strategy information on how to position oneself to develop torque and thrust at the feet which is transposed into lateral forces.

To evaluate trunk posture, as well as the applied forces and moments directions during two-handed pushing, Granata and Bennett (2005) used an experimental test bench composed of a 6-DOF (Degree of Freedom) load cell, electromagnetic sensors for kinematic evaluation, and a ground reaction force plate. Although the COM and the hand force application point were calculated relative to the L5-S1 vector instead of being measured, interesting conclusions emerged from this study. For postural evaluations, it was found that foot placement in side-by-side stance was nearly at half distance between the front and rear foot position of when adopting a split stance. During the trials, all the subjects leaned a minimum of 15 ° when pushing the handle, and substantial out of the sagittal plane loads were observed. Finally, the mean horizontal force was 33% greater for waist height handle height compared to shoulder height indicating that subjects transfer a portion of the gravitational bodyweight force into horizontal force, which is in line with the observations seen in the literature (Haslegrave, et al., 1997).

Hoffman, Reed, and Chaffin (2007b) also developed an experimental test bench to evaluate pushing and pulling tasks in laboratory conditions. This test bench was equipped with a 6-DOF load cell on which a handle was attached and was used in conjunction with a motion capture system and 29 body landmarks. Ground reaction forces were measured with moveable force plates. The main conclusions of this study on two-handed tasks were that in a side-by-side stance, the projected COM would tend to exit the BOS, whereas in a split stance the projected COM would stay inside the BOS. It was also established that upper limb postures facilitate the maximization of applied shoulder and elbow torques while lower limb postures support balance maintenance. In a later study, Hoffman, Reed, and Chaffin (2008) conducted similar experiments using the previous experimental test bench, however in this new study one-handed pushing and pulling tasks were evaluated. The main difference between two-handed and one-handed tasks is that exerted forces will be asymmetrical for one-handed tasks instead of symmetrical, which generates more lateral forces. Because feet position were not constrained, subjects were free to position themselves in relation to the task, hence the observation that subjects adjust their body position to align it with the direction of the applied force in order to reduce lateral & transverse forces and only apply sagittal plane forces. It was also observed that one-handed tasks are defined by forward or backward axial rotation of the torso with respect to the hand position reducing the rotational trunk torques, by varying the pelvis position.

This experimental test bench has been reused multiple times over the years which seems to have given the researchers accurate results for posture evaluation (Hoffman et al., 2007a, 2010; Jones et al., 2013). Through these studies, the researchers have covered various evaluations of human postures during one-handed and two-handed tasks for pushing and pulling. Outcomes include shoulder positioning being above the handle location when lower forces are applied and moving towards handle height during higher forces. Regression models were developed to estimate the actual hand forces that should be applied to obtain a specific vertical or horizontal force considering the added lateral forces that will be produced. The impact of bracing on the force capabilities of humans has even been evaluated with this test bench. Results showed that applied forces can increase on average by 43% across all

studied conditions (Jones et al., 2013). The experimental protocol in their study defined task height locations scaled to each subject (43, 59, and 76% of stature) as well as anterior-posterior axis distances between the bracing obstacle and the target (26 and 44% of stature).

The use of a hand force capture system combined with motion capture cameras and force platforms seems to be the preferred configuration for evaluating both human kinetics at kinematics. A recent study by Weston, Aurand, Dufour, Knapik, and Marras (2018) developed a sophisticated experimental test bench to evaluate one-handed and two-handed pushing and pulling tasks. Subjects were required to displace a moveable rig equipped with a braking system that added linear and rotational resistance proportional to the absolute displacement. The defined protocol provided researchers with data on muscle contraction as well as force magnitude and direction to evaluate lumbar spine load in terms of task position.

### 2.3 Conclusion

A total of 26 articles were covered in this literature review given their potential contribution to this project and the research questions. Undoubtedly, the conducted article search has not made it possible to recover all the studies present in the literature. However, a considerable number of studies have been collected to explain and demonstrate specific concepts that will be used throughout this thesis.

The stability model proposed by Popovic et al. (2000) is adequate for developing foot prediction models as it details when a specific postural strategy should be used according to the position of the COP. When comparing the high preference region to the natural sway of humans, results reveal a similarity to what is present in the literature (Holbein, et al. 2007; Lucy & Hayes, 1985). The unstable region, limit where stepping is triggered, was fixed in the anterior-posterior direction at 59% of the foot length, representing an inevitable step must be taken at 23.5% of the BOS anterior limit. With regard to this stepping threshold, results were similar to those obtained by Pai et al. (1998). The mean stepping trigger across all groups for the middle perturbation during the study by Pai et al. (1998) was between 25% and 30% of the BOS anterior limit.

A challenge regularly encountered when using current foot placement prediction models is the difficulty to evaluate more complex tasks as the existing models are often based on general experimental data which doesn't incorporate the assessment for complex material handling or tool manipulation tasks. Additional experiences should be conducted in specific scenarios for data-based models to have a more precise representation. Even though the zero moment point is currently mainly used in the robotics field, it appears to be an exploitable parameter for assessing stability and generating plausible postures in digital human models.

In light of what was identified in this chapter, no study has yet conducted experiments in industrial conditions to evaluate human posture when performing tasks involving hand tools. By evaluating the various experimental test bench designed in previous studies, it is possible

to mitigate the risk related to the design of a non-functional system. As mentioned by other researchers, the direction and amplitude of loads out of the sagittal plane greatly influence the different postural strategies used by humans (De Looze, Van Greuningen, Rebel, Kingma & Kuijer, 2000; Granata & Bennett, 2005). Therefore it has been determined that a 6-DOF load cell would best fulfill the requirements needed for the test bench and that an interface adapter similar to that of Kong et al. (2007) would be added to allow the use of various hand tools during experiments. The postural evaluation will be conducted with a motion capture system and reflective markers affixed on landmarks. As for ground reaction forces, they will be assessed with a force platform that will measure feet COP positions and magnitudes. All these components will be detailed in section 3.3 of this thesis.

No study evaluated tasks out of the sagittal plane using obstacles to impose spatial constraints without preventing whole-body movement or prescribing specific feet placement. Although one-handed tasks have been studied for feet placement, no obstacles were present which allowed subjects to position themselves freely to the tasks which aren't always possible in industrial settings due to environmental constraints. Also, most studies constrained subjects' feet during experiments which have been seen to greatly influence whole-body posture as well as force exertion capabilities.

Nonetheless, there is insufficiency in the variety of experimental data available for tasks other than perturbed standing, maximal force exertion, and foot positioning during box manipulation tasks. Experimental observations are predominant to studies in industrial settings and usually impose specific feet placement or don't evaluate stability with respect to a controlled variable. Given that no convenient experimental data has yet been produced to validate the model of Zeighami et al. (2019), the developed experimental test bench was designed to allow the assessment of a variety of industrial tasks requiring different postural strategies mainly focusing on feet position.



## CHAPTER 3

### METHODOLOGY

This chapter presents the experimental methods fulfilled during this research project. The first section will present an evaluation aiming at determining task postures frequently observed in the industrial sector. The second section covers elements leading to the development of the experimental test bench used to capture experimental subject data. The third section will outline the components defined to design the full experimental protocol and the data collection protocol which was used to obtain the experimental results.

#### 3.1 Industrial task posture evaluation

This section is intended to assess the various industrial task postures observed in the automotive assembly industry. A total of sixteen (16) assembly lines, organized in Table 3.1, were analyzed for seven (7) different automotive companies using online video data.

Table 3.1 Automotive companies  
& Assembly lines assessed

Company	Assembly lines
<b>Ford</b>	→ Focus 2019 → Ranger 2019 → Mustang 2019
<b>Toyota</b>	→ Prius 2017 → Mirai → Corolla
<b>Honda</b>	→ Accord 2019 → Civic 2017 → Odyssey
<b>Volkswagen</b>	→ Golf 2017 → Touareg 2017 → Touareg India
<b>Mercedes</b>	→ Actros
<b>PACCAR</b>	→ Kenworth → DAF
<b>Rolls-Royce</b>	→ Phantom

Figure 3.1 illustrates examples of assessed tasks. Defining the occurrence of each task permitted the determination of the essential task postures that will be performed by the subjects. Here it is possible to view kneeling, standing straight, and squatting postures. The assigned postures are listed in Table 3.2.



Figure 3.1 Task assessment examples

Table 3.2 Task assessment examples legend

Image	Posture
Figure 3.1 a)	→ Half Kneeling
Figure 3.1 b)	→ Standing Straight with Step
Figure 3.1 c)	→ Standing Straight without Step
Figure 3.1 d)	→ Leaning with Step
Figure 3.1 e)	→ Leaning without Step
Figure 3.1 f)	→ Leaning with Step
Figure 3.1 g)	→ Standing Straight without Step
Figure 3.1 h)	→ Stride Kneeling
Figure 3.1 i)	→ Seated
Figure 3.1 j)	→ Squatting with Step

### 3.1.1 Grouping of postures

Table-A II-1 through Table-A II-9 in APPENDIX II group the task postures that have been extracted from the assembly line videos for different car companies. Tasks were first grouped according to the generic postures defined in the Assembly Specific Force Atlas (Schaub et al., 2015). The nine (9) groups are namely: Standing Upright, Standing Bent, Standing Above the head, Squatting, Seating Upright, Seating Bent, Kneeling Upright, Kneeling Bent, and Kneeling Above the head and can be viewed in the distribution graphic at Figure 3.2. In total 165 different tasks were observed and retrieved from the videos. As can be seen, standing tasks paired with leaning tasks represent 88% of all evaluated tasks.

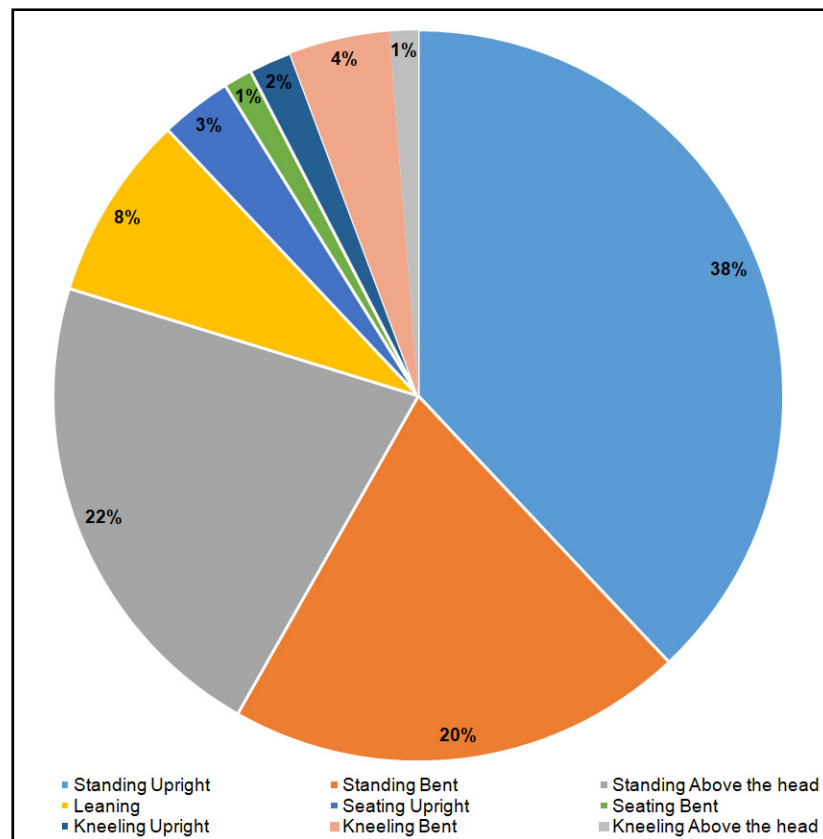


Figure 3.2 Distribution by grouping of postures

An external assessment was performed within a company for two automotive baselines by visually observing workers onsite to validate the accuracy of the online data used. Because of distribution agreements, the identity of the company will remain confidential.

Table 3.3 presents the evaluation of data acquired onsite compared to online videos. Although when comparing "task postures by group", data might seem different, several inferences can be made to "task postures by class". Indeed, the evaluation conducted for this thesis found for the standing and the leaning task differences of 1% and 1.5% respectively with the inter-data means, which is negligible considering the variability in assembly task requirements.

Table 3.3 Comparison of task assessments for three data sets in the automotive industry

Task Posture by Class	Task Posture by Group	Data Sets						
		Onsite Baseline N° 1		Onsite Baseline N° 2		Inter-data Mean	Online videos (Internal evaluation)	
Standing	Standing Upright	59%	75%	58%	83%	79%	38%	80%
	Standing Bent	5%		14%			20%	
	Standing Above the head	11%		11%			22%	
Leaning	Leaning	14%		5%		9.5%	8%	
Seating	Seated Upright	5%	11%	9%	11%	11%	3%	4%
	Seated Bent	6%		2%			1%	
Kneeling	Kneeling Upright	0%	0%	0%	1%	0.5%	2%	7%
	Kneeling Bent	0%		1%			4%	
	Kneeling Above the head	0%		0%			1%	
Number of Tasks evaluated		466 Tasks evaluated		400 Tasks evaluated		100%	165 Tasks evaluated	

As for seating and kneeling tasks, although the occurrences vary, the summation of these two tasks by group are relatively similar. In fact, they are respectively 11%, 12%, and 11%. It is assumed that different strategies are used throughout the automotive industry. For lower tasks, some companies might prefer employees to work seated whereas other companies would prefer kneeling. These results indicate the data is accurate for posture classification.

### 3.1.2 Posture strategies classifications

To accurately evaluate task occurrences, a classification based filter technique was used. Task postures were first assessed according to five primary posture strategies (Standing Straight, Leaning, Squatting, Kneeling, and Seating), that have been defined in Table 3.4.

Table 3.4 Primary Posture Strategies Definitions

<b>Standing Straight</b>	→ Flexion or Extension of the trunk inferior to 15 °. → Flexion at the knee inferior to 15 °.
<b>Leaning</b>	→ Flexion or Extension of the trunk superior to 15 °. → Flexion at the knee inferior to 15 °.
<b>Squatting</b>	→ Flexion of the trunk superior to 15 °. → Flexion at the knee superior to 15 °. → Flexion at the ankle superior to 15 °.
<b>Kneeling</b>	→ At least one knee touching the ground.
<b>Seating</b>	→ Inferior posterior chain touching a supporting object.

The primary strategies are then subdivided into five secondary posture strategies that are defined in Table 3.5. When it is unclear in the images what secondary posture strategy the subject is using, the task is considered unclassifiable. Therefore, the interpretations of tasks in the unclassifiable category will only be evaluated by their primary strategy classification.

Table 3.5 Secondary Posture Strategies Definitions

<b>Stepping</b>	<b>Anterior-posterior:</b> → Stance with the middle of the front foot passing toes of the rear foot. <b>Transverse:</b> → Stance wider than shoulder-width. <b>Rotation:</b> → Foot rotational angle superior to 45 ° with a neutral position.
<b>Bracing</b>	→ Body touching a supporting object.
<b>Half Kneeling</b>	→ One knee is in contact with the ground.
<b>Stride Kneeling</b>	→ Both knees are in contact with the ground.
<b>Unclassifiable</b>	→ Images don't allow to determine what strategy the subject is performing.

### 3.1.3 Posture strategies occurrences

Once all the tasks were classified according to their primary and secondary posture strategies, an occurrence evaluation was conducted. Figure 3.3 represents the distribution of tasks according to primary and secondary strategies. It is noted that in this graphic, the Unclassifiable tasks were kept to display their importance and also allow a full representation of primary posture strategies. In this distribution, it is obvious that Standing Straight and Leaning tasks represent a vast majority of all the analyzed tasks.

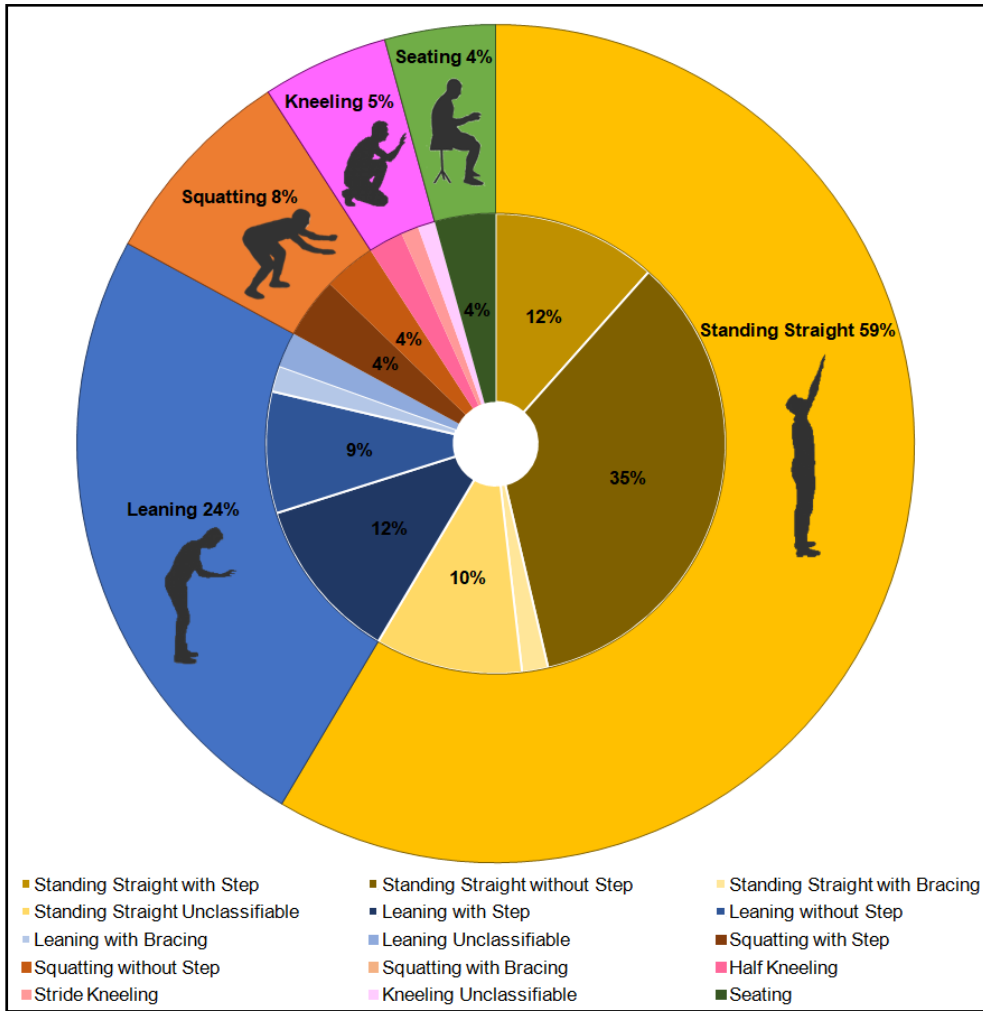


Figure 3.3 Distribution of Occurrences grouped by Primary Posture Strategies

The following graphic represented in Figure 3.4 illustrates the distribution of all the tasks evaluated excluding the tasks that were considered Unclassifiable. This new representation allows an evaluation of the number of occurrences for each primary posture strategies. The first notion that can be mentioned about this distribution is that contrary to when Standing Straight, subjects tend to step more when using the Leaning or Squatting strategy. In fact, for Standing Straight tasks subjects are three times more likely to execute tasks without stepping.

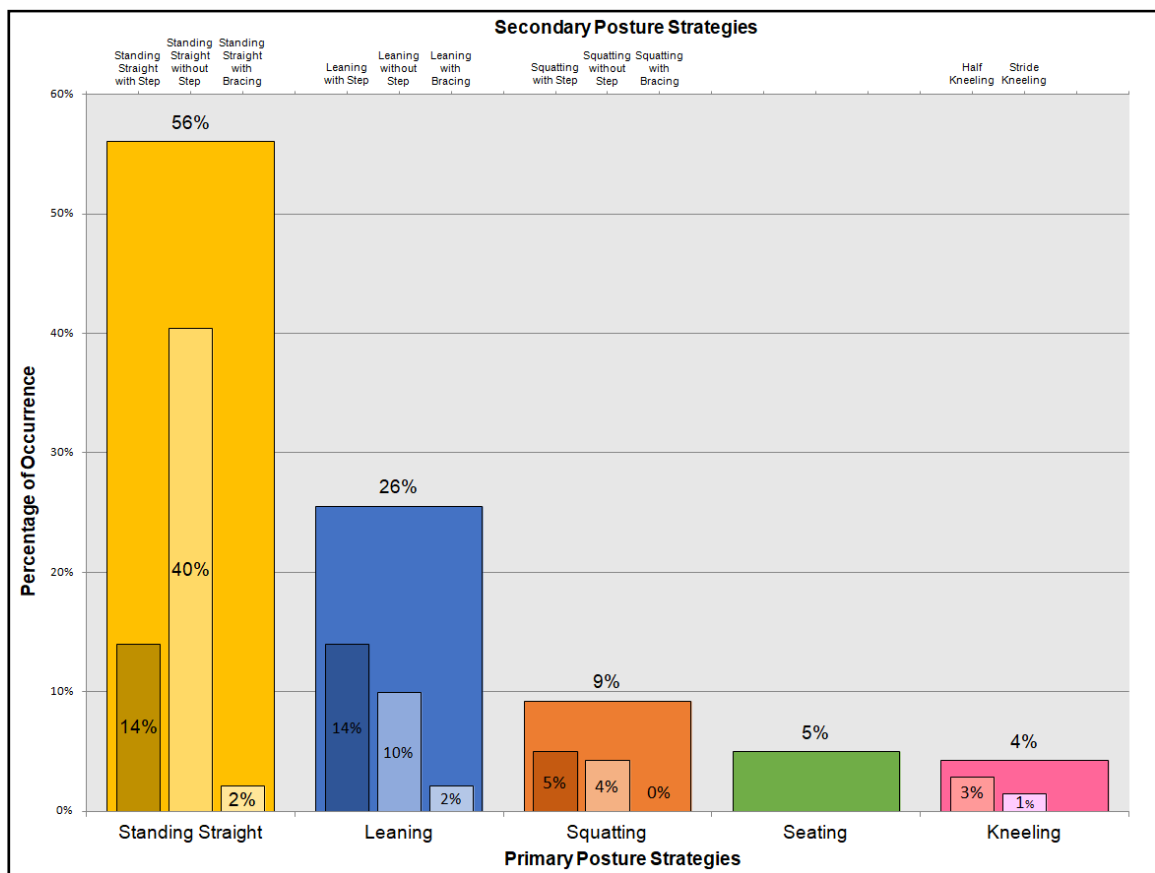


Figure 3.4 Distribution of Secondary Posture Strategies in terms of Occurrence classified by Primary Posture Strategies

In the final graphic in Figure 3.5, all the evaluated tasks were grouped by secondary posture strategies with seating and kneeling grouped in the category Other. Once again, the Unclassifiable tasks were removed. This representation allows an estimation of the number of occurrences when no stepping, stepping, or bracing was used. It is possible to see that stepping is a considerable strategy to evaluate as it represents about a third of all evaluated secondary posture strategies.

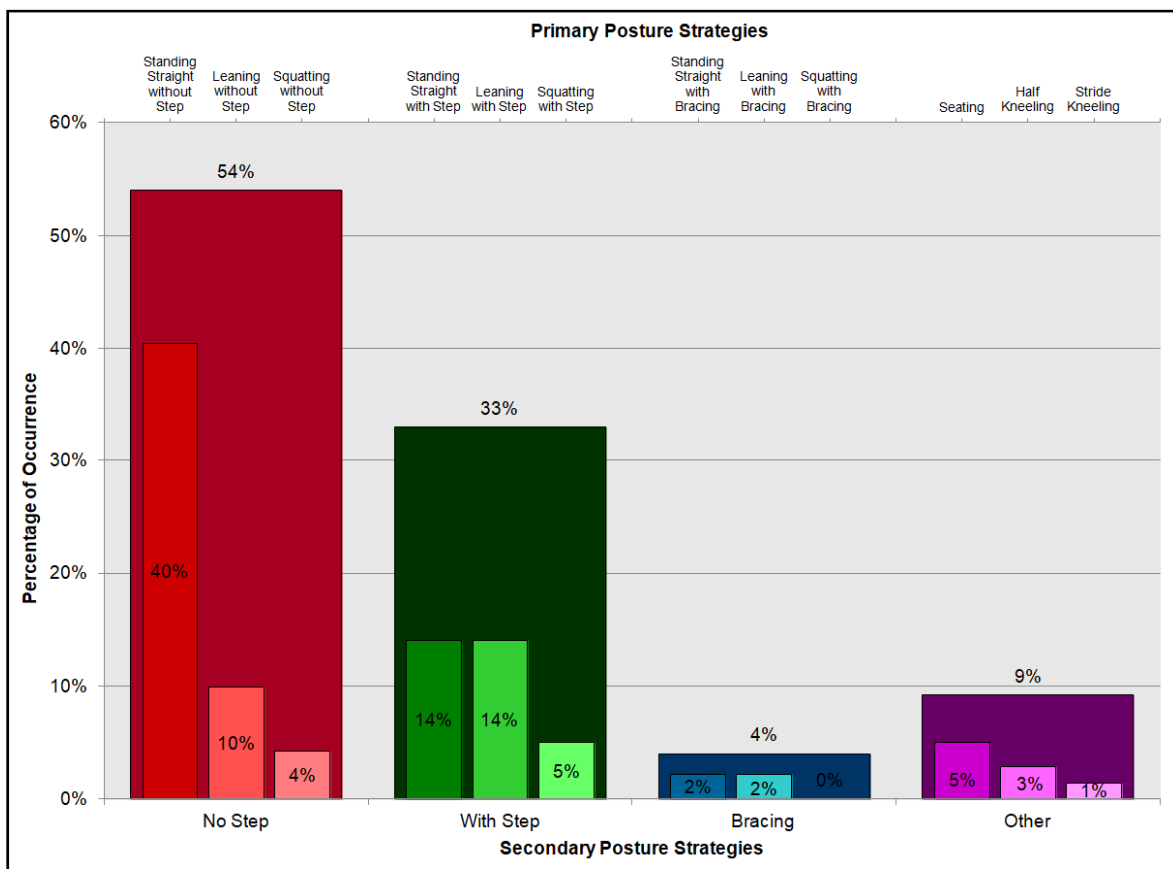


Figure 3.5 Distribution of Primary Posture Strategies in terms of Occurrence classified by Secondary Posture Strategies

### 3.1.4 Conclusion

In conclusion, results were consistent with those found by Baril-Gingras and Lortie (1995). Leaning was almost the same during the transport company handling study with an occurrence of 25.4% compared to 26%. Squatting seems to be used less often in the automotive industry than in the material handling sector with occurrences respectively of 9% compared to 11.7%. This can be due to the fact that kneeling wasn't assessed in the previous study which accounted for 4% of all automotive posture strategies. As mentioned by Baril-Gingras and Lortie (1995), a form of stepping was seen in 34.6% of all the handlings requiring upper limb movement or exertion. This is comparable to the 33% found in the automotive industry.

This evaluation allowed the identification of nine (9) typical postures often used by workers in industrial conditions. An in-depth analysis of these postures permits the division of these tasks into two groups: simple and complex tasks (Figure 3.6). The three standing task postures (Standing Upright, Standing Bent, and Standing Above the head) will be considered as simple tasks. The Leaning task posture will also be considered simple. The two seating (Seating Upright and Seating Bent) and the three kneeling (Kneeling Upright, Kneeling Bent, and Kneeling Above the head) task postures compose the complex tasks. Seated tasks are considered complex because multiple surfaces are in contact with the environment and the worker. When detailing the different tasks that will be experimentally tested, it will be taken into account to develop situations that will require the subjects to use the stepping strategy.

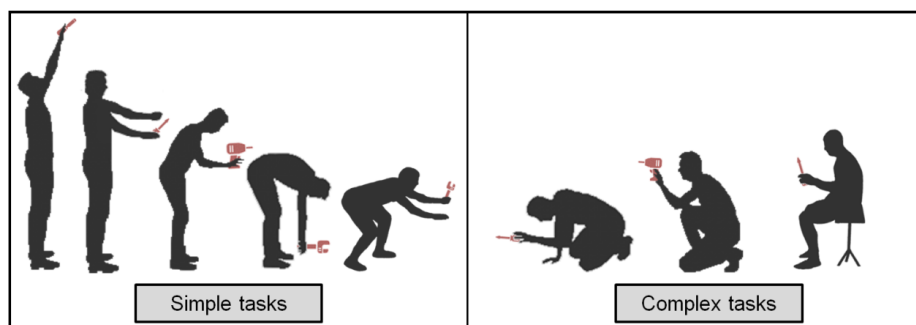


Figure 3.6 Summary of postural evaluation tasks

## **3.2 The conception of an experimental test bench**

The following section presents the functional and technical elements defined when developing the experimental test bench.

### **3.2.1 Requirements**

The main objective of developing an experimental test bench is to conceive a data acquisition device that will allow the evaluation of external forces and moments applied by the human body when performing standing industrial tasks. The test bench must also simultaneously allow the use of a motion capture system to obtain subject kinematics.

#### **3.2.1.1 Attributes**

Attributes are needs and expectations that need to be fulfilled as best as possible. Within the framework of this thesis, the following attributes were determined.

##### **Functionality**

- The device allows the evaluation of simple tasks (Standing & Leaning);
- The device is adaptable to allow the evaluation of complex tasks (Crouching & Kneeling);
- The device permits the measurement of ground loads (Reaction forces & moments);
- The device measures the loads exerted by the hands (Reaction forces & moments);
- The measurements acquired with the device are repeatable (Variation between the measurements taken by the same person several times);
- The measurements acquired with the device are reproducible (Variation between the mean measurements taken by several people);
- The device permits the kinematic measurements of the human body;
- The device enables the use of various industrial tools;

### **General**

- The adjustments are resistant to usage;
- The device is robust to the loads applied;
- The collected data is compatible with the other equipment in the research laboratory;
- The device is affordable;
- The measurements are accurate (Can tolerate an uncertainty if repeatable);

#### **3.2.1.2 Constraints**

Constraints are elements that any concept must meet to be considered a potential solution that can achieve the project limits. Within the framework of this thesis, the following constraints were determined.

- The device must be safe;
- The device must be adjustable to allow the evaluation of various task postures;
- The adjustments must be kept during the acquisitions;
- The device must not be permanently affixed;
- The device must be stable;
- The external load capture system must be interchangeable for the left & right hand;

#### **3.2.1.3 Good to have**

The following is a list of elements to consider when developing the experimental test bench for future works that would require the usage of this device.

- The device permits the integration of the VIVE virtual reality helmet;
- The device permits the movement of the feet without constraining their position;
- The device permits the support of the contralateral or ipsilateral upper limb for future bracing usage (Hand, Forearm & Elbow);

### 3.2.2 Design

After reviewing previous studies and determining the requirements for the experimental test bench, the device was conceived. The following schematic diagram, Figure 3.7, illustrates the different modules, as well as the different interactions between each one.

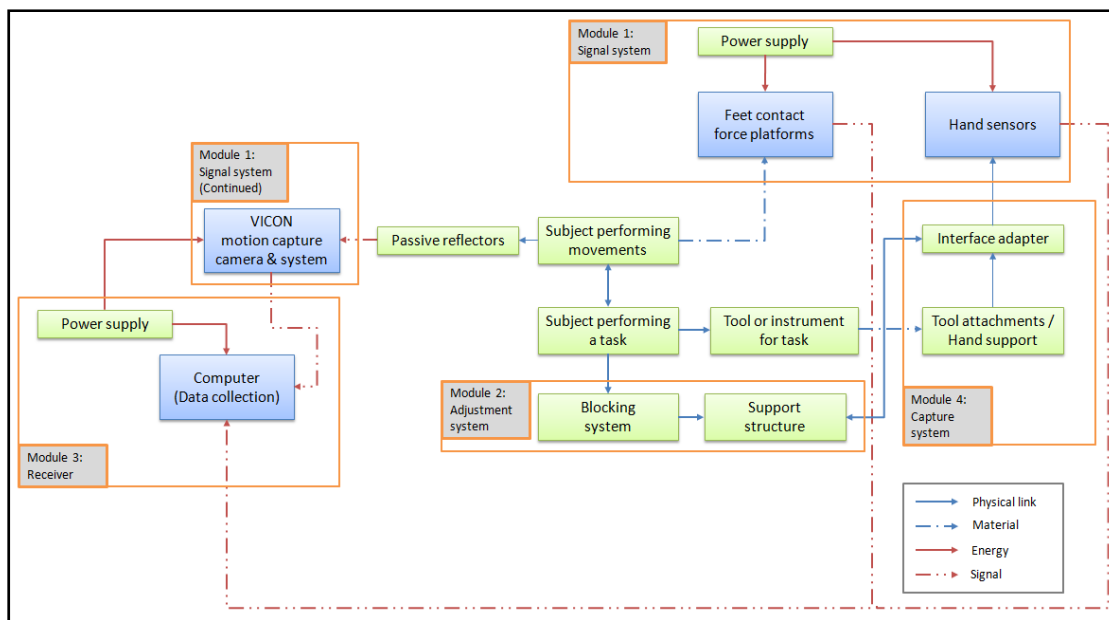


Figure 3.7 Experimental test bench schematic diagram

The test bench was designed in such a manner to allow the assessment of different tasks, which in terms allows the visualization of different postures. Two sliding rails mounted on articulated pantograph arms enable adjustment of the bench to vary target position. All adjustments are lockable to ensure no displacement will occur when forces are applied.

Figure 3.8 displays the test bench design. An anterior and a posterior pantograph arm establish the positioning of the two sliding rails for task height, anterior task, or obstacle position. It can be seen, that the structure is equipped with wheels to facilitate its displacement. However, during experiments, the wheels are disengaged and the test bench is affixed to the laboratory floor using two M10 screws to securely anchor it.



Figure 3.8 Experimental test bench design

Two standard anthropometric dimensions were used to proportion the test bench properly: stature and arm span (Gordon et al., 2014). Thus the maximum usable height is 218 cm (10 cm over maximum stature), the largest transverse offset from the sagittal plane is 65 cm in both directions and the maximum anterior reach is 122 cm with one pantograph arm and 218 cm with both pantograph arms.

The load cell is mounted on the sliding rails and can be moved in the transverse direction. This final adjustment allows for a three-dimensional variation of the target position. A capture interface is used for tool assessment (Figure 3.9) and can be changed for the assessment of different tools (Figure 3.10).

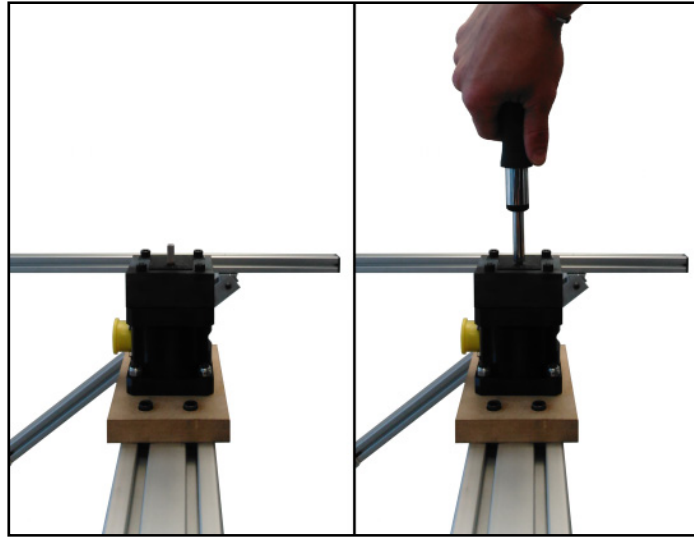


Figure 3.9 Screwdriver capture interface

Important aspects of the interface adapter are the transfer of the applied forces and moments while generating an adequate representation of a workpiece. This denotes that some degrees of freedom, either translation or rotation, remain unconstrained.

The capture interface can be equipped with alternative interfaces seen in Figure 3.10 to evaluate different tools, such as screwing with feed, tube insertion, or drilling.

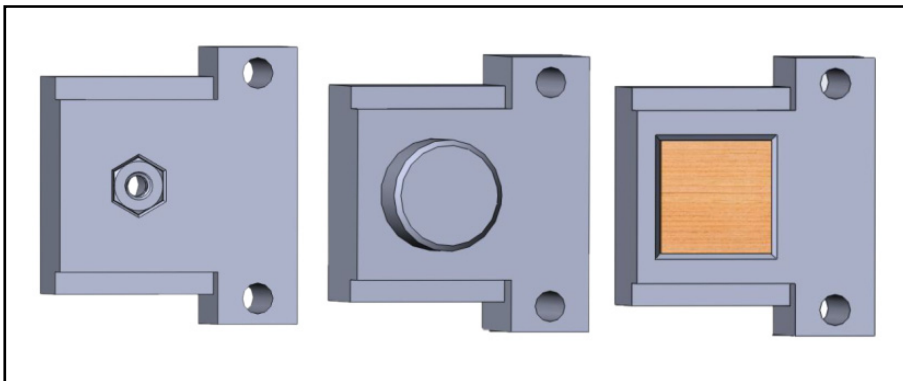


Figure 3.10 Alternative tool interfaces

For evaluating pushing and pulling, a  $5 \frac{3}{16}$ " (131.7 mm) handle system with a projection of 2" ( 50.8 mm) represented in Figure 3.11 was built. It consists of a high-friction rubber handle with a special anti-slip shape that enhances hand-handle grip. These characteristics are important to create a strong and sturdy coupling interaction between the hand and the load cell.

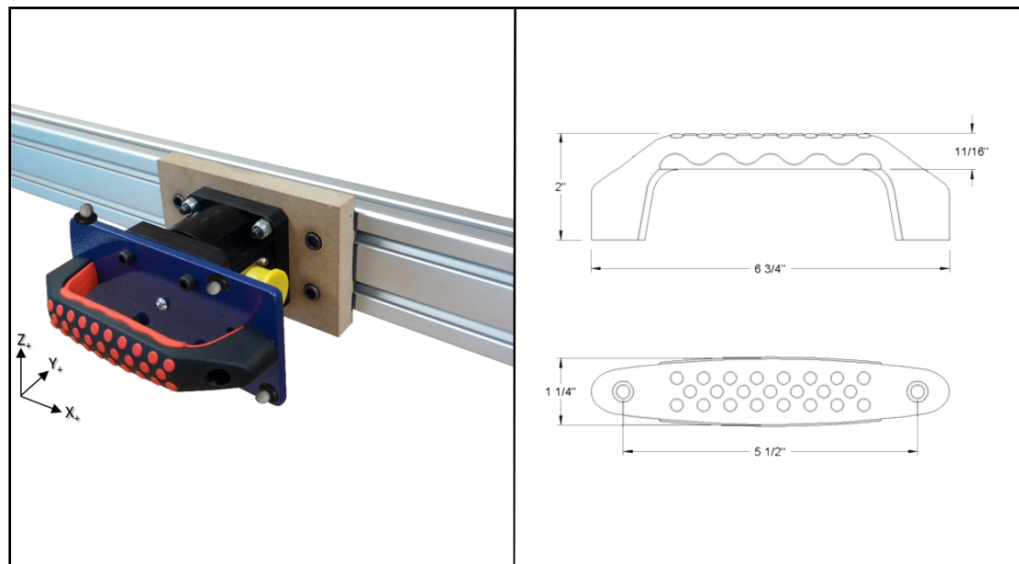


Figure 3.11 Pushing and Pulling handle capture interface

The design of the handle system imposes the adoption of a typical power grip. Also, limiting the total projection between the load cell face and the handle reduces the out of plane moments created by the handle lever arm.

Figure 3.12 illustrates how the device is installed in the laboratory. It is possible to see that the anterior pantograph arm is parallel to the transverse plane, serving as an anterior obstacle, were as the posterior pantograph arm is vertical to simulate a wall.

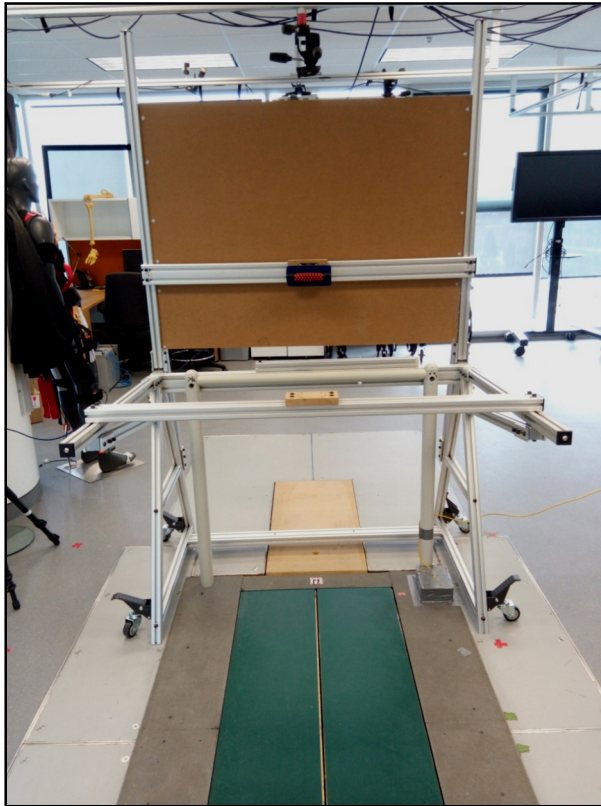


Figure 3.12 Installed experimental test bench

In this position, the anterior pantograph arm can also be used to reproduce tasks that require bracing. A second load cell can be mounted on the anterior sliding rail to acquire supporting hand reaction forces and moments.

To reproduce tasks out of the sagittal plane, a transverse obstacle can be positioned accordingly. This element has not been evaluated in previous studies. Instead of imposing spatial constraints, fixed feet positions are usually imposed on the studied participants, which isn't representative of industrial settings where workers are free to assume preferred postures.

The example presented in Figure 3.13 requires a step to ensure sufficient foot torque can be developed to apply the required hand forces considering a distant transverse reach is needed.

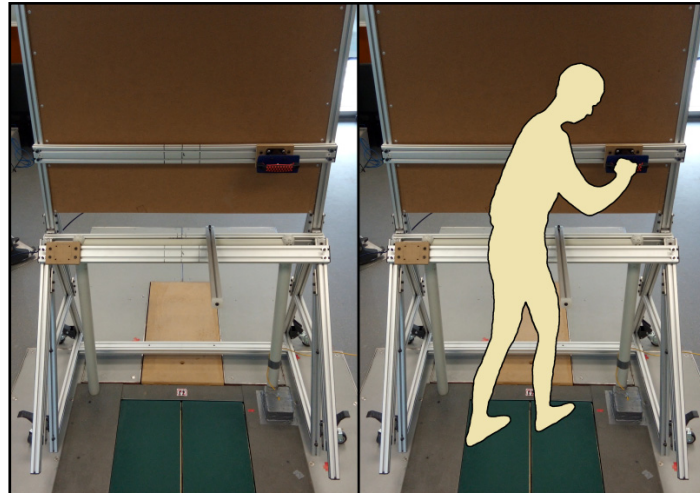


Figure 3.13 Task requiring a transverse obstacle

In the configuration shown in Figure 3.14, the anterior pantograph arm is used to reproduce tasks that require stooping or crouching to go under an obstacle to access the target.

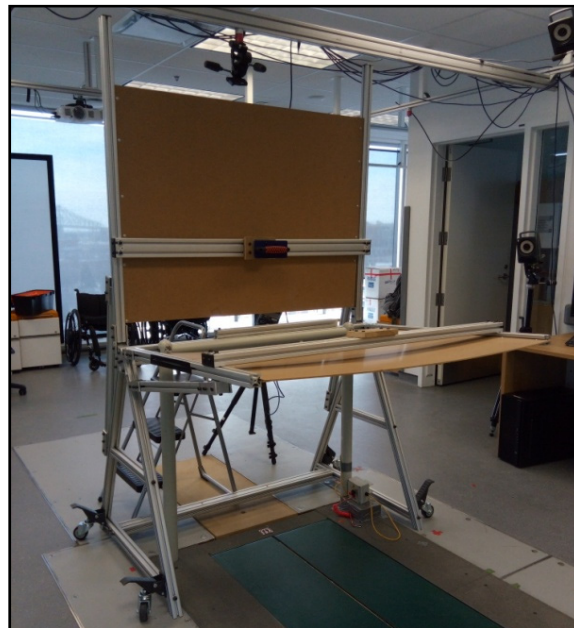


Figure 3.14 Tasks underneath an obstacle

### **3.3 Case study**

In this section, elements leading to the acquisition of human kinematics and kinetic data corresponding to the loads and positions of contact between the human body and the environment under industrial task conditions will be described.

As part of this thesis, experimental data was collected with a pilot subject according to a data collection protocol. This allowed validation of the test bench functionalities, the verification of elements within the full experimental protocol, and the assessment of the repeatability as well as the quality of the acquired data.

Experimental trials were carried out with synchronized acquisition systems allowing the evaluation of external forces and kinematic parameters of stability during one-handed standing tasks. The collected data was used to determine a relationship between the task requirements and the different feet placement.

#### **3.3.1 Experimental methodology**

The following subsection will detail the components covering the experimental data methodology. Elements presented in this section were approved by the research ethics committee of the CRCHUM and by the ethics committee of the ÉTS.

##### **3.3.1.1 Setup**

The experiments were conducted in the imaging and engineering laboratory of the CRCHUM. Three synchronized acquisition systems were used to collect human kinematics and kinetic data (Figure 3.15): (1) AMTI MC3A 6-DOF load cell attached to the capture interface, (2) Twelve VICON MX T20-S motion capture cameras, and (3) ground force platforms. As shown in Figure 2, the experimental test bench is centered with the force platforms and is affixed in this position using anchor screws.

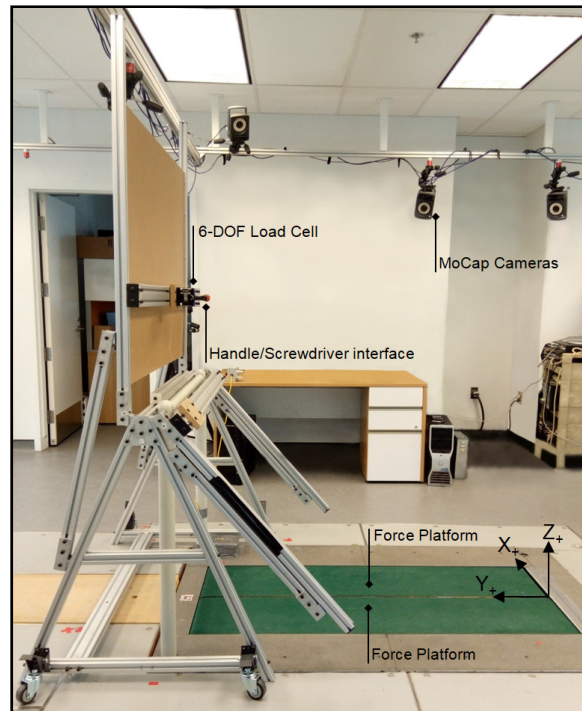


Figure 3.15 Experimental setup

### 3.3.1.2 Data collection equipment

Kinetic data were measured at a sampling frequency of 1000 Hz. Hand forces and moments were captured with an AMTI MC3A 6-DOF load cell presented in Figure 3.16. Static calibration was verified by applying known weights (3.0-20.5 kg) and verifying the loading and unloading values.



Figure 3.16 AMTI MC3A load cell

Feet kinetic was measured with an AMTI side-by-side treadmill with force platforms integrated (Figure 3.17). Static calibration was also verified by adding a known weight (2.27 kg). During this verification, the COP calculation was visually validated by placing a passive reflective marker on the center of the weight and verifying that the resultant calculated reaction force intersected with the recorded marker position.



Figure 3.17 ATMI Side-By-Side Treadmill

The treadmill was preferred to individual force platforms as the large usable area enables the recording of subjects walking towards the task and doesn't confine foot placement to a specific position. The available recordable surface is 152.20 cm long and 64.59 cm wide.

The kinematic data were captured at 200 Hz simultaneously with the kinetic data using VICON Nexus 2.8, a data capture software. Twelve VICON System (Oxford Metrics, Ltd) MX T20-S cameras (Figure 3.18) were positioned in the laboratory in a way to mitigate the occlusion created by the wood panels and the structure of the experimental test bench.



Figure 3.18 VICON  
MX T20-S camera

Three reflective markers were fixed on each capture interface which is attached to a load cell and three other markers were affixed on the screwdriver, to locate their position in the environment (Figure 3.19). Positions of the body landmarks used are defined under subsection 3.3.1.4.

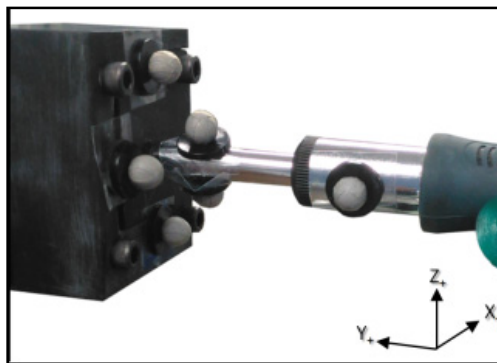


Figure 3.19 Markers used with a tool

Finally, a Digital Video Camera was used to record trials at 30 Hz with a quality of 480p (720 x 480 pixels). The video capture system permitted visual verification of the adopted postural strategies and obtained foot placement results.

### 3.3.1.3 Test tasks, locations, and conditions

Experimental trials are distinguished by a task, a location, and a condition. Arising from the industrial task posture evaluation (Section 3.1), simple and complex tasks were defined for the design of the experimental trials. Ten tasks (Figure 3.20) varying in height, reach and spatial constraints were designed for the full experimental protocol, based off-target positions retrieved in the literature review (Granata & Bennett, 2005; Haslegrave et al., 1997; Hoffman et al., 2008; Jones et al., 2013).

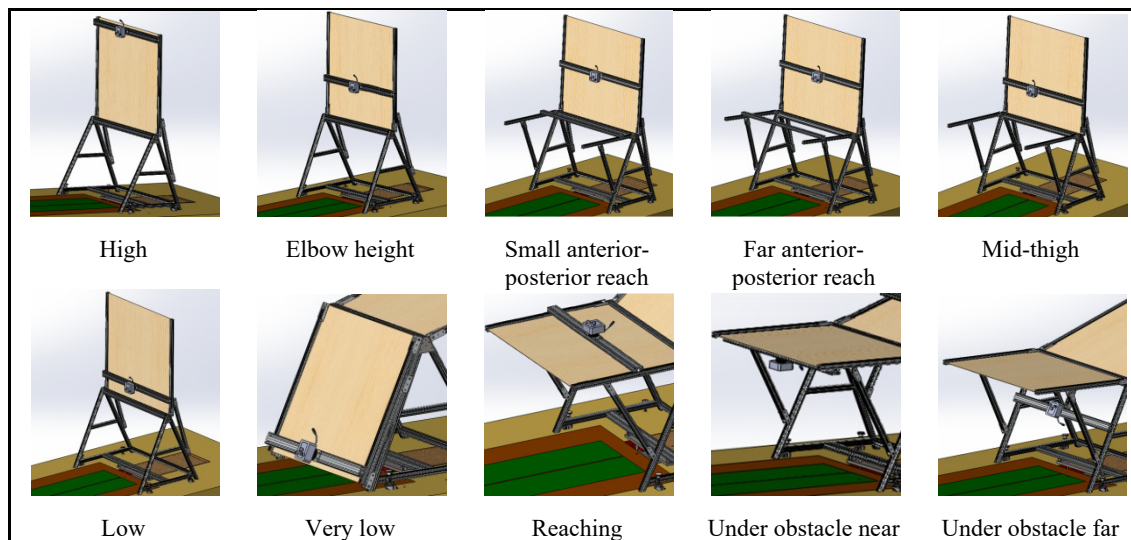


Figure 3.20 Designed test tasks

The test tasks presented in Figure 3.20 are defined as follows:

1. **High:** Coronal plane target at 0.1 m overhead;
2. **Elbow height:** Coronal plane target at 63% of stature;
3. **Small anterior-posterior reach:** Coronal plane target with a reach of 26% of stature;
4. **Far anterior-posterior reach:** Coronal plane target with a reach of 44% of stature;
5. **Mid-thigh:** Coronal plane target at 41% of stature;
6. **Low:** Coronal plane target at heights of 35% & 25% of stature;
7. **Very low:** Coronal plane target at 0.2 m from the ground;

8. **Reaching:** Transverse plane target at 1m from the ground while varying anterior-posterior reach;
9. **Under obstacle near:** Transverse plane target at 1 m from the ground at 0.2 m from the edge of the obstacle;
10. **Under obstacle far:** Coronal plane target at 0.6 m from the ground at 1 m from the edge of the obstacle;

The second test characteristic is the test locations (Table 3.6). For a same task, multiple target locations are evaluated to assess the influence of the target position on the posture adopted.

Table 3.6 Test location lexicon

Vertical Axis		Anterior-posterior Axis		Transverse Axis	
Location	Description	Location	Description	Location	Description
VertiHead	Target at 0.1 m overhead	A-P26	Obstacle at 26% of stature from the target	Trans25	Target in (X+) or (X-) at 25% of arm span
Verti63	Target at 63% of the stature	A-P44	Obstacle at 44% of stature from the target	TransHip	Obstacle in (X+) or (X-) at hip width minus 5 cm
Verti41	Target at 41% of the stature	A-P1m	Obstacle at 1 m from the target		
Verti35	Target at 35% of the stature	A-P0.2m	Obstacle at 0.2 m from the target		
Verti25	Target at 25% of the stature				
Verti1m	Target at 1 m from the ground				
Verti0.6m	Target at 0.6 m from the ground				
Verti0.2m	Target at 0.2 m from the ground				

Experimental trials are performed under four different test conditions: reach a target, forward pushing, backward pulling, and with a tool using a screwdriver.

The screwdriver was chosen as this tool limits out of plane moments created by tool dimension and shape. When comparing the three different tools presented in Figure 3.21, several conclusions can be made from these characteristics.

For the screwdriver, the applied external force is roughly in line with both the tool center of mass and the hand center of mass which are almost superimposed. Also, the applied moment is around the line of action. Over time, this tool's weight and shape have little to no effect on the applied loads.

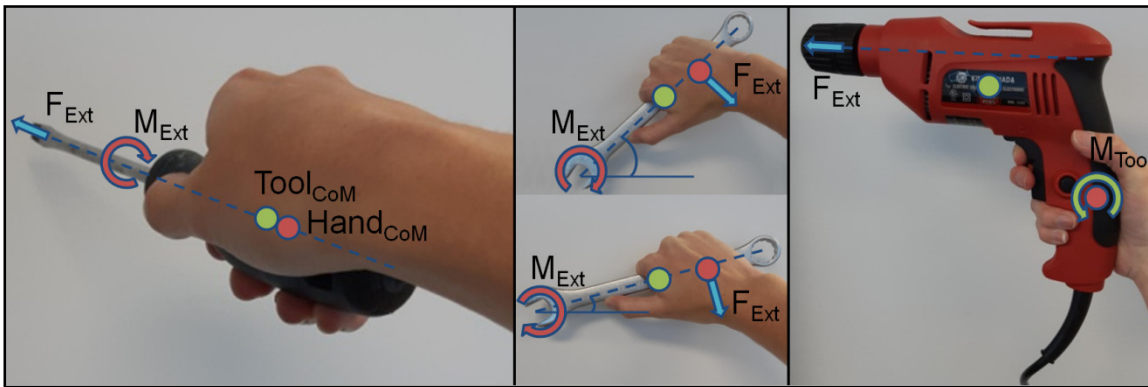


Figure 3.21 Tool shape effect comparison

When viewing the wrench, the effect of tool characteristics over time can be seen. Despite the tool and the hand center of masses being in line with the applied moment, the reaction hand force direction varies greatly over time. Also, the tool center of mass is located further away from that of the hand which creates a greater tool moment compared to the screwdriver.

The drill represents well the impact of tool shape and weight on the hand. The hand reaction forces will be significantly different due to the moment created by the distance between the end of the drill and the hand in addition to its weight which generates a tool moment.

Thus, the screwdriver will best represent a pure torsion applied to the center of the hand using a diagonal volar grip, hence simplifying the data modeling by neglecting the effects of the tool weight and shape.

Table 3.7 describes an overview of the trials designed that have been developed.

Table 3.7 Full experimental protocol overview

1.		2.		3.		4.	
<b>High (VertiHead)</b>		<b>Elbow height (Verti63)</b>		<b>Small anterior-posterior reach (Verti63)</b>		<b>Far anterior-posterior reach (Verti63)</b>	
a.) -Centered	Reach Push Pull Tool	a.) -Trans25(X-) -TransHip	Reach Push Pull Tool	-Centered -A-P26	Reach Push Pull Tool	-Centered -A-P26	Reach Push Pull Tool
b.) -Trans25(X+) - TransHip	Reach Push Pull Tool	b.) -Trans25(X+) -TransHip	Reach Push Pull Tool				
c.) -Trans25(X-) - TransHip	Reach Push Pull Tool	c.) -Centered	Reach Push Pull Tool				
5.		6.		7.			
<b>Mid-thigh (Verti41)</b>		<b>Low (Verti35)</b>		<b>Low (Verti25)</b>		<b>Very low (Verti0.2m)</b>	
a.) -Centered	Reach Push Pull Tool	-Centered	Reach Push Pull Tool	-Centered	Reach Push Pull Tool	-Centered	Reach Push Pull Tool
b.) -Trans25(X+) -TransHip	Reach Push Pull Tool						
c.) -Trans25 (X-) -TransHip	Reach Push Pull Tool						
8.		9.		10.			
<b>Reaching without step (Verti1m)</b>		<b>Reaching with step (Verti1m)</b>		<b>Under obstacle near (Verti1m)</b>		<b>Under obstacle far (Verti0.6m)</b>	
-Centered	Reach	-Centered	Reach	-Centered -A-P0.2m	Reach Push Pull Tool	-Centered -A-P1m	Reach Push Pull Tool

During trial task 8 without step, the subjects cannot step or lift their heels. An anterior-posterior obstacle is placed between the subject and the target. The target is then moved in the anterior direction until the subject indicates a step is needed. The experimental trial is completed with the target moved back 1 cm from the indicated position. In regards to task 8 with step, the same procedure is completed, however, for this trial subjects are permitted to take as big a step as they desire and lift their heels.

#### **3.3.1.4 Experimental protocol**

The full experimental protocol consists of completing every test task for all locations under each condition once. Prior to the experimental trials, subjects are required to accomplish at least one practice trial of the presented target configuration. The purpose of the practice trial is to ensure preferred postures are adopted and that subjects are comfortably achieving the required force levels at the presented target position. Each experimental trial target position is scaled to the subject stance, arm span, and hip-width measurements, initially taken.

Subjects will start facing the target with feet side-by-side outside the posterior end of the treadmill. A verbal indication, given by the experimental supervisor, will instruct subjects the trial has started. At this moment subjects are required to take a few steps towards the target and adopt a preferred posture while, with their dominant hand, executing and maintaining for 5 seconds the required condition. After the specified time, another verbal indication will instruct subjects to stop and return to the start position.

Applied force and torque levels are monitored for each experimental trial. For the reaching condition, subjects are asked to approach as close as possible the target with their working hand without touching it. During the pushing and pulling conditions, the minimum exertion required is 40 N and the maximum exertion is 100 N which has been determined from values presented in previous studies (Hoffman et al., 2007b; Singh & Khan, 2010). Audio feedback is produced once the minimum force has been obtained, announcing the posture must be maintained for 5 seconds. A different sound is produced if the maximum force is exceeded, indicating the subject to unload. For the tool condition using a screwdriver, the minimum required torque is 3 Nm and the maximum torque is 6.5 Nm. These values were determined from the maximal torque ranges found for different screwdrivers studied by Kong et al. (2007). Audio feedback is also produced once the minimal torque was achieved and if the maximal torque is exceeded.

Figure 3.22 illustrates the monitor used for pushing and pulling conditions. The region in white represents forces under the minimum required values (-40 N to 40 N). The light blue regions represent the desired zones where applied subject forces should be situated (-40 N to -100 N; 40 N to 100 N). Consequently, the remaining dark blue regions represent the undesired zone where applied subject forces are too important ( $< -100$  N;  $< 100$  N).

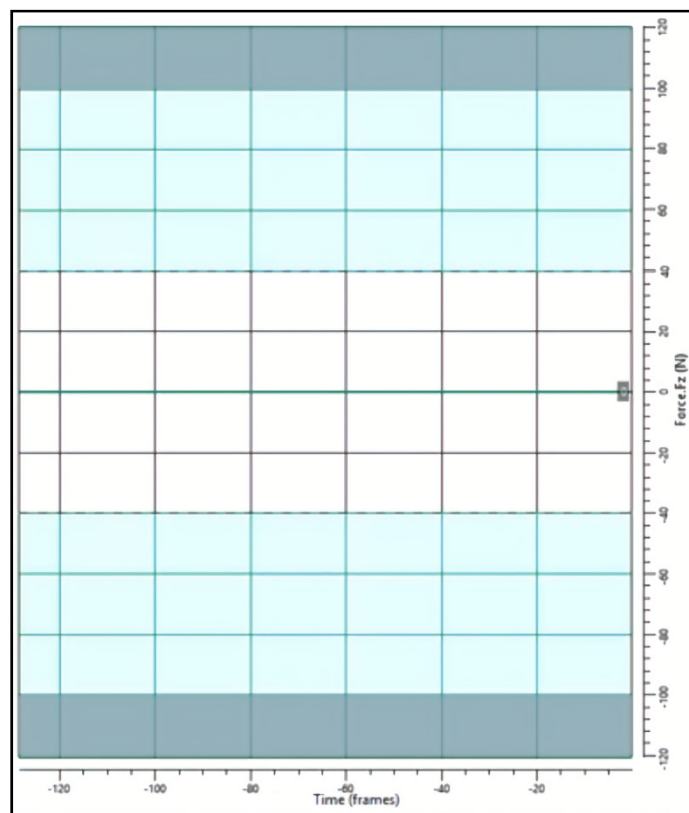


Figure 3.22 Applied hand force monitor ( $F_z$ )

Trials are considered invalid if any form of bracing is used, either with the opposing hand or with the inferior limbs. A trial is also invalid if stepping is seen for tasks where stepping isn't allowed. Lastly, for force and torque requirements if the minimal values aren't achieved or if more than half of the trial is performed over the maximal limit, the trial is considered invalid.

Marker assignment was divided into the following four regions, which are presented in Figure 3.23. Anatomical landmarks proposed by Dempster (1955) were used to assign rigid body segments representing those of the human body. A total of 50 passive reflective markers were positioned on body landmarks:

- **Hands:** Single-segment composed of four markers with the wrist as joint with the forearm;
- **Head & Neck:** Three markers are used for the head and the neck with the center of mass located between the C7 vertebrae and the axis between the tragus of the ears. (Dempster, 1955; Tyan et al., 2017);
- **Feet:** One segment define each foot and are jointed with the tibias at the malleolus;
- **Body:** Ten segments make up the rest of the body (Upper arms, Forearms, Trunk, Thighs, and Tibias).

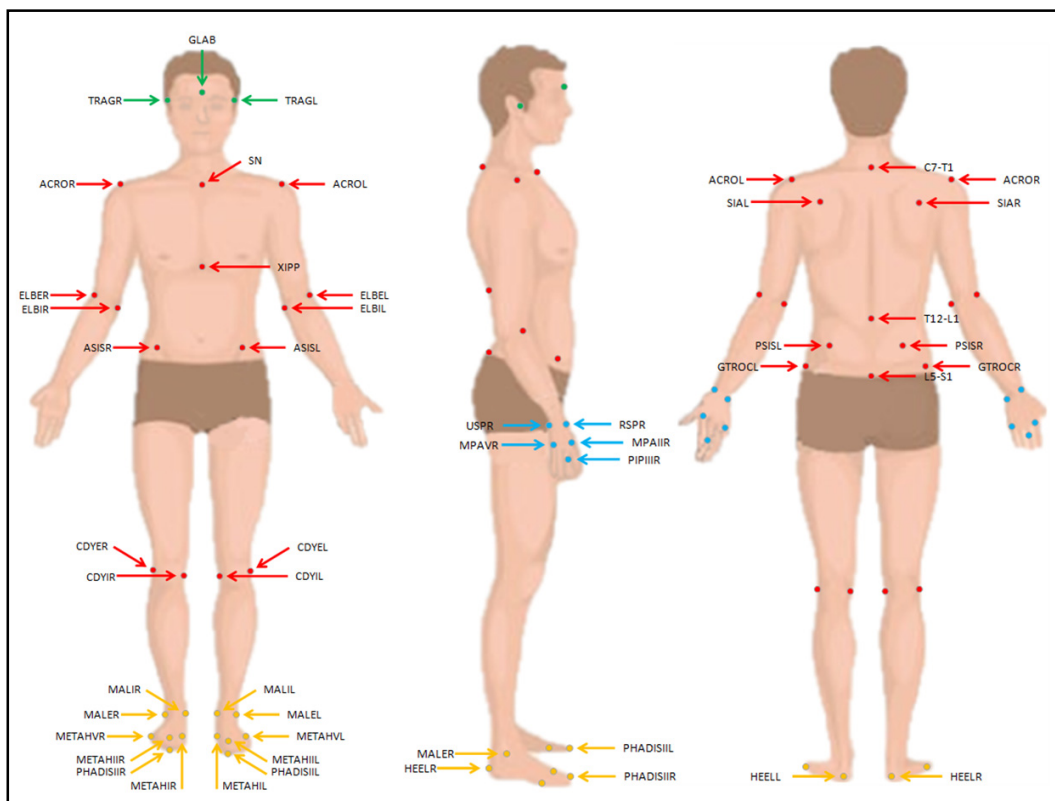


Figure 3.23 Anatomical landmarks for markers

The body landmarks are defined as presented in Table 3.8:

Table 3.8 Body landmarks lexicon

Head		Hands	
GLAB	Glabella	USPR	Ulnar Styloid Process Right
TRAGR	Tragion Right	USPL	Ulnar Styloid Process Left
TRAGL	Tragion Left	RSPR	Radial Styloid Process Right
<b>Body</b>		RSPL	Radial Styloid Process Left
ACROR	Acromion Right	MPAVR	Metacarpophalangeal Articulation V Right
ACROL	Acromion Left	MPAVL	Metacarpophalangeal Articulation V Left
SN	Suprasternal Notch	MPAIR	Metacarpophalangeal Articulation II Right
ELBER	Elbow External Right	MPAIL	Metacarpophalangeal Articulation II Left
ELBEL	Elbow External Left	PIPIIR	Proximal Interphalangeal Articulation III Right
ELBIR	Elbow Internal Right	PIPIIL	Proximal Interphalangeal Articulation III Left
ELBIL	Elbow Internal Left	<b>Feet</b>	
XIPP	Xiphoid Process	MALER	Malleolus External Right
ASISR	Anterior Superior Iliac Spine Right	MALEL	Malleolus External Left
ASISL	Anterior Superior Iliac Spine Left	MALIR	Malleolus Internal Right
CDYER	Condyle External Right	MALIL	Malleolus Internal Left
CDYEL	Condyle External Left	METAHVR	Metatarsal Head V Right
CDYIR	Condyle Internal Right	METAHVL	Metatarsal Head V Left
CDYIL	Condyle Internal Left	METAHIIR	Metatarsal Head II Right
SIAR	Scapula Inferior Angle Right	METAHIIL	Metatarsal Head II Left
SIAL	Scapula Inferior Angle Left	PHADISIIR	Phalanx Distal II Right
C7-T1	Spine Vertebrae C7-T1	PHADISIIL	Phalanx Distal II Left
T12-L1	Spine Vertebrae T12-L1	METAHIR	Metatarsal Head I Right
PSISR	Posterior Superior Iliac Right	METAHIL	Metatarsal Head I Left
PSISL	Posterior Superior Iliac Left	HEELR	Heel Right
GTROCR	Greater Trochanter Right	HEELL	Heel Left
GTROCL	Greater Trochanter Left		
L5-S1	Spine Vertebrae L5-S1		

For the hands, it was decided, to facilitate marker attachment and comfort, to use gloves equipped with markers. Tests were conducted to ensure that the trajectory of the markers is continuous and that it does not make many irregular zigzags that can come from the relative movement between the hand and the glove (Figure 3.24).

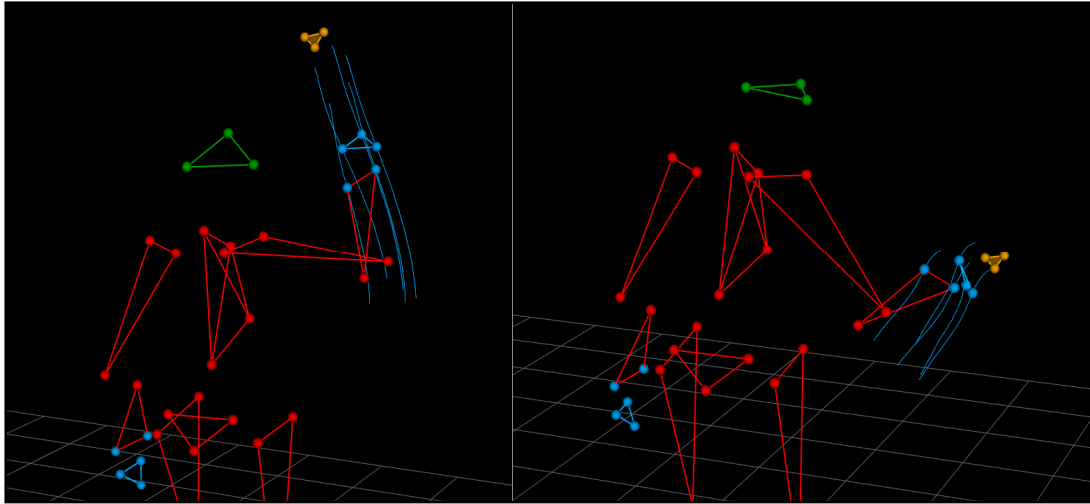


Figure 3.24 Verification of gloves with markers

These verifications have shown by the blue trajectories that the marker positions on the hands were continuous with their previous and the subsequent frames. Therefore, the use of such equipment was considered adequate for kinematic assessment. The final equipment was produced in three different sizes: 6/7, 7/8, and 8/9 to fit tightly different morphologies (Figure 3.25). Also, the markers are secured on the gloves using Velcro where the hand landmarks are located. This makes it possible to make small adjustments if needed to fit specific subjects.



Figure 3.25 Hand marker gloves

### 3.3.2 Data collection protocol

Experiments were conducted as presented in Table 3.9 with the right hand only. Prior to each experimental condition, at least one practice trial of the presented target configuration was required to ensure that the preferred posture was adopted and that the subject was comfortable achieving the required force levels. For the transverse offset trials, the target was placed at 25% of the subject's arm span in X+ direction. The obstacle was fixed at the waist level and hip-width minus 5 cm transverse to the center of the force platforms. These positions were chosen to account for subject variability in arm span as well as anthropometric measurements that could influence reach and physical limitations in the experimental setup.

Table 3.9 Pilot subject data collection protocol test conditions and number of trials analyzed

Task Height	Handle location	Condition	Number of trials analyzed
High	Centered	Reach	5
		Push	5
		Pull	5
		Tool	5
	Transverse offset	Reach	5
		Push	5
		Pull	5
		Tool	5

Experimental trials assessed in this study with the pilot subject were conducted with a target height of 0.1 m over stature (overhead), which was also studied by Hoffman et al. (2008), as it is a position where the stepping strategy is isolated since the use of other postural stability strategies is limited. At this height, subjects won't favor the use of the squatting strategy as it will not benefit the vertical reach of the target. An overhead target has been seen to create more balance perturbation when leaning in a side-by-side stance and limit the use of body mass to increase applied hand force (Haslegrave et al., 1997; Wilkinson et al., 1995).

Although overhead work isn't a preferred working posture, it remains present in some industrial sectors (Forde & Buchholz, 2004; Marchand & Giguère, 2010) and its study is important as it still represents a high impact risk from an ergonomic point of view (van der Molen, Foresti, Daams, Frings-Dresen & Kuijer, 2017; van Rijn, Huisstede, Koes & Burdorf, 2010). Forde and Buchholz (2004) found that workers in the construction ironwork sector spend between 6 and 21% of their work time with arm(s) in an overhead posture. Marchand and Giguère (2010) studied the upper limb risks related to the automotive maintenance sector, where overhead work was seen to represent 50 to 80% of work time for observations of screwing under the hood. In their study, a total of 252 different instances of overhead work lasting more than 30 seconds were observed for ten different maintenance tasks, where the average minimum time spent overhead was 7.5% of the work, whereas the average maximum time was 29.3% of the work.

The data collected with this reduced protocol was used in part to validate the performance of the experimental test bench and to verify elements of the full experimental protocol. A Matlab program was developed to process the raw data and to retrieve postural stability parameters such as support length, center of gravity position, and zero moment point position. The results obtained from the collected data are presented in CHAPTER 4.

### 3.3.2.1 Pilot subject

Experiments have been conducted on a pilot subject and the results presented in this thesis come from this subject. The characteristics of the subject are presented in Table 3.10.

Table 3.10 Pilot subject characteristics

<b>Sex</b>	→ Female
<b>Age</b>	→ 24
<b>Weight</b>	→ 67 (kg)
<b>Height</b>	→ 165 (cm)
<b>Arm span</b>	→ 167 (cm)
<b>Hip-width</b>	→ 31.12 (cm)
<b>Hand dominance</b>	→ Right

The subject was informed of the different risks, read the data collection protocol, and signed an information & consent form. Figure 3.26 displays the subject during the experiment with all passive reflective markers affixed.

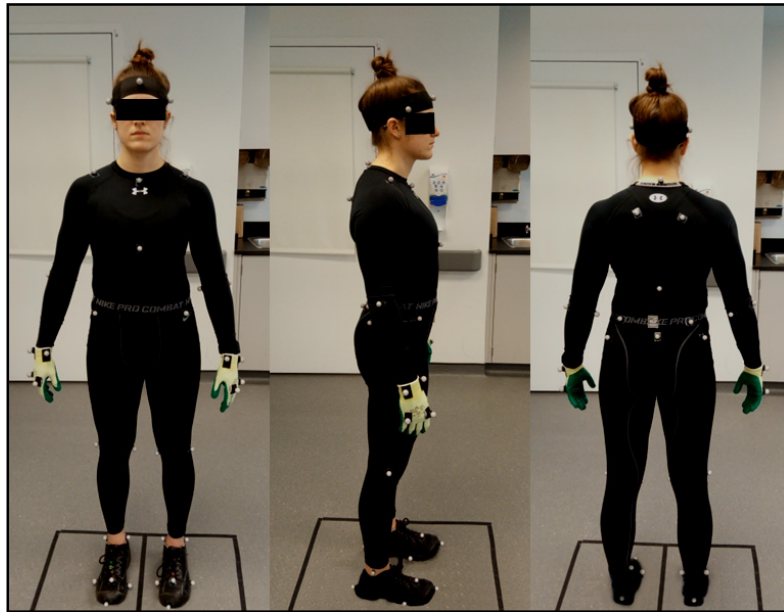


Figure 3.26 Passive reflective marker affixed on the pilot subject

### 3.3.3 Data preparation

All the collected data were processed before any results were extracted. However, the experimental data was not filtered during the data preparation so as not to filter trajectories, hand forces, and ground reaction forces before modeling the data.

First of all, the reflective markers used were labeled in each trial according to the body landmarks previously defined. Although an automated labeling program was used, a manual verification was accomplished to ensure every marker was well labeled, as the same marker nomenclature is used for the Matlab data processing program. When possible, gaps in trajectories of markers associated with rigid body segments were filled using the translations and rotations of the remaining marker cluster to fill gaps having a maximum size of 50 frames (Figure 3.27). Rigid body segments are segments that are composed of four or more markers. For gaps of 5 frames and less that were not linked to a rigid body, a Woltering quintic spline was used to fill the missing marker positions. All other gaps were left in their original state.

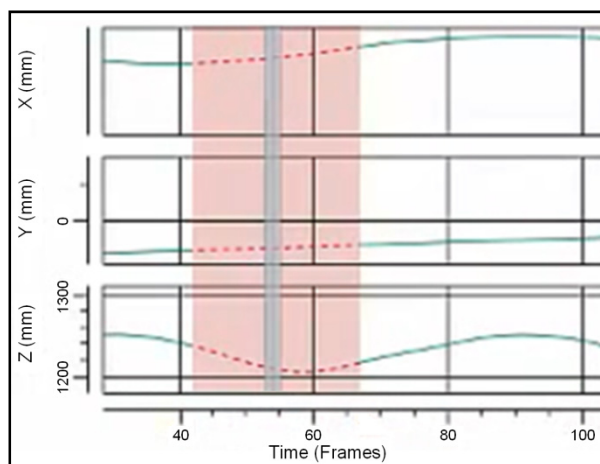


Figure 3.27 Gap filling

The above figure presents the filling of a gap, illustrated by the red zone, for a marker belonging to a rigid body segment.

Subsequently, once the raw data was processed, it was trimmed to separate the static five-second portion from the entire dynamic trial. The static phase represents the terminal posture adopted by the subject for the required task and condition. Figure 3.28 presents the three phases that are seen in every trial by viewing the variation of the center of mass in the vertical axis.

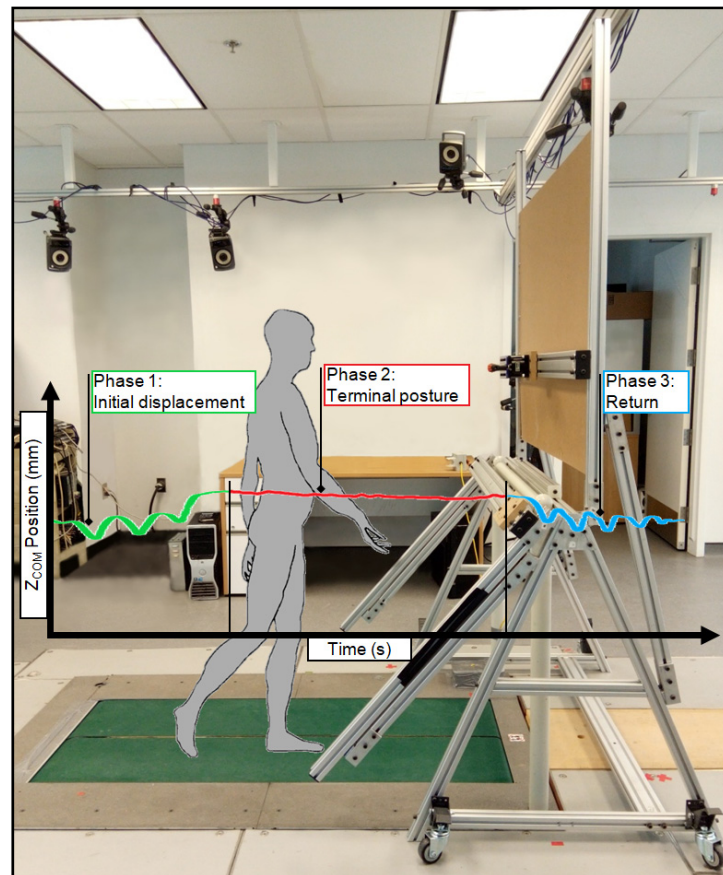


Figure 3.28 Three phases of a trial

The first phase is the initial displacement where the subject walks towards the task and uses the required strategies to reach the location of the target. The second phase is considered the static posture phase as it's the moment where the terminal posture is observed. At this stage, the target is reached and the hand conditions are achieved resulting in a noticeable stabilization of the subject's posture. The final phase captures the unloading of the hand condition and the return to the starting position.

### 3.3.3.1 Evaluated parameters

The parameters assessed in this thesis consist of postural stability parameters such as the support length and the BOS area. Other evaluated parameters are the COM, the COP, and the ZMP, which all need to be computed from the three-dimensional marker positions and/or end effectors (feet and hands) reaction forces. The parameters are assessed by projecting the vertical component (Z-axis) on the ground.

The body COM was calculated using the center of mass segmental distances presented by Dempster (1955). The individual adjusted segmental weight ratios presented by Clauser, McConville, and Young (1969) were used. These ratios were adjusted because the sum of Dempster's (1955) ratios equaled 97.7% of total body mass. The body COM was estimated using a 14 segment model presented in Table 3.11 (Head, Trunk, Upper Arms, Forearms, Hands, Thighs, Tibias, and Feet) arising from individual marker position and subject mass.

Table 3.11 Center of mass calculation points

<b>Segment</b>	<b>Human landmarks</b>
Head & Neck	C7-T1 and 1st rib/ Ear canal
Upper arms	Glenohumeral axis/ Elbow axis
Forearms	Elbow axis/ Ulnar Styloid
Hands	Wrist axis/ Knuckle II middle finger
Trunk	Greater trochanter/ glenohumeral joint
Thighs	Greater trochanter/ Femoral condyles
Tibias	Femoral condyles/ Medial malleolus
Feet	Lateral malleolus/ Head metatarsal II

The net center of pressure is calculated using the equations presented in subsection 2.1.1. As for the zero moment point, it is calculated using the equations presented in subsection 2.1.3. Validations of these computed parameters are presented in section 4.1.

### 3.3.3.2 Data modeling

Subject modeling was accomplished using the computing environment Matlab. The processing program gathered both the kinematic and the kinetic data whereupon it was trimmed according to the hand position relative to the target as well as the applied loads.

As seen in Figure 3.29, which represents the modeled data, there is a coordinate system for each force platform as well as one for the hand load cell that is located spatially by markers. These coordinate systems were positioned orthogonally with the global coordinate system. The red vertices and edges describe the left side of the subject, whereas the green ones describe the right side.

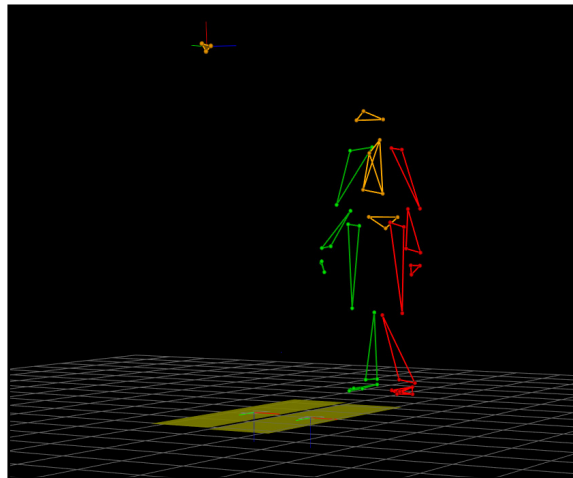


Figure 3.29 Data modeling representation

Screwdriver weight was neglected for the tool conditions because it was determined, in subsection 3.3.1.3, that pure torsion is applied directly in the center of the hand. Considering that a diagonal volar grip is used for this condition, the tool COM should almost coincide with the hand COM which is nearly situated in the line of action of the applied moment.

Before generating results, marker position data and kinetic data were subsequently low-pass filtered at specific cut-off frequencies (5-10 Hz, 4<sup>th</sup> order zero-lag Butterworth).

During a quiet standing trial, the subject should be perfectly aligned to the global coordinate system, but experimentally this isn't the case. The results presented with respect to the subject's position in the following CHAPTER 4 were calculated from the local coordinate system (e.g., anterior-posterior sway, high preference standing zone position, validation of net COP and COG position). Figure 3.30 illustrates how the ML and MR points are determined, thus how the support length is measured. ML and MR were found to be 40.8% of the subject's foot length from the heel with the pilot subject. The BOS includes the left and right foot regions in contact with the ground as it is defined by the external polygonal line of the points of contact between the feet with the ground.

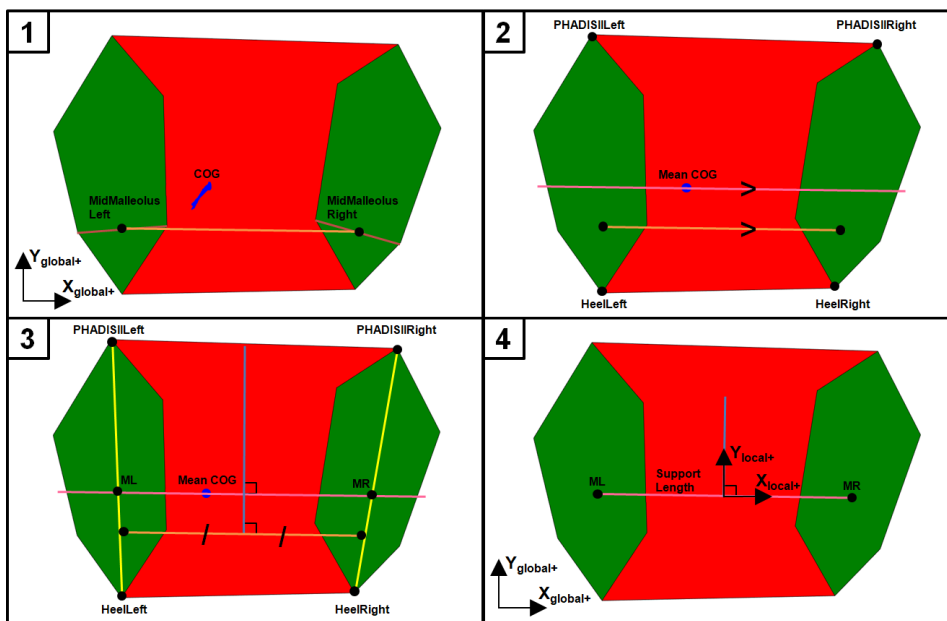


Figure 3.30 ML and MR points, support length, and local coordinate system definition during quiet standing

Ground contact regions of the feet were estimated by comparing the vertical position of the feet markers against their vertical positions in the reference quiet standing trial. If a marker was 3 mm above the reference position, the part of the left or right foot was considered raised. The 3 mm threshold was set to account for possible variations (e.g., foot soft tissue deformation) (Mochimaru, Kouchi & Dohi, 2000).

The lead foot distance from the target and the orientation of the support length with respect to the global transverse axis were evaluated as presented in Figure 3.31. The lead foot distance from the target was calculated from the difference between the lead foot support length ML or MR point against the target position (i.e., load cell). This is illustrated in Figure 3.31 (a) and (c). For the centered reach trials the distance was calculated from the local coordinate system of the support length as feet were predominantly side-by-side, refer to Figure 3.31 (b). An angle of  $0^\circ$  indicates the subject is oriented square to the target with their lower limbs predominantly side-by-side.

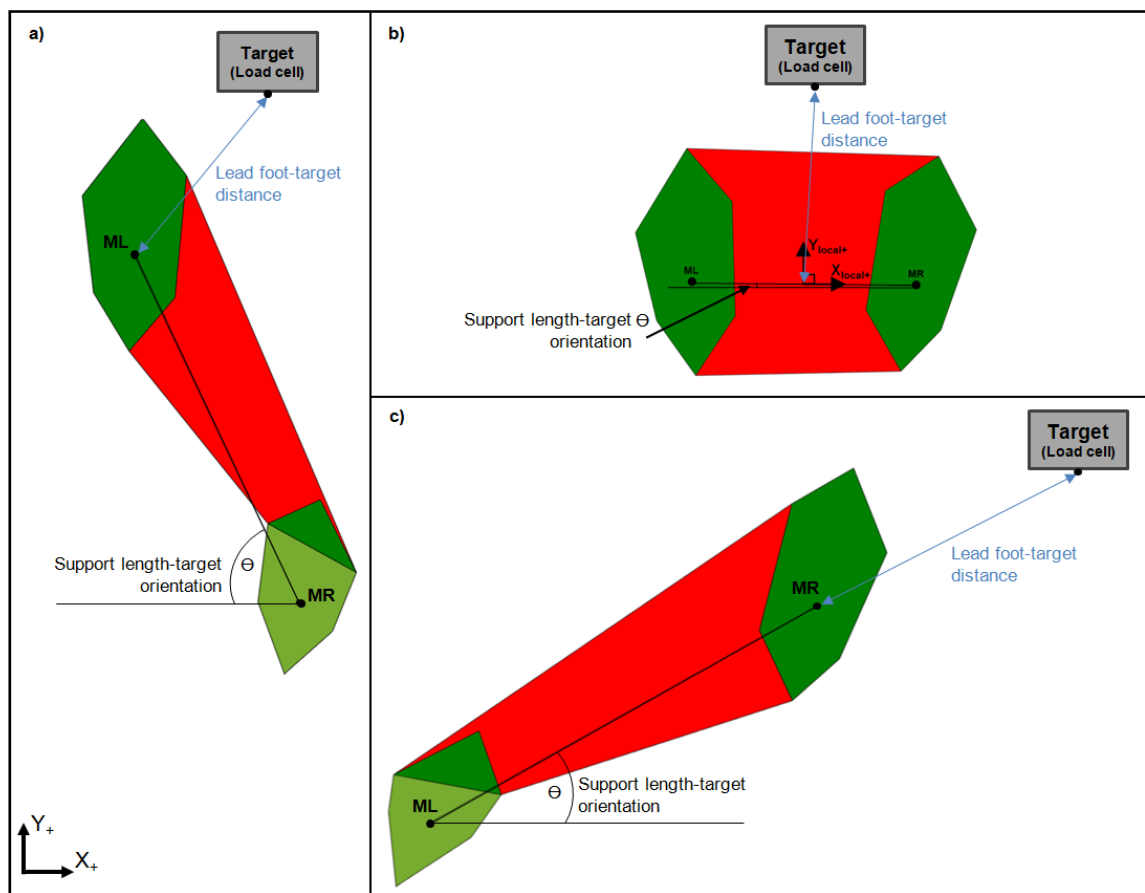


Figure 3.31 Lead foot-target distance and support length-target orientation definition



## CHAPTER 4

### RESULTS & ANALYSIS

This chapter will present the different results as well as an analysis of these results obtained with the pilot subject from the previously described methodology. Verifications and validations of the calculated and computed parameters are first presented.

#### 4.1 Data verification & validation

A visual verification was first accomplished across all the trials to ensure repeatability could exist for the adopted postures. Table 4.1 groups the trials for the task high centered.

Table 4.1 Visual repeatability representation task high centered

Task High Centered					
Condition	Trial N° 1	Trial N° 2	Trial N° 3	Trial N° 4	Trial N° 5
Reach					
Push					
Pull					
Tool					

It is evident that the subject is very repeatable in terms of the intra-condition postural strategy used. This repeatability can be quantitatively viewed by evaluating the variation of the vertical component for the whole body center of mass. The following graphic (Figure 4.1) illustrates this repeatability which varies less than 1 cm during the terminal posture phase. A similar pattern can be viewed across the five presented trials throughout the three phases.

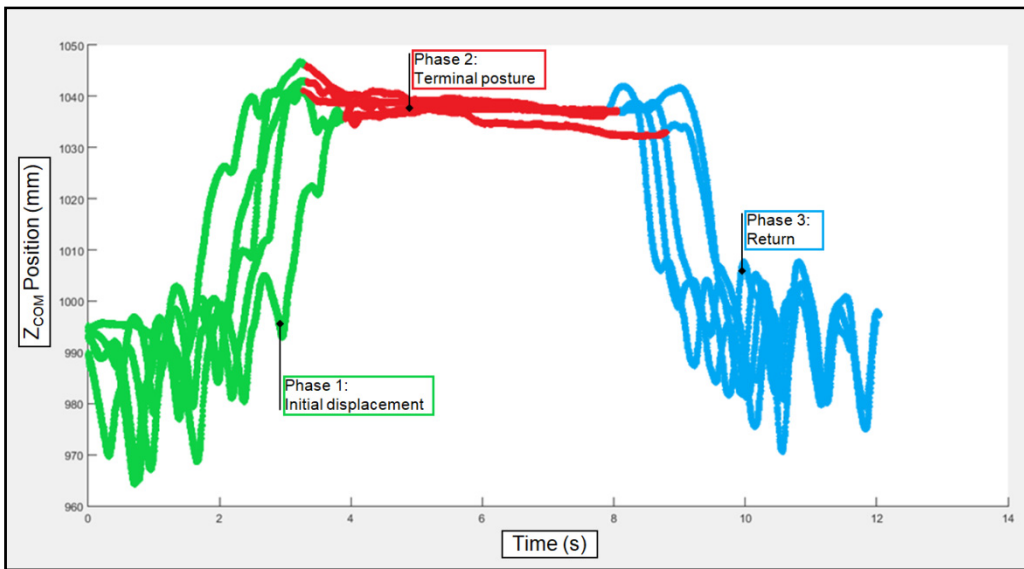


Figure 4.1 Repeatability over 5 trials  
(Pushing a Centered High task)

Because the center of mass and the zero moment point are computed parameters and not measured points, a validation of these parameters was completed. The first validation was conducted by comparing the NetCOP,  $COP_C$  and  $COP_V$  obtained from equations (2.1), (2.2), and (2.3), with the left and right force platform center of pressures.

Figure 4.2 plots the computed NetCOP,  $COP_L$ , and  $COP_R$  during a 5-second quiet standing trial with feet side-by-side where the subject was asked to position herself in front of the target at a reaching distance. The plot shows a correlation between the three parameters, with the net COP almost in the middle, which is consistent with what is presented in the study of Winter et al. (1993). The entering slope (0-0.5 s) represents the approach to the static terminal posture, whereas the exiting slope (4.7-5 s) represents the departure back to the start position.

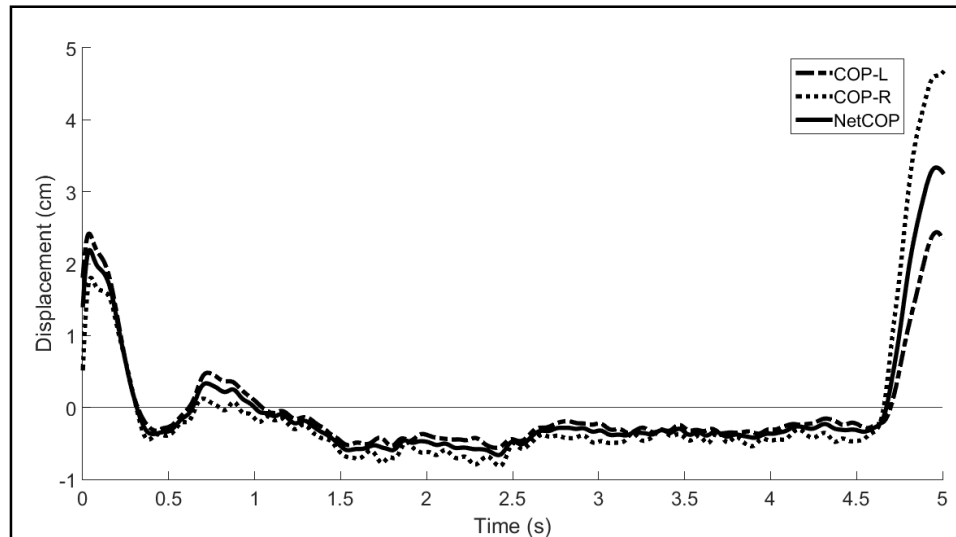


Figure 4.2 NetCOP,  $COP_L$ , and  $COP_R$  in the anterior-posterior direction  
(*Quiet side-by-side standing*)

Figure 4.3 and Figure 4.4 plot the contributions from body adjustments to maintain the static posture. When viewing Figure 4.3, it is observed that the majority of the net COP changes in the anterior-posterior direction are almost entirely accomplished from ankle muscle control ( $COP_c$ ) whereas the vertical loading and unloading component ( $COP_v$ ) is virtually null.

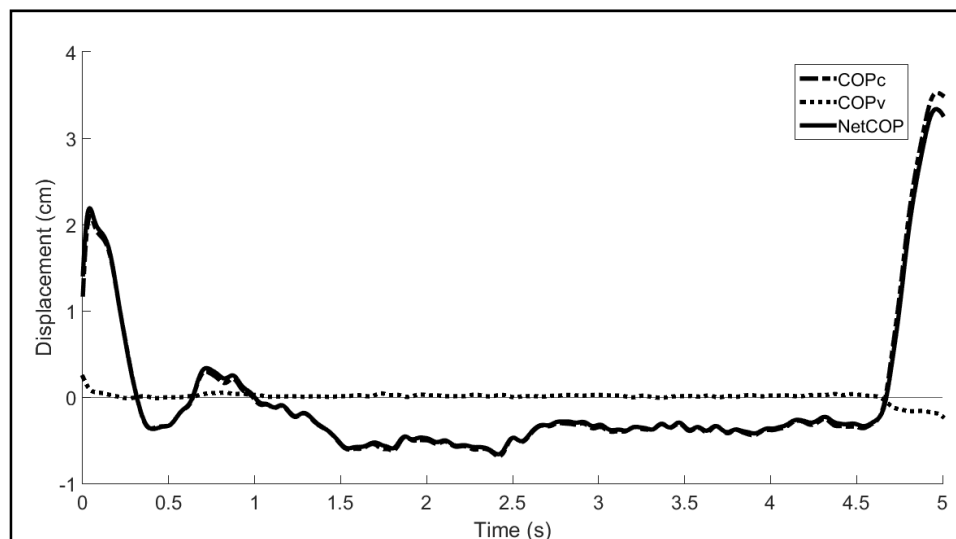


Figure 4.3 NetCOP,  $COP_c$ , and  $COP_v$  in the anterior-posterior direction  
(*Quiet side-by-side standing*)

However, when viewing the net COP changes in the transverse direction (Figure 4.4), a different strategy is present. In fact, in this direction, there is almost no contribution from ankle muscle control ( $COP_C$ ). Instead, the loading and unloading component ( $COP_V$ ) strongly contributes to the changes in the net COP.

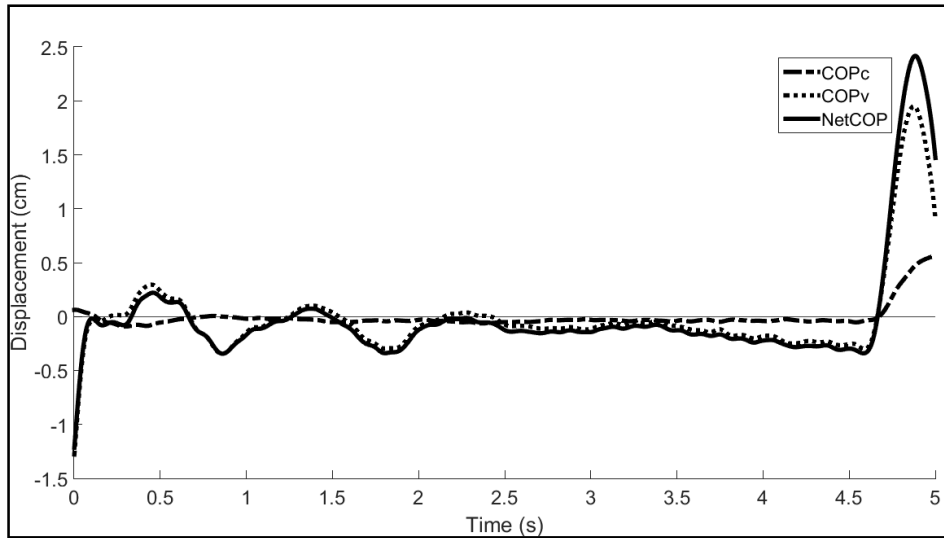


Figure 4.4 NetCOP,  $COP_C$ , and  $COP_V$  in the transverse direction  
(*Quiet side-by-side standing*)

The results of the contributions from the ankle muscles ( $COP_C$ ) and due to loading and unloading of each limb ( $COP_V$ ) are also in line with what has been seen in the literature (Winter et al., 1993). The contribution of each parameter is explained by the ankle axis, assuming both ankle joints are aligned, is almost perpendicular to the anterior-posterior axis, hence in this direction, it is easier to control about this joint. However, in the transverse direction, it is difficult to use the ankle invertor and evertor muscles to control stability. That said this can easily be done by loading and unloading each limb which could be the cause of the hip abductor and adductor muscles variations (Winter et al., 1993).

The second validation is verifying the computed center of gravity (COG) which is the vertical projection of the calculated center of mass (COM). Figure 4.5 plots the COG and the net COP for the same quiet standing trial. For this new plot, because side-by-side standing is

defined by both ankle joints being along the same axis, the ankle joint axis was approximated by a line passing through the middle of the external and internal malleolus for the left and the right foot.

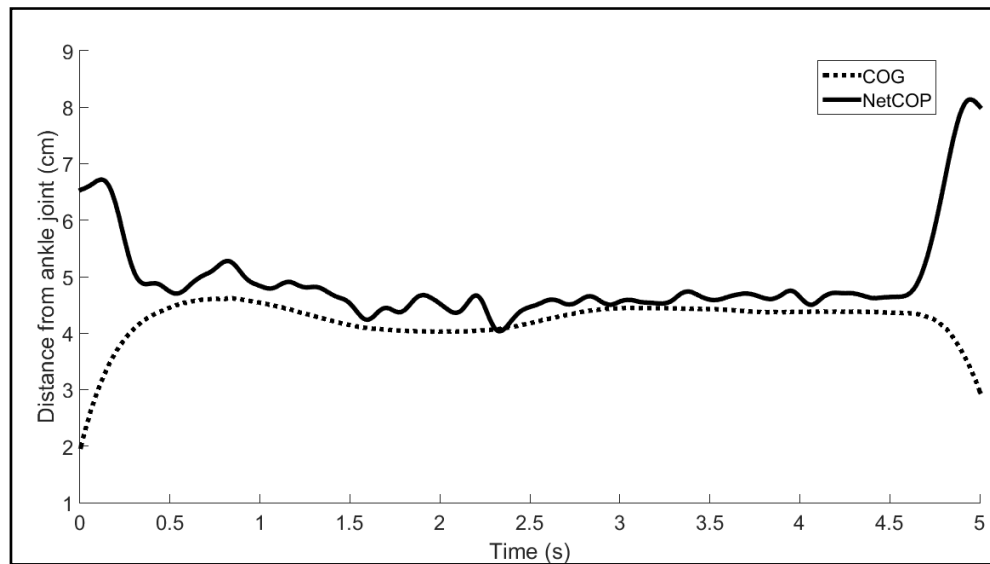


Figure 4.5 COG and NetCOP fluctuations in the anterior-posterior direction (*Quiet side-by-side standing*)

Several fundamental elements can be extracted from this plot. Foremost, it is apparent that the subject was able to remain very stable throughout this trial. In fact, the total anterior-posterior sway of the net COP during the terminal stable posture (0.5-4.7 s) is only 1.25 cm, which is consistent with the most stable proportion for subjects of the same age group in the study of Holbein-Jenny et al. (2007).

During quiet standing, the whole body can be assumed as an inverted pendulum, rotating about the ankle joint (Winter et al., 1990). As the subject is approaching the terminal posture, the net COP shifts anterior of the COG to decrease forward-leaning velocity which helps stabilize the body. The angular acceleration of the body will then reverse, moving the net COP back towards the COG (0-0.5 s) (Winter et al., 1990). The mean net COP should be equal to the mean COG over an extended period. Thus, when the net COP and the COG are close, angular acceleration will switch from forward to backward oscillating the net COP and

maintaining body stability. Figure 4.5 also shows that the net COP displacement is in accordance with the observations of Stapley et al. (2000) that characterized its displacement as a three-phase trajectory sequence in order to achieve a terminal position.

For this trial, the difference between mean net COP and mean COG during the terminal stable posture (0.5-4.7 s) is 0.31 cm (Figure 4.6). The mean COG also respects the condition of being situated 2-5 cm in front of the ankle joint during quiet standing (Badler et al., 1993).

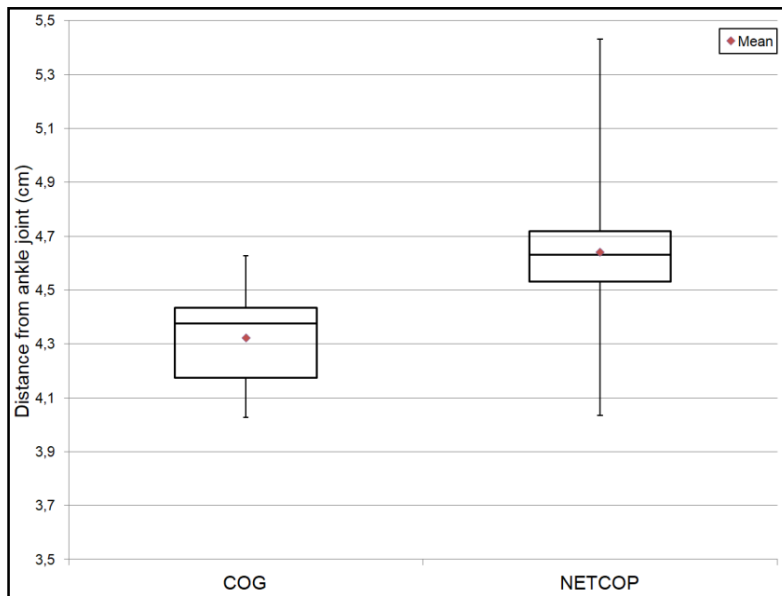


Figure 4.6 Comparison between the COG and the net COP anterior-posterior distance from the ankle joint

With the computed net COP and COG validated, the third and final validation consisted of verifying the calculated zero moment point (ZMP) given from equation (2.5). Ideally, the ZMP concurs with the COG in the absence of external forces or moments and nearly corresponds to the net COP when external loads are present during balanced gait. The validation was conducted with the previous quiet standing trial along with a pushing high centered task trial. The projection of the measured parameters from these trials is shown in Figure 4.7 and the absolute error about the references is presented in Table 4.2.

Table 4.2 Summary of feet positioning and parameters projection

Trial	Direction	ZMP	COG	net COP	Absolute error
Quiet standing	Anterior-posterior	46.42 cm	46.39 cm	N/A	0.03 cm
	Transverse	0.57 cm	0.59 cm	N/A	0.02 cm
Pushing	Anterior-posterior	34.71 cm	N/A	35.00 cm	0.29 cm
	Transverse	0.89 cm	N/A	0.76 cm	0.13 cm

It can be observed for the pushing trial that the COG position is not shown as forces are present and the interpretations of the error between the COG and the ZMP are not relevant.

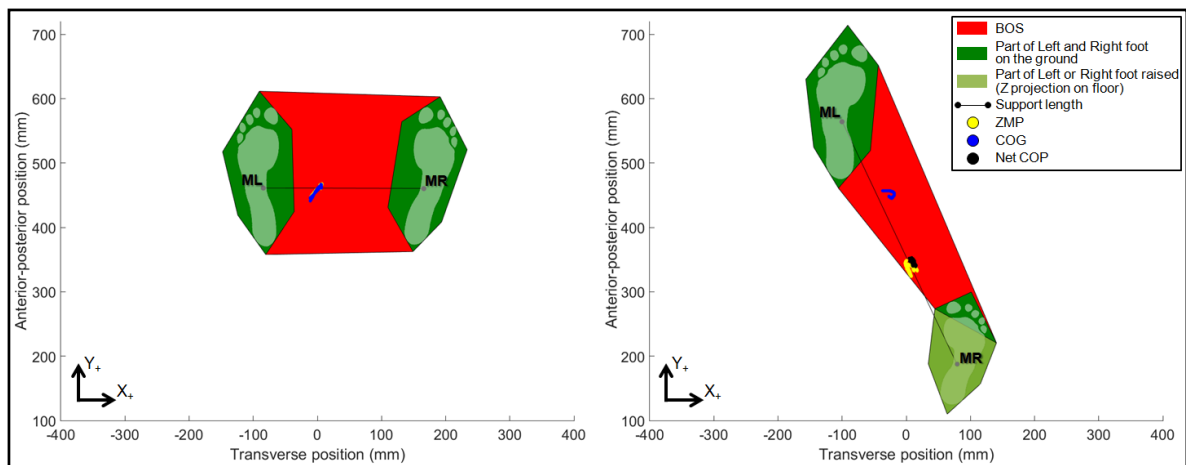


Figure 4.7 Quiet side-by-side standing and pushing trial feet positioning projection

From these trials, it is evident that the calculated ZMP respects the correlations with the computed COG and the net COP. Indeed, when referring to equation (2.5), when no forces or moments are present ( $M_b$  and  $F_b$  are zero),  $ZMP_x$  equals  $X_{COG}$  and  $ZMP_y$  equals  $Y_{COG}$ . When forces and moments are present in a balanced gait, the ZMP coincides with the net COP as it represents the acting point on the contact surface for the reaction force vector (Vukobratović & Borovac, 2004).

The total maximum error found by the calculated zero moment point validation was a true position error of 0.64 cm, as defined by equation (4.1), with  $net\ COP_{A/P}$  and  $ZMP_{A/P}$  along with  $COP_{Trans}$  and  $ZMP_{Trans}$  corresponding respectively to the net COP and ZMP position in the anterior-posterior and transverse directions.

$$\text{True position error} = 2 * \sqrt{(\text{net COP}_{A/P} - \text{ZMP}_{A/P})^2 + (\text{net COP}_{\text{Trans}} - \text{ZMP}_{\text{Trans}})^2} \quad (4.1)$$

The measured error is considerably less than the errors Wilkinson et al. (1995) stated of 39 mm for the COG and 38 mm for the COP. In their study, the COP was calculated from the handle reaction force vector and the extreme posture assumptions made when calculating the COG from 22 digitized points and anthropometric tables, which generated these positioning errors. Whereas in this thesis, the net COP was directly measured with the force platforms and the COG was calculated using twice as many anatomical reference points.

Succinctly, it was presented in this subsection that the computed center of pressure, the computed center of gravity as well as the calculated zero moment point are accomplished adequately, hence accurate results can be collected.

## 4.2 Results from experiments

Of the forty trials that were analyzed, one transverse offset-reach trial and one transverse offset-pull trial were removed from the analysis because it was seen on the digital video camera that the subject braced against the obstacle which in terms alters the assessment that could have been done. Thereby, a total of 38 trials were used for the pilot subject analysis.

The visual repeatability representation showed limited forward and backward leaning and presented limited use of the hip strategy (squatting) as the target would have been more difficult to reach. Both observations support the use of the overhead target for isolating the stepping strategy.

When comparing the net COP and COG distances from the ankle joint over the 5 centered reaching trials, where no loads are applied, they are found to be closely correlated, as illustrated in Figure 4.8, with a correlation coefficient of 0.895 ( $p < 0.001$ ). This indicates a strong relationship between the two variables and that the COG is well calculated.

The trendline represents the linear behavior of the data. The adjusted R-squared statistics between these two variables is 80.14%. The correlation coefficient represents the linear relationship between the net COP and the COG, whereas the adjusted R-squared represents the percentage of variations in the net COP that are predictable from the COG changes.

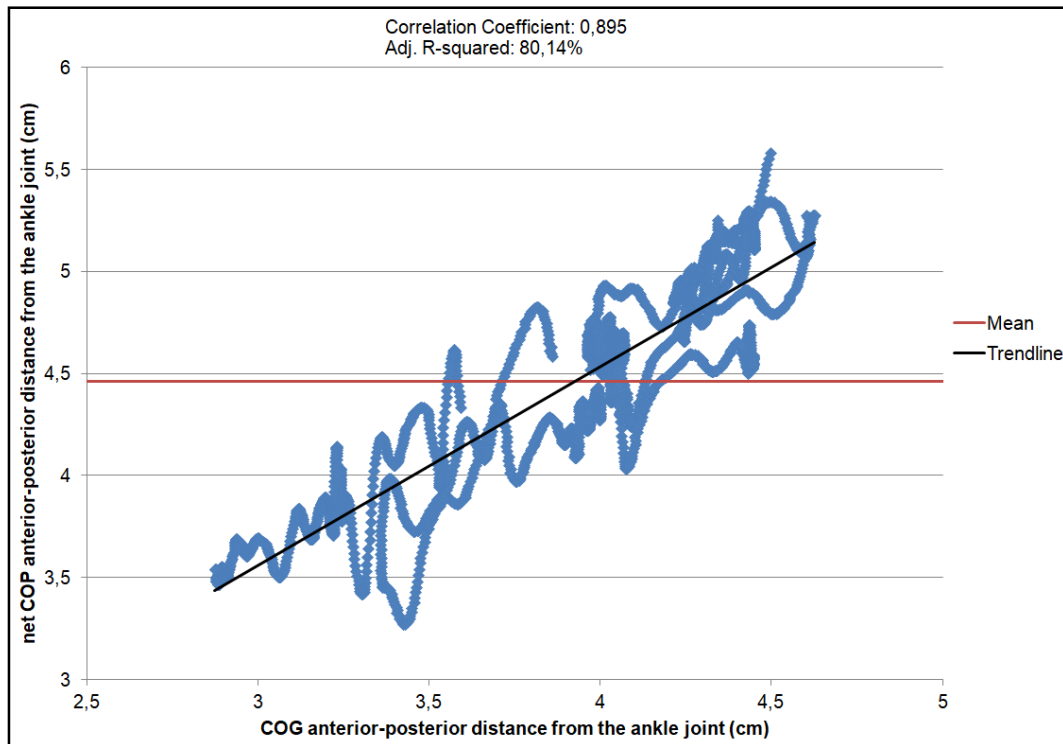


Figure 4.8 COG and net COP correlation distribution

### 4.3 ZMP projection

The zero moment point projection is defined by the  $D_2$  ratio on the support length. External forces and moments influence the position of the ZMP projection as loads applied to the hand will displace the ZMP in the direction of the reaction force or moment application.

#### 4.3.1 Results

After processing the raw data, parameters were obtained as illustrated in Figure 4.9. The  $D_2$  ratio is a normalized ratio between 0.00 and 1.00 from the root foot (trailing leg), specified by the square projection ( $D_2$ ) of the mean 5-second static posture ZMP position ( $ZMP_X$  and  $ZMP_Y$ ) on the support length (SL). This is calculated using equation (4.2). Consequently, if the  $D_2$  ratio is superior to 1.00 the ZMP projection is situated outside of the support length, which can be seen in Figure 4.13 for the centered pull condition.

$$D_2 \text{ratio} = \frac{D_2}{SL} ; \text{ where } SL(\text{support length}) = D_1 + D_2 \quad (4.2)$$

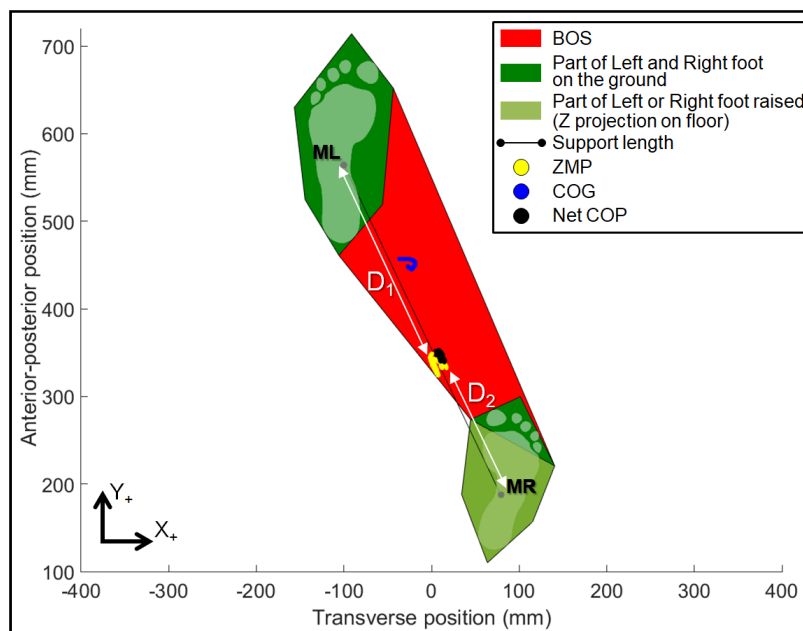


Figure 4.9 Processed trial parameters (XY plane projection) for a pushing centered trial

Individual trial statistics of the calculated normalized D<sub>2</sub> ratio, the support length magnitude, and the occurrence of the dominant right foot being the lead foot are presented in Table 4.3. This data is also presented graphically in Figure 4.10 for each condition.

Table 4.3 Mean normalized (and standard deviations) D<sub>2</sub> ratio, support length magnitude and lead foot occurrence across trials

Handle location	Condition	D <sub>2</sub> ratio	Support length magnitude (mm)	Occurrence of right foot being lead foot
Centered	Reach	0.65 (0.04)	256.79 (10.15)	1/5
	Push	0.42 (0.04)	425.47 (34.98)	0/5
	Pull	1.11 (0.06)	470.62 (32.68)	0/5
	Tool	0.88 (0.05)	356.30 (30.35)	0/5
Transverse offset	Reach	0.40 (0.05)	317.38 (45.87)	4/4
	Push	0.59 (0.06)	418.32 (21.64)	5/5
	Pull	0.95 (0.04)	403.59 (8.88)	4/4
	Tool	0.28 (0.06)	325.30 (13.89)	5/5

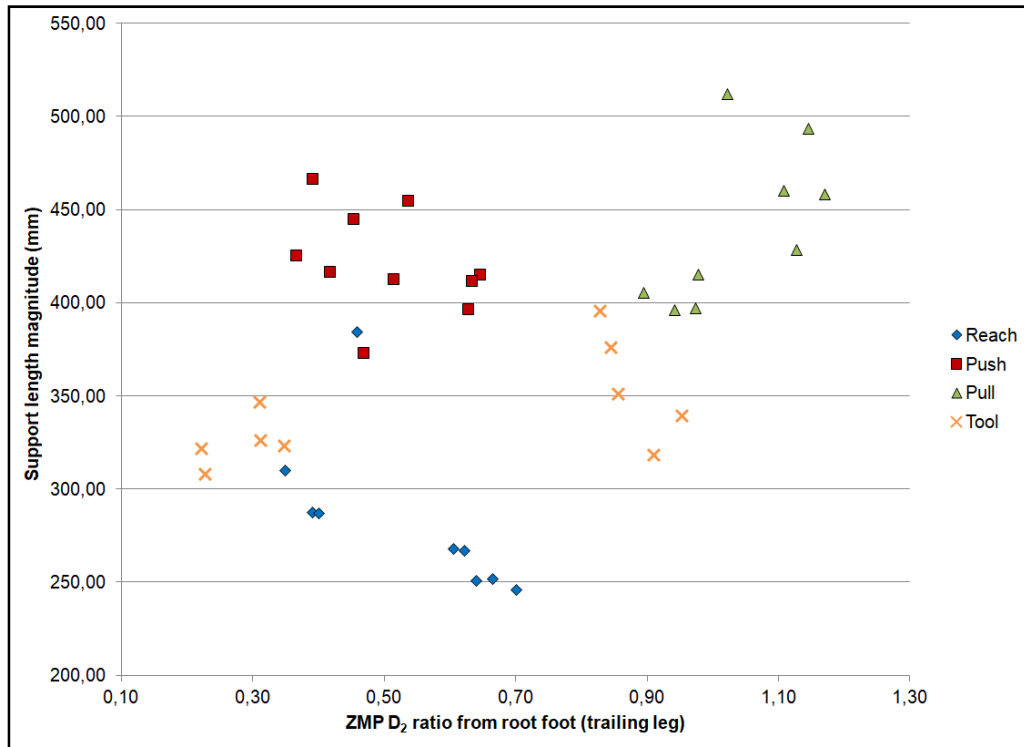


Figure 4.10 Scatter plot of Support length magnitude with respect to the ZMP D<sub>2</sub> ratio from the root foot grouped by conditions

When viewing the data by handle location (Figure 4.11), a squared-X (quadratic) model can be fitted. This type of regression model was determined appropriate as it can represent an inverted bell where the summit indicates the smallest support length and the extremities tend towards the largest useable support length. Figure 4.11 illustrates the proposed single factor regression fitted model and the calculated statistics.

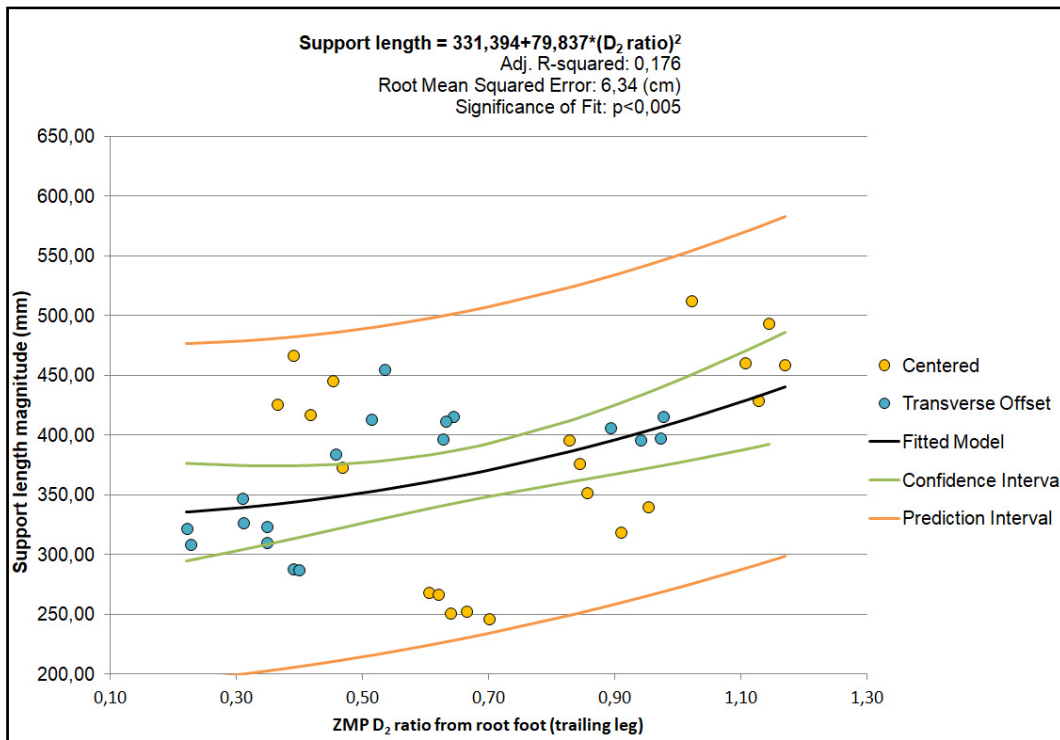


Figure 4.11 Scatter plot of Support length magnitude with respect to the ZMP D<sub>2</sub> ratio from the root foot grouped by handle location. Single-factor regression fitted model displayed with confidence and prediction intervals

The confidence interval is a 95% probability that the true best-fitted regression model lies within the interval. The prediction interval is an estimated interval based on the previous observations where 95% of the support length magnitude to be estimated from the ZMP D<sub>2</sub> ratio measurements will be within the interval about the fitted regression model.

The Root Mean Squared Error (RMSE) is calculated using equation (4.3), with  $X_{obs}$  corresponding to the observed ZMP  $D_2$  ratio,  $X_{model}$  corresponding to the estimated ZMP  $D_2$  ratio, and  $n$  is the number of trials. For this model,  $n$  is equal to 38. This error represents the average absolute difference between the observed values and the estimated values.

$$RMSE = \sqrt{\frac{\sum_{i=1}^n (X_{obs,i} - X_{model,i})^2}{n}} \quad (4.3)$$

When verifying the relevance of the fit by evaluating the residuals of the proposed model (Figure 4.12), it can be observed that the regression model is well adapted to the evaluated data. The plot shows that the variance of the residuals is centered around 0.00 as well as being constant. Also, no outliers are present outside of the 95% confidence interval and there doesn't seem to be any drift, which supports the relevance of the proposed model.

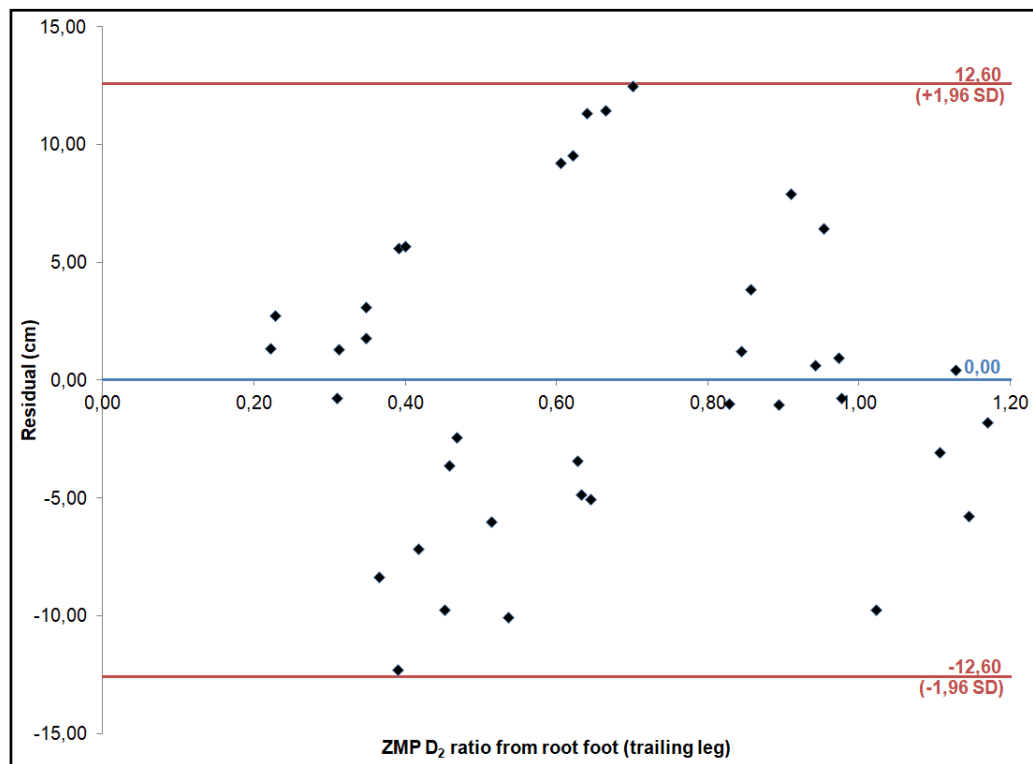


Figure 4.12 Plot of residuals and limits with a confidence interval of 95%

### 4.3.2 Analysis

First of all, the presented model gives respectable results compared to what is seen in the literature. Dijkstra and Gutierrez-Farewik (2015) found a total anterior-posterior and transverse relative RMSE (rRMSE) of  $22.5 \pm 6.02\%$  for their ZMP model to predict the ground reaction forces. Where rRMSE is the normalized RMSE to the average amplitudes of the observed trials and the predicted model.

Wagner, Reed, and Chaffin (2005) found a total anterior-posterior and transverse RMSE of 6.47 cm for the predicted COG and 11.11 cm for the predicted trailing foot position, with a varying adjusted  $R^2$  ( $0.16 < R^2 < 0.67$ ) according to the different independent variables (stature, load carry hand(s), pickup height) that had a significant effect ( $p < 0.05$ ). Wagner et al. (2010) also developed a regression model for foot placement using  $p < 0.01$  for variable effect along with requiring an adjusted  $R^2$  greater than 0.1 as criteria of significance. Their adjusted  $R^2$  also varied ( $0.19 < R^2 < 0.57$ ) depending on the variables used that had a significant effect.

Although the model in this thesis can only indicate that 17.6% of the variability in the support length is due to the ZMP  $D_2$  ratio, the model was found to be adequate according to previous criteria of significance presented. All the more, only one independent variable is used for this model. To vary the support length, it can be hypothesized that one of the following variables could be the cause: tool weight, task height or reach distance, subject anatomical differences (e.g., lower limb length), or hand dominance.

A statistically significant relationship was found between the support length magnitude and the ZMP  $D_2$  ratio from the root foot ( $p = 0.005$ ). The RMSE of this model is only  $6.34 \pm 3.09$  cm and the rRMSE is  $23.8 \pm 11.6\%$  ( $p < 0.05$ ) which is comparable to results found in previous studies (Dijkstra & Gutierrez-Farewik, 2015; Wagner et al., 2005, 2010).

The contralateral lead foot was seen across all load required conditions for the centered trials. This observation is consistent with the other studies that found this behavior as being the most frequent observation (Wagner et al., 2010). In this thesis, imposing a transverse obstacle allowed us to see that spatial constraint might have an opposite effect on this conclusion as it was seen across all trials with the obstacle that the ipsilateral lead foot was the preferred behavior.

Finally, the mean support length magnitude appeared smaller for the handle location with a transverse offset which indicates hand-target reach might have been favored over stability. It is notable in Figure 4.10 that the push and pull conditions both seem to be relatively clustered together for both handle location. Which is not the case for the reach or the tool conditions. This could be due to the low force application, but the fact that the reaching requirements are still present. Thus, the subject maintained a similar support length, but the applied hand torque varied the ZMP position. The support length magnitude difference between the reach and the tool condition for the transverse offset location was only 2.5%. This possibly indicates that the subject only adjusted their feet orientation to overcome applied hand moments, while maintaining the same support length.

## 4.4 Feet adjustments

The following subsection presents results covering postural changes accomplished from feet adjustments, which can potentially explain variations in the stepping strategy.

### 4.4.1 Results

When evaluating the lead foot distance of the respective support length point (ML or MR) from the target (Table 4.4), a statistically significant relationship was found with the support length ( $p < 0.001$ ). The strength of the correlation coefficient between both variables was moderately strong ( $R = -0.64$ ). The negative correlation indicates that the closer the lead foot is to the target, the larger the support length will be. Thereby, it is deduced that the further the subject is from the target, the smaller a step will be taken. This distance was calculated from the lead foot ML or MR point against the target position as presented in section 3.3.3.2. For the centered reach trials the distance was calculated from the local coordinate system of the support length as feet were predominantly side-by-side, as illustrated in Figure 3.31 (b). Table 4.4 presents these results as well as the orientation of the support length with respect to the global transverse axis, refer to Figure 3.31. An angle of  $0^\circ$  indicates the subject was oriented square to the target with lower limbs predominantly side-by-side.

Table 4.4 Mean (and standard deviations) lead foot-target distance and Support length-target orientation by condition

Handle location	Condition	Lead foot-target distance (mm) (ML/MR to target)	Support length-target orientation ( $^\circ$ )
Centered	Reach <sup>†</sup>	328.49 (22.69)	2.87 (4.21)
	Push	282.48 (24.86)	61.11 (3.18)
	Pull	174.50 (16.14)	65.90 (4.87)
	Tool	276.19 (8.65)	51.31 (6.20)
Transverse offset	Reach	310.08 (13.87)	24.77 (7.50)
	Push	313.42 (22.31)	21.55 (13.19)
	Pull	328.54 (16.00)	12.53 (2.84)
	Tool	329.39 (17.13)	3.66 (9.57)

<sup>†</sup> Calculated from the middle of support length to target.

The orientation of the support length with respect to the target transverse axis is considerably different ( $p < 0.05$ ) for both handle locations across all paired conditions. This displays that the subject was adopting a predominantly anterior-posterior step for the centered handle location and a predominantly transverse step for the transverse offset handle location.

Figure 4.13 presents the mean feet placement, the mean projected ZMP, and the mean projected COG on the support length for each condition and handle location are also illustrated. As hypothesized, the ipsilateral and contralateral legs moved accordingly to ensure the ZMP displacement remained collinear to the support length in the most stable direction. Across conditions requiring load exertions, the  $D_2$  ratio varied in the direction of the hand reaction load. The ZMP and COG nearly coincide for the reach condition as no external force is present. The ZMP and COG nearly coincide for the reach condition as no external force is present.

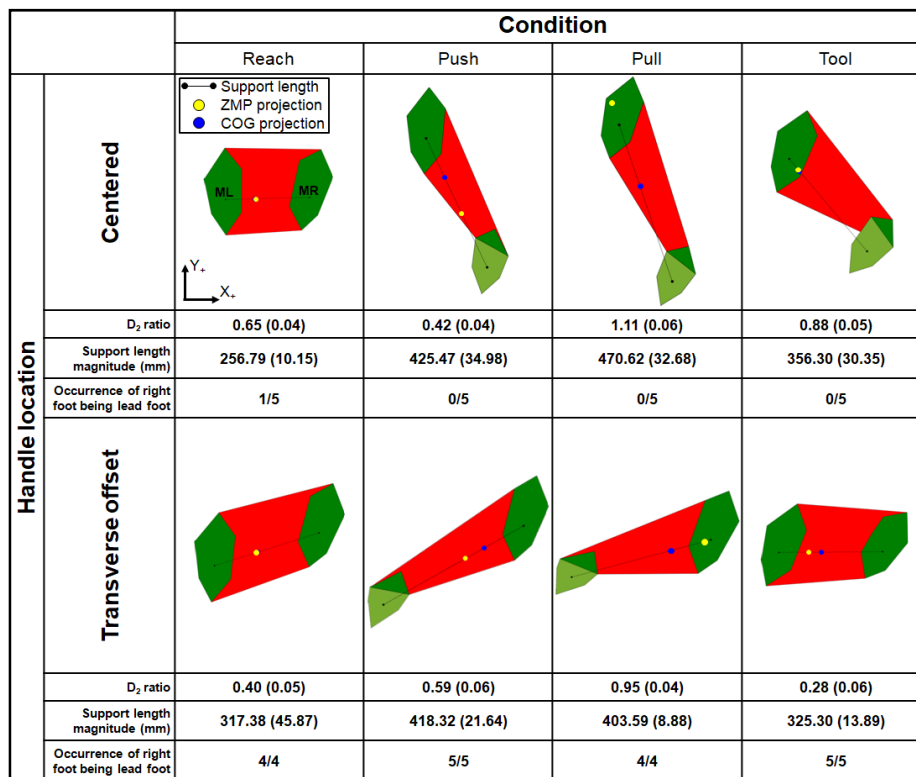


Figure 4.13 ZMP projection in yellow and COG projection blue on the support length between ML and MR. Mean normalized (and standard deviations)  $D_2$  ratio, support length magnitude, and lead foot occurrence across trials. Reference quiet standing trial support length of 250.73 mm

#### 4.4.2 Analysis

With respect to the lead foot position, it was presented that the further the subject is positioned from the target, the smaller of a support length will be adopted, representing a smaller stepping, presumably to achieve other objectives such as maximizing hand-target reach. It was presented regarding the support length orientation that for the transverse offset handle location, a less anterior-posterior foot orientation was adopted, likely indicating transverse balance was preferred for this location. In contrast, during the centered push and pull trials, a larger anterior-posterior step was used conceivably to maximize applied hand forces and stability. These observations agree with Hoffman et al. (2008), who stated that when possible subjects will prefer to position their body in line with the applied force direction to maximize applied forces by limiting lateral forces.

During the centered task, since the subject was able to center herself with the applied force direction, she preferred to maximize her stability by expanding the BOS in the same direction as the force. In regards to the transverse offset location, because the obstacle prevented the subject from positioning herself in line with the force, a specific more transverse foot placement strategy was used to develop sufficient torque at the foot base to compensate for the moment created from the hand force and the out of plane distance. This observation is consistent with Wilkinson et al. (1995), where out of sagittal plane forces required the production of feet moments to ensure stability when standing with feet centered to the target.

The orientation of the support length during the tool transverse offset trials suggest foot placement were such as to only counter applied hand moments, with a difference of 85.2% when compared to the reach transverse offset trials. Little anterior-posterior stepping is seen compared to transverse stepping, which supports what was seen when comparing the support length magnitudes of the reach and the tool conditions. Experimental trials also indicate that the projected COG is not predominantly located at a half distance (0.50) between feet. The mean COG for each trial was found in a range varying from 0.40 to 0.86 normalized to the support length from the root foot.

## 4.5 Postural stability control

In this subsection of the results, postural control by the pilot subject with respect to what has been seen in the literature will be evaluated from the postural sway and the net COP high preference zone as presented by Popovic et al. (2000) during side-by-side standing.

### 4.5.1 Results

When standing without any perturbations, humans continuously compensate for small variations to keep the center of gravity stable by naturally swaying. In regards to the sway for the quiet standing trial, the sway of the net COP during the terminal stable posture with respect to the local coordinate system was only 1.25 cm in the anterior-posterior direction and 0.52 cm in the transverse direction. Across the 5 reaching trials for the centered handle location, the mean anterior-posterior, and transverse sway were respectively  $1.37 \pm 0.15$  cm and  $0.75 \pm 0.23$  cm.

These results are consistent with the most stable proportion for subjects of the same age group in the study of Holbein-Jenny et al. (2007) where the mean anterior-posterior sway was found to be  $2.3 \pm 0.6$  cm and  $1.0 \pm 0.3$  cm in the transverse direction. Because feet orientation and trunk rotation influence the direction of the true local coordinate system during postures other than standing with feet side-by-side, it was determined to use the resultant total postural sway. When comparing the sway during the centered handle location against the transverse offset handle location, it was observed that the obstacle increased the instability of the subject across all the conditions (Table 4.5). The subtotal sway grouped by each handle location displays a 60% higher sway for the transverse offset location.

Table 4.5 Mean (and standard deviations) of the total postural sway by condition

Handle location	Condition	Total Anterior-posterior & Transverse postural sway (cm)
Centered	Reach	1.57 (0.22)
	Push	2.07 (0.45)
	Pull	2.89 (0.44)
	Tool	1.72 (0.52)
	<b>Subtotal</b>	<b>2.06 (0.65)</b>
Transverse offset	Reach	1.82 (0.52)
	Push	3.27 (1.18)
	Pull	6.20 (1.67)
	Tool	2.22 (0.70)
	<b>Subtotal</b>	<b>3.31 (1.95)</b>

During the quiet standing trial, the mean anterior-posterior net COP position was measured at 43.1% of the subject's foot length. Although this value varies from the center established at 47.0% by Popovic et al. (2000), the high preference zone center measured across their 10 subjects varied in a range between 36.6% and 77.7%. Considering all centered handle location reach trials, this high preference zone center is found to be  $42.9 \pm 2.4\%$  of the subject's foot length.

The position of the mean ZMP, which remains within the BOS across all the trials (Figure 4.14), indicates that the subject adopted stable postures to execute each condition as she is considered dynamically stable (Vukobratović & Borovac, 2004). The adopted posture is considered less stable when the ZMP is close to the edges of the BOS.

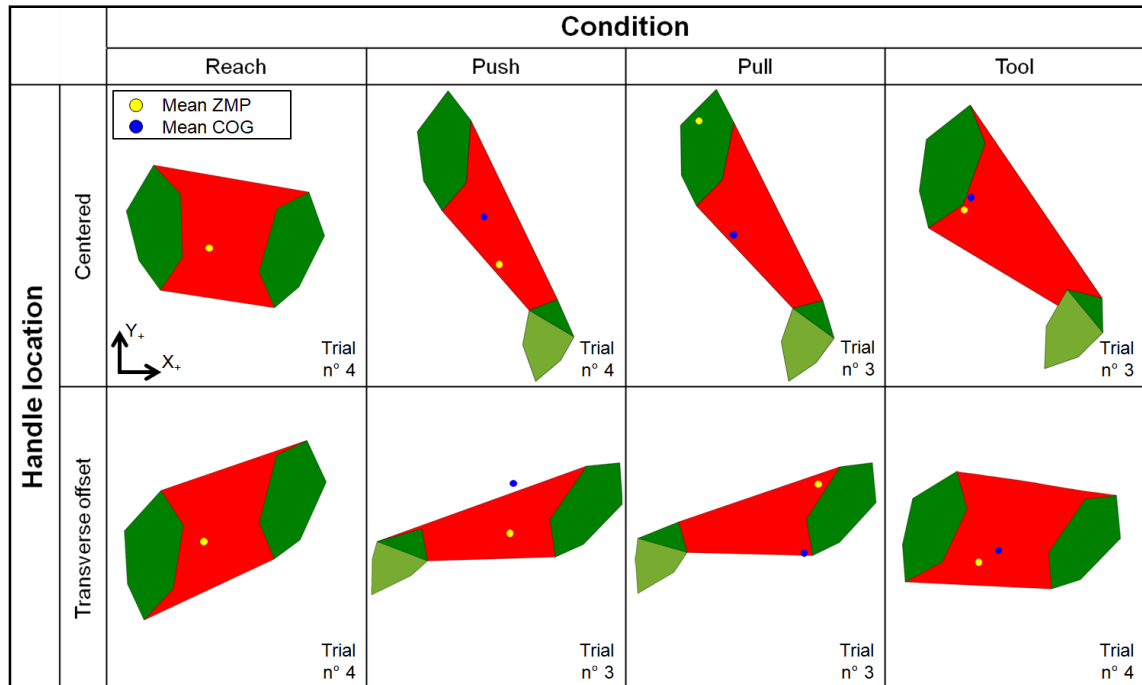


Figure 4.14 Mean ZMP in yellow and mean COG in blue over the 5-second static trial

In regards to the mean COG position, it can indicate as to if the adopted posture is ideal. When the COG is close to or outside of the BOS edge, it indicates that the posture is not ideal. If the force is removed, the subject will no longer be considered stable as the COG will be located outside the BOS. As shown during the transverse offset trials n° 3 for the push and pull conditions.

#### 4.5.2 Analysis

The sway analysis across trials allows us to quantify the control of stability by the subject during the 5-second acquisition. The transverse offset with load application trials indicated that stability was dependably more difficult to maintain. For the centered standing reaching trials, this sway oscillates around the high preference zone center established for this study at  $42.9 \pm 2.4\%$  of the subject's foot length and centered between feet. Despite, the fact that this center has not been calculated for the other conditions, it was observed that the results are in agreement with Popovic et al. (2000).

## 4.6 Limitations

Although the results obtained during this thesis have the potential of improving existing DHM stepping models, certain limitations need to be addressed. First of all, the sample size is insufficient to ensure that the proposed ZMP projection estimation model can account with certainty for an accurate stepping prediction model. Ideally, subjects of different ages and anthropometry should be included to have an accurate representation of what is seen in the industrial field. Further experimentations would without a doubt change the model as it would include the intersubject variability and the different foot placements used. However, the presented pilot subject allowed the verification that each condition was executed with enough repeatability and that 5 trials are not needed for each condition.

The second limitation is that the number of tasks evaluated with the pilot subject is limited. The full experimental protocol presented in section 3.3.1.4, where the target heights and positions vary, should be used to evaluate additional tasks and handle locations. The variation of target position would allow the full integration of target parameters in a stepping prediction model.

The third limitation of this study is that the model does not predict the support length position or orientation about the target and the hand load direction requirements. It also does not incorporate tool characteristics as it was simplified in this study that the screwdriver weight and shape were negligible.

Despite that, throughout this thesis, an experimental test bench was presented and was able to measure hand forces and acquire parameters of postural stability at the feet. The modeled raw data was able to project accurately the zero moment point on the support length so that it could be estimated. The experimentations on two different handle locations for multiple conditions provided enough validation as to the proposed methodology for future work to build on.

## CONCLUSION & RECOMMENDATIONS

This study presents an experimental test bench capable of measuring hand forces and moments simultaneously with feet position when completing tasks in industrial conditions. It is noted that the sample size is limited, hence the conclusions remain partial.

The literature review presented gaps in digital human models that integrate accurate stepping behavior models derived from specific industrial task experiments providing human movement coordination. It was also raised that a large majority of studies proposed feet positioning models arising from general two-handed push-pull tasks. No feet prediction model assessed tasks involving hand tools. Also, no study evaluated the effects of a transverse obstacle imposing spatial constraints and requiring subjects to execute tasks out of the sagittal plane without prescribing specific feet placement, which has been underlined by Wilkinson et al. (1995) to require further investigation.

Experimental trials covered different target positions and hand conditions, in which spatial constraints and a tool were studied. The trials statistically confirmed that a ZMP projection model can estimate the support length with respect to task requirements. Our exploratory experiments showed that task requirements vary the position of feet placement whether an obstacle is present or not. Over all trials, the subject moved the contralateral leg backward when the transverse obstacle was present, as feet were not constraint.

The overhead task was effective for isolating the stepping strategy. Being that the task necessitated the subject to reach vertically, this limited the use of the hip strategy (squatting) as the subject wouldn't have been able to reach the target as easily. Also, this target height restricted the use of forward and backward leaning by the subject to use bodyweight in order to support applied hand forces, which can result in adopting non-ideal postures.

During the centered trials, because the subject was able to center in line with the applied force direction, stability was maintained by expanding the BOS in the same direction as the

applied force. These observations agree with Hoffman et al. (2008), who stated that when possible subjects will prefer to position their body in line with the applied force direction to maximize applied forces by limiting lateral forces.

During the transverse offset location trials, because the obstacle prevented the subject from positioning in line with the applied force, a more transverse feet placement strategy was used, possibly to develop sufficient torque at the foot base to compensate for the moment created by the hand force and the out of plane distance. This observation is consistent with Wilkinson et al. (1995), where out of sagittal plane forces required the production of higher feet torque to ensure stability when standing with feet centered to the target.

The mean support length magnitude appeared smaller for the transverse offset trials which indicates hand-target reach might have been favored over stability. The postural sway analysis supports this conclusion as the transverse offset location affected the total sway more compared to the centered location.

The contributions of this research enabled progress in the DHM field as follows:

- This work developed an experimental test bench to assess accurately postural parameters.
- This work proposed a preliminary model to estimate the support length with respect to the ZMP position.
- This work studied the effect of an obstacle and the use of tools on feet placement.

In addition, this research project has been presented and published at the 6th International Digital Human Modeling Symposium (DHM2020) (Latour, Zeighami, Hagemeister, Charland & Aissaoui, 2020), and has been awarded a scholarship for publication in Substance, the scientific journal of l'École de technologie supérieure.

The preliminary results from this project contributed to validate the new stepping prediction model proposed by Zeighami et al. (2019) which will optimize the already developed Smart Posture Engine. The observed behaviors in the ZMP and the feet adjustments mentioned in this work, in addition to the proposed support length regression model appearance will be continuously improved as more experiments are completed. The future implementation of this new stepping prediction model in the Dassault Systèmes digital human model will be a considerable advancement as it will eliminate manual manipulations previously required to position the virtual manikin and ensure postures with accurate foot placement are simulated. Technological transfer to Dassault Systèmes is ongoing.

In future works, it should be intended to carry out the presented full experimental protocol (See Table 3.7) on a larger population size in order to develop a more robust regression model able of predicting the support length with respect to the ZMP position.

The new prediction model should be able to predict the orientation of the support length about the target and the hand load direction requirements. Future experimentations should also evaluate the different stability subregions found when stepping. Thus, prediction models could incorporate stability zones as proposed by Popovic et al. (2000) which would allow models to quantify more precisely the stepping behaviors. This thesis has shown the capability of evaluating the high preference zone for the centered reach trials. Another element that future works should study is the effect of more complex tools on feet placement as not all tools are used the same way.

This new evaluation could observe the influence of heavier tools, awkwardly shaped tools, or even unstable tools such as swivel sockets on adopted postures. It would also be interesting to assess the influence of assembly tasks on postures or even complex hidden tasks, which are often seen in the automotive field.



## APPENDIX I

### LITERATURE REVIEW SUMMARY TABLES

Table-A I-1 Literature review summary table of postural strategies assessment

Title	Authors	Date	Objectives & Article Type	Number of subject's	Evaluation criteria's & Conclusions	Tasks & Requirements	Specifications & Positions
<i>Medial-lateral and anterior-posterior motor responses associated with centre of pressure changes in quiet standing</i>	Winter, D.A., Prince, F., Stergiou, P. & Powell, C.	1993	Evaluate effect anterior-posterior and medial-lateral changes on calculated Net COP	10 subjects	Net COP is the integrated control variable and CoM is the controlled variable.  In A/P direction, Left and Right COP are perceived by Net COP, but not in M/L. Loading/unloading was predominant in M/L.	Quiet standing feet at 20 cm apart for acquisitions of 16 sec.  <b>Conditions:</b> -Eyes open -Eyes closed	Standing side-by-side
<i>The handling of objects other than boxes: Univariate analysis of handling techniques in a large transport company</i>	Baril-Gingras, G. & Lortie, M.	1995	Identify postural strategies used for material handling	31 males 3217 efforts & 944 handling tasks observed	More Horizontal pulling/pushing (48.2%) than Vertical lifting/lowering (26.6%). <b>Hand position:</b> 2 hand symmetrical 6.9%, 1 hand 55.4%, 2 hands asymmetrical 35.6%. <b>Forward or Lateral leaning:</b> 64.5%. <b>Squatting:</b> 11.7% of efforts. <b>Stepping:</b> Feet along the axis of movement only 9.2%.	<b>Tasks evaluated:</b> -9 effort types -25 object types  <b>Plane/Axis/Direction:</b> 21.9% in transverse axis of efforts. 4.3% in sagittal axis. 19.6% in vertical axis.	Standing  Object manipulation  Grid of 36 variables was developed
<i>Functional stability limits while holding loads in various positions</i>	Holbein, M.A. & Redfern, M.S.	1997	Investigate stability limits while standing and holding loads	15 males Age between 18 & 36	Theoretical stability region is the BOS. FSR may be smaller. External loads lowered COG & extended FSR limits. Ankle rotation allowed to avoid the effects of postural strategies on stability.  <b>FSR from the Center of BOS:</b> 53.7% leaning forward 61.5% leaning backward 62.2% lateral directions	<b>Tasks:</b> Leaning as far as possible in 4 directions.  <b>Conditions:</b> -No loads -Load(s) 11.4kg	Standing  1 Hand at waist 2 Hands at waist 1 Hand at side 2 Hands at sides 1 Hand High
<i>Force exertion in awkward working postures strength capability while twisting or working overhead</i>	Haslegrave, C.M., Tracy, M.F. & Corlett, N.E.	1997	Evaluate applicable force in 3 awkward work situations	24 males Age between 20 & 35 Divided into 2 groups	<b>Baseline:</b> max pushing force at shoulder level & max reach distance. Limit body weight to increase the force. <b>Twisted:</b> Handle height of 142 cm--shoulder <b>Overhead:</b> Handle at 4 locations above the right foot position (15° forward, 15° rearward & 15° each side of the vertical axis). Reach measured from the shoulder with arms extended above the head.	<b>Facing forward:</b> 0° shoulder level, right foot max reach <b>Twisted:</b> -90° right, foot-handle antero-distance 45.7 cm -135° right, foot handle distance 53.9 cm	Standing  Lying supine on the floor  Right foot position was specified

Table-A I-1 Literature review summary table of postural strategies assessment (cont'd)

Title	Authors	Date	Objectives & Article Type	Number of subject's	Evaluation criteria's & Conclusions	Tasks & Requirements	Specifications & Positions
<i>Static versus dynamic predictions of protective stepping following waist-pull perturbations in young and older adults</i>	Pai, Y.-C., Rogers, M.W., Patton, J., Cain, T.D., Hanke, T.A.	1998	Evaluate stepping threshold with perturbations for balance recovery	13 young, 18 older non-fallers & 18 fallers	Normalized foot to CoM position and CoM velocity of stability region and Forward stepping region.  Once the COM is within 10% of the boundary stepping is imminent. (Safety margin of 10% to govern their decision to step)	<b>Perturbation conditions:</b> -Low 0.045m 0.09m/s -Middle 0.09m 0.18m/s -High 0.135m 0.27m/s	Standing side-by-side
<i>Investigating centre of mass stabilisation as the goal of posture and movement coordination during human whole body reaching</i>	Stapley, P., Pozzo, T., Grishin, A. & Papaxanthis, C.	2000	Investigate if whole-body reaching movements can be executed by keeping CoM fixed in the horizontal axis	6 subjects Age between 18 & 35 Kinematic simulation-based from experimental data	CoM stabilized by axial synergies or anticipatory postural adjustments. CoM position verified with Toe and Heel markers, to ensure posture control movements to stay in BOS.  Maintaining CoM at constant horizontal position results in smaller ankle peak flexor & extensor torques.  Stabilizing CoM is associated with greater backward hip displacement, but not strategy chosen for reaching.  <b>COP displacement:</b> 1) Initial backward displacement. 2) COP pass in front of the CoM. 3) Finish at anterior limit of BoS.	Reach and Lift object of 1.8kg  <b>Anterior-posterior axis distance:</b> -5% of stature -30% of stature  <b>Conditions:</b> -Reach -Grasp a wooden dowel (0.4m*0.07m, 1.8kg) -Lift the object to shoulder height	Reaching forward while standing  Leaning forward  <b>Object height:</b> -Navel level
<i>Stability criterion for controlling standing in able-bodied subjects</i>	Popovic, M.R., Pappas, I.P.L., Nakazawa, K., Keller, T., Morari, M. & Dietz, V.	2000	New stability criterion for standing based on COP	10 subjects Mean age of 28.6	Established a relationship between COP position and stability.  <b>Stability zones:</b> High Preference(HP) 99% quiet standing Low Preference(LP) 1% quiet standing Undesirable(UN) postural changes to maintain balance. An unstable step is imminent to stay stable Subjects normalized (x & y COP coordinates divided by feet length)	HP center is at 0.47*L (L=Foot length)  <b>Ellipse Regions:</b> (AP/ML) HP: 0.16/0.07 LP: 0.43/0.57 UN: 0.59/0.97	Quiet standing  Standing postural with changes  Standing with stepping
<i>Validity of functional stability limits as a measure of balance in adults aged 23-73 years</i>	Holbein-Jenny, M.A., McDermott, K., Shaw, C. & Demchak, J.	2007	Validation of functional stability limits (FSL) with respect to the balance	52 subjects (16 males & 36 females) Aged between 23 & 73	Projection of the COP inside BOS.  <b>FSL (%):</b> Forward (57.8%), Backward (54.7%), Right (65.8%) Left (67.0%), 45° Right (69.0%), 45° Left (66.9%)	<b>Conditions:</b> -Forward -Backward -Left -Right -45° Left -45° Right	Standing  Leaning until fall limit

Table-A I-2 Literature review summary table of foot placement prediction models

Title	Authors	Date	Objectives & Article Type	Number of subject's	Evaluation criteria's & Conclusions	Tasks & Requirements	Specifications & Positions
<i>A Task-Based Stepping Behavior Model for Digital Human Models</i>	Wagner, D.W., Reed, M.P. & Chaffin, D.B.	2006	Develop a model based on laboratory experiments of foot behaviors, placements, and motions.	10 male and 10 female Paid subjects	Move loads between shelves located in various positions one to five steps apart.  Foot behavior matrix developed (lateral position, stride width, fore-aft position, forward foot, angular rotation of the foot, heel up & toe down times)	3 start/8 delivery tower locations.  <b>One-handed loads:</b> 0.5/2.27/4.54 kg <b>Two-handed loads:</b> 1.0/4.54/13.61 kg	Standing  <b>Task Heights:</b> -Low (15% ) -Middle (53%) -High (90% of stature)
<i>Optimization-Based Posture Prediction for Analysis of Box Lifting Tasks</i>	Marler, T., Knake, L. & Johnson, R.	2011	A new model for the global position and orientation of body as well as foot position, while considering balance.	A model compared to motion-capture data and literature-based data	Balance is measured by ZMP restricted to be inside the trapezoid foot support area (FSR). Upper & lower limit of hand(s) & feet placement reach constraints from anthropometric data. Present a minimum joint torque solution.	Posture predicted by external forces  Incorporation of balance & torque based performance measures.	Box lifting from the ground  Feet are not fixed but free in boundaries on the ground.
<i>Introducing Stability of Forces to the Automatic Creation of Digital Human Postures</i>	Delfs, N., Bohlin, R., Hanson, L., Högberg, D. & Carlson, J.S.	2013	A new model for assessing the stability and balance of DHM.	A human model containing 162 DOF	Inverse kinematics solver find end effector(s) position and orientation, by maximizing scalar comfort function (Joint angles, joint moments, object distance, etc.). Feet allowed to slide and rotate around the z-axis. (Remaining 3 DOF locked). Stability measure combined in comfort function and given importance ( $\alpha$ -required stability).	<b>Balance:</b> Sum of internal & external forces = 0. <b>Stability:</b> Forces & Torques derived from potential function $V(q)$ stable if $\Delta V > 0$ for every nonzero displacement $\Delta q$ .	Box holding. Tunnel bracket assembly. Seat mounting.
<i>Optimal Posture and Supporting Hand Force Prediction for Common Automotive Assembly One-Handed Tasks</i>	Howard, B., Yang, J. & Ozsoy, B.	2014	Develop a model to predict optimal posture and supporting hand forces using stability techniques	A human model containing 56 DOF based on 50 <sup>th</sup> percentile female	All postures predicted with respect to joint torque & supporting hand forces. Increase stability: lower COG, increase distance ZMP stability axis. The excursion of ZMP was only such that it adhered to the minimal stability requirements.  Experimental data needed to determine actual ZMP excursions resulting from the supporting hand forces.	Postures validated visually to postures from an experimental study.  External forces are assessed using stability analysis. Measures are based on joint torque.	Standing postures with a supporting hand.  Stability criteria based on the ZMP position.
<i>Stepping behavior for stability control of a digital human model</i>	Zeighami, A., Lemieux, P.O., Charland, J., Hagemeister, N. & Aissaoui, R.	2019	Develop a new stepping behavior prediction model.	A human model containing 95 DOF based on 50 <sup>th</sup> percentile	ZMP computed from COG and external loads. If ZMP needs to exit FSR for the target to be reached, stepping is required.  If target can be reached without ZMP leaving FSR no stepping is required. Experimental validation was conducted on 5 lifting trials.	<b>One-handed loads:</b> -Pulling +100N -Pushing -100N -No force 0N	Standing postures  Stability criteria based on the ZMP position with respect to the FSR.

Table-A I-3 Literature review summary table of industrial tasks using hand tools

Title	Authors	Date	Field of study	Force and moment capture system	Kinematics capture system	Results and conclusions
<i>Power grip strength as a function of tool handle orientation and location</i>	Megorry, R.W. & Lin, J.-H.	2007	30 subjects inexperienced & experienced	<ul style="list-style-type: none"> <li>• <b>Strain gauges (N)</b></li> <li>• <b>Angular position dial (°):</b></li> </ul>	Visual evaluation of ankle positioning	Height and reach decrease grip strength, but orientation also influences this strength.
<i>Evaluation of handle design characteristics in a maximum screwdriving torque task</i>	Kong, Y.K., Lowe, B.D., Lee, S.J. & Krieg, E.F.	2007	12 males	<ul style="list-style-type: none"> <li>• <b>Torque transducer (Nm):</b> TQ202, 0–30 Nm</li> <li>• <b>Force sensor (N):</b> FlexiForce</li> <li>• <b>EMG (%CVM)</b></li> </ul>	N/A	Evaluate 24 screwdriver handles. Individual finger & phalange forces-contribution as a function of the handle.
<i>Effect of feed force and duration on discomfort level using a hand drill machine</i>	Singh, J. & Khan, A.A.	2010	9 males	<ul style="list-style-type: none"> <li>• <b>Triaxial accelerometer (m/s<sup>2</sup>):</b> Onosoki</li> </ul>	N/A	The force and the time of application have considerable effects on subject discomfort.
<i>Contraintes biomécaniques exercées aux membres supérieurs lors de l'utilisation de petits outils dans le secteur des services à l'automobile</i>	Marchand, D. & Giguère, D.	2012	19 students	<ul style="list-style-type: none"> <li>• <b>EMG (%CVM):</b> Evaluate muscle fatigue</li> <li>• <b>Torque transducer (Nm):</b> IMADA DL-1M</li> <li>• <b>Strain gauges (N):</b></li> </ul>	Subjects equipped with LED lights at on the joints (SONY HDRCX110)	<u>Assessment of 3 tasks:</u> Bolting (16 cond.), Sanding (26 cond.), Painting (8 cond.) Ergonomic positions reduce joint stress.
<i>Linear Modeling of Human Hand-Arm Dynamics Relevant to Right-Angle Torque Tool Interaction</i>	Ay, H., Sommerich, C.M. & Luscher, A.F.	2013	40 subjects from an automotive industry	<ul style="list-style-type: none"> <li>• <b>Rate gyro (rad/s):</b> Analog Devices™ADXRS150EB</li> <li>• <b>Strain gauges (N)</b></li> <li>• <b>Torque transducer (Nm):</b> Stanley™ E44LA19-70 RA</li> </ul>	N/A	The gauges measured an offset in the bending moment when the subjects performed only static grip.
<i>A laboratory study of a low-cost system for measuring coupling forces</i>	Rakheja, S., Marcotte, P., Kalra, M., Adewusi, S. & Dewangan, K.	2016	9 males	<ul style="list-style-type: none"> <li>• <b>Force sensor (N):</b> Kistler 9212 &amp; FlexiForce 1230</li> <li>• <b>6-DOF Load cell (N-Nm):</b> Kistler 9317b</li> <li>• <b>Accelerometer (m/s<sup>2</sup>):</b> PCB SEN026</li> </ul>	N/A	Comparison of Tekscan 9811, FlexiForce 1230 & QTC (Peratech). Tekscan & FlexiForce best. Resistive sensors are less precise than capacitive & less expensive.
<i>Instrumentation of a grinding tool for capturing dynamic interactions with the workpiece</i>	Phan, G.-H., Kana, S. & Campolo, D.	2017	1 operator	<ul style="list-style-type: none"> <li>• <b>6-DOF Load cell (N-Nm):</b> ATI mini 40</li> <li>• <b>Bellows coupling:</b> CPBSC 25-10-10 MISUMI</li> <li>• <b>Encoder (rad-rad/s):</b> HEDL 5400#A12</li> </ul>	N/A	Developed a robotic model to reproduce repetitive tasks.

Table-A I-4 Literature review summary table of experimental test bench designs

Title	Authors	Date	Objectives & Article Type	Number of subject's	Evaluation criteria's & Conclusions	Tasks & Requirements	Specifications & Positions
<i>Relationships between one-handed force exertions in all directions and their associated postures</i>	Wilkinson, A.T., Pinder, A.D.J. & Grieve, D.W.	1995	Evaluate the relationship between three-dimensional forces and adopted postures	11 subjects (All males, 9 right-handed & 2 left-handed)	<p><b>Hand forces:</b> Triaxial force sensor</p> <p><b>Kinematics:</b> Photographs in the horizontal and vertical plane with 22 body landmarks</p> <p><b>Ground reaction forces:</b> N/A</p> <p>CoG &amp; COP error of 39 mm &amp; 38 mm because calculated not measured. CoG of upper limbs was based on an assumed position.</p> <p>Postural stability diagram used to assess postures. Vertical plane provides posture information in terms of force magnitude. The horizontal plane provides posture strategies to develop torque &amp; thrust at the foot base to generate lateral forces.</p> <p>Off-axis forces generated horizontal feet moments of up to 50 Nm. Off sagittal plane forces require body strategies to stay stable.</p>	<p>One-handed pull &amp; push</p> <p>Use only the right hand used.</p> <p>Feet positioned predominantly side-by-side. Required to be equidistant from the centerline of the target.</p> <p><b>Conditions (26):</b> Forward/Backward Left/Right Up/Down</p>	<p>Standing</p> <p><b>Handle heights:</b> -0.5 m -1.0 m -1.5 m</p> <p><b>Handle positions:</b> -Central</p> <p>The horizontal heel-to-second-toe lines of the feet defined the forward direction</p>
<i>Low-Back Biomechanics and Static Stability During Isometric Pushing</i>	Granata, K.P. & Bennett, B.C.	2005	Investigate low-back risk factors associated with pushing	11 subjects (7 males & 4 females) Force level was randomized	<p><b>Hand forces:</b> 6-DOF load cell</p> <p><b>Kinematics:</b> Electromagnetic sensors</p> <p><b>Ground reaction forces:</b> Ground reaction force plate</p> <p>CoM and hand positions were calculated relative to L5-S1 positions not measured.</p> <p>Trunk posture, Force direction &amp; Trunk moment are influenced by exertion level, the elevation of the handle, and foot positioning.</p> <p>Foot placement distance in parallel stance was almost exactly mid-way between the front and rear feet during a staggered stance. All participants leaned forward at least 15° for pushing. For waist-height trials mean horizontal force was 33% more than the max horizontal force when pushing at shoulder height.</p>	<p>Two-handed push</p> <p>Feet positions not constrained.</p> <p><b>Conditions:</b> Force levels at Max Voluntary Effort (MVE), 30% of BW, 15% of BW</p>	<p>Standing side-by-side</p> <p>Standing staggered stance</p> <p><b>Handle heights:</b> -Shoulder height -ASIS height (waist) -Midway within shoulder and waist height (midheight)</p> <p><b>Handle positions:</b> -Central</p>

Table-A I-4 Literature review summary table of experimental test bench designs (cont'd)

Title	Authors	Date	Objectives & Article Type	Number of subject's	Evaluation criteria's & Conclusions	Tasks & Requirements	Specifications & Positions
<i>Predicting Force-Exertion Postures from Task Variables</i>	Hoffman, S.G., Reed, M.P. & Chaffin, D.B.	2007	Exploratory evaluation of the effects of hand force location, magnitude, and direction on whole-body posture for standing tasks	20 subjects (7 males & 8 females) No randomization	<p><b>Hand forces:</b> 6-DOF load cell</p> <p><b>Kinematics:</b> Motion capture system (29 body landmarks)</p> <p><b>Ground reaction forces:</b> Moveable force plates</p> <p>-Parallel stance (CoM out of BOS) -Split Stance arms flexed/extended (CoM in BOS)</p> <p>Lower-extremity postures favor balance maintenance. Upper-extremity postures maximize shoulder &amp; elbow torque. Straight-arm pushing &amp; pulling minimize torque &amp; joint moment (Seitz et al., 2005)</p>	<p>Two-handed pull &amp; push</p> <p>Subjects had to achieve/maintain requested forces</p> <p>Feet positions not constrained. Force feedback present.</p> <p><b>Conditions:</b> Force levels at 25%, 50%, 75%, 100% (MVE)</p>	<p>Standing</p> <p><b>Handle heights:</b> Elbow height</p> <p><b>Handle positions:</b> The subject free to position himself.</p> <p>Maximal exertion trials of 6 secs. Then a practice trial.</p>
<i>Postural Behaviors during One-Hand Force Exertions</i>	Hoffman, S.G., Reed, M.P. & Chaffin, D.B.	2008	Exploratory evaluation of postural behaviors during one-hand force exertions	19 subjects (9 males & 10 females, all right hand dominant) No randomization A split-plot design was employed	<p><b>Hand forces:</b> 6-DOF load cell</p> <p><b>Kinematics:</b> 8 camera Qualysis Proreflex (29 body landmarks)</p> <p><b>Ground reaction forces:</b> Moveable force plates</p> <p>Allowed to brace off own body but not externally.</p> <p>When possible, subjects align their bodies with the direction of the force to convert potential crossbody exertions (asymmetric) into sagittal plane exertions (symmetric).</p> <p>In the hand-force plane, the pelvis position favors the postural objective of reducing rotational trunk torques. One-handed postures are defined by axial rotation of the torso towards or away of force application point.</p>	<p>One-handed pull &amp; push</p> <p>Required to take steps to handle.</p> <p>Feet positions not constrained. Force feedback present.</p> <p><b>Conditions (6):</b> Forward/Backward Left/Right Up/Down</p> <p><b>Conditions:</b> Force levels 25%, 50%, 75%, 100% (MVE)</p>	<p>Standing</p> <p><b>Handle heights:</b> -Elbow height (63% of stature) -Mid-thigh (41% of stature) -0.1 m overhead</p> <p><b>Handle positions:</b> The subject was free to position himself.</p> <p>Maximal exertion trials of 6 secs. Then a practice trial.</p>
<i>Biomechanically determined hand force limits protecting the low back during occupational pushing and pulling tasks</i>	Weston, E.B., Aurand, A., Dufour, J.S., Knapik, G.G. & Marras, W.S.	2018	Establish hand force limits according to the forces perceived by the lumbar spine	62 subjects (31 males & 31 females) Handle heights and directions randomized	<p><b>Hand forces:</b> Bertec HT0825 transducers</p> <p><b>Kinematics:</b> OptiTrack 36 motion capture cameras (41 markers)</p> <p><b>Back activation:</b> EMG Motion Lab Systems MA300-XIV system</p> <p><b>Ground reaction forces:</b> N/A (Force plate only for model calibration)</p> <p>Task, force direction &amp; height significantly influence spinal load, hand forces &amp; turning torque. Obtained values are up to 30% lower than existing pushing &amp; pulling risk assessment tools &amp; task recommendation guides.</p>	<p>One-handed pull</p> <p>Two-handed pull &amp; push</p> <p><b>Conditions:</b> Straight or Turning</p>	<p>Standing</p> <p><b>Handle heights:</b> -81.3 cm -101.6 cm -121.9 cm</p> <p>Subjects move a rig on rails brake adds linear or rotational resistance proportional to displacement.</p>

## APPENDIX II

### INDUSTRIAL TASK EVALUATION

Table-A II-1 Grouping of tasks "Standing Upright"

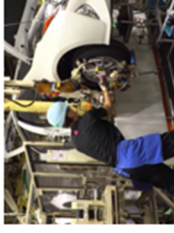
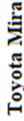
Standing Upright			
 <b>Ford Focus 2019</b>	 <b>Ford Focus 2019</b>	 <b>Ford Focus 2019</b>	 <b>Ford Focus 2019</b>
 <b>Ford Focus 2019</b>	 <b>Ford Ranger 2019</b>		 <b>Ford Ranger 2019</b>
 <b>Ford Ranger 2019</b>	 <b>Ford Mustang 2019</b>	 <b>Toyota Prius 2017</b>	 <b>Toyota Mirai</b>
			 <b>Ford Ranger 2019</b>
			 <b>Toyota Mirai</b>

Table-A II-1 Grouping of tasks "Standing Upright" (cont'd)

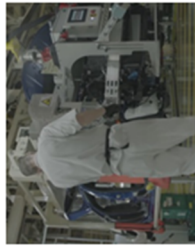
 <p><b>Toyota Mirai</b></p>	 <p><b>Toyota Mirai</b></p>	 <p><b>Toyota Mirai</b></p>	 <p><b>Toyota Mirai</b></p>	 <p><b>Toyota Corolla</b></p>
 <p><b>Toyota Corolla</b></p>	 <p><b>Toyota Corolla</b></p>	 <p><b>Toyota Corolla</b></p>	 <p><b>Toyota Corolla</b></p>	 <p><b>Honda Accord 2019</b></p>
 <p><b>Honda Accord 2019</b></p>	 <p><b>Honda Accord 2019</b></p>	 <p><b>Honda Civic 2017</b></p>	 <p><b>Honda Civic 2017</b></p>	 <p><b>Honda Civic 2017</b></p>

Table-A II-1 Grouping of tasks "Standing Upright" (cont'd)

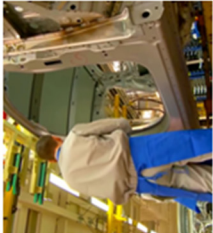
 Honda Civic 2017	 Honda Civic 2017	 Honda Odyssey	 Honda Odyssey	 Volkswagen Golf 2017
 Volkswagen Golf 2017	 Volkswagen Golf 2017	 Volkswagen Touareg 2017	 Volkswagen Touareg 2017	 Volkswagen Touareg 2017
 Volkswagen Touareg 2017	 Volkswagen Touareg 2017	 Volkswagen Touareg 2017	 Volkswagen Touareg 2017	 Volkswagen Touareg 2017
 Volkswagen Touareg 2017	 Volkswagen Touareg 2017	 Volkswagen Touareg 2017	 Mercedes Actros	 Mercedes Actros

Table-A II-1 Grouping of tasks "Standing Upright" (cont'd)

 <p>Mercedes Actros</p>	 <p>Mercedes Actros</p>	 <p>Mercedes Actros</p>	 <p>Mercedes Actros</p>	 <p>Mercedes Actros</p>
 <p>Mercedes Actros</p>	 <p>Mercedes Actros</p>	 <p>Mercedes Actros</p>	 <p>PACCAR</p>	 <p>PACCAR</p>
 <p>Rolls-Royce</p>		 <p>Rolls-Royce</p>		

Table-A II-2 Grouping of tasks "Standing Bent"

Standing Bent				
 <p>Ford Focus 2019</p>	 <p>Ford Ranger 2019</p>	 <p>Ford Ranger 2019</p>	 <p>Ford Ranger 2019</p>	 <p>Ford Mustang 2019</p>
 <p>Ford Mustang 2019</p>	 <p>Toyota Prius 2017</p>	 <p>Toyota Prius 2017</p>	 <p>Toyota Prius 2017</p>	 <p>Toyota Prius 2017</p>

Table-A II-2 Grouping of tasks "Standing Bent" (cont'd)

				
<b>Toyota Mirai</b>	<b>Toyota Mirai</b>	<b>Toyota Corolla</b>	<b>Toyota Corolla</b>	<b>Toyota Corolla</b>
				
<b>Honda Accord 2019</b>	<b>Honda Accord 2019</b>	<b>Honda Accord 2019</b>	<b>Honda Civic 2017</b>	<b>Honda Civic 2017</b>
				
<b>Honda Civic 2017</b>	<b>Honda Civic 2017</b>	<b>Volkswagen Golf 2017</b>	<b>Volkswagen Golf 2017</b>	<b>Volkswagen Golf 2017</b>

Table-A II-2 Grouping of tasks "Standing Bent" (cont'd)

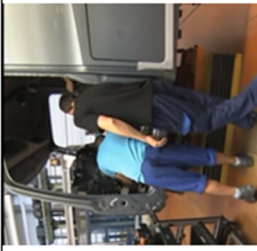
 <p><b>Volkswagen Golf 2017</b></p>	 <p><b>Volkswagen Touareg 2017</b></p>	 <p><b>Mercedes Actros</b></p>	 <p><b>Mercedes Actros</b></p>	 <p><b>Mercedes Actros</b></p>
 <p><b>PACCAR</b></p>		 <p><b>Rolls-Royce</b></p>		

Table-A II-3 Grouping of tasks " Standing Above the head"

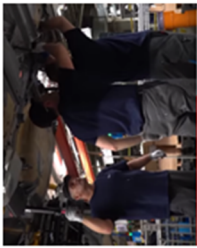
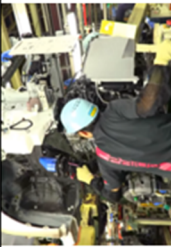
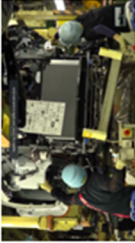
Standing Above the head				
				
Ford Focus 2019	Ford Focus 2019	Ford Focus 2019	Ford Ranger 2019	Ford Mustang 2019
				
Ford Mustang 2019	Toyota Prius 2017	Toyota Prius 2017	Toyota Prius 2017	Toyota Prius 2017
				
Toyota Prius 2017	Toyota Prius 2017	Toyota Mirai	Toyota Mirai	Toyota Mirai
				
Toyota Corolla	Honda Accord 2019	Honda Accord 2019	Honda Accord 2019	Honda Civic 2017

Table-A II-3 Grouping of tasks " Standing Above the head" (cont'd)

 <b>Honda Civic 2017</b>	 <b>Honda Odyssey</b>	 <b>Honda Odyssey</b>	 <b>Volkswagen Touareg 2017</b>	 <b>Volkswagen Touareg 2017</b>
 <b>Volkswagen Touareg 2017</b>	 <b>Volkswagen Touareg 2017</b>	 <b>Mercedes Actros</b>	 <b>Mercedes Actros</b>	 <b>Mercedes Actros</b>
 <b>Mercedes Actros</b>	 <b>PACCAR</b>	 <b>PACCAR</b>	 <b>Rolls-Royce</b>	

Table-A II-4 Grouping of tasks "Leaning"

Leaning				
 <p><b>Ford Ranger 2019</b></p>	 <p><b>Toyota Prius 2017</b></p>	 <p><b>Toyota Prius 2017</b></p>	 <p><b>Toyota Mirai</b></p>	 <p><b>Toyota Mirai</b></p>
 <p><b>Toyota Corolla</b></p>	 <p><b>Volkswagen Touareg 2017</b></p>	 <p><b>Volkswagen Touareg 2017</b></p>	 <p><b>Volkswagen Touareg 2017</b></p>	 <p><b>Mercedes Actros</b></p>
 <p><b>Mercedes Actros</b></p>	 <p><b>Mercedes Actros</b></p>	 <p><b>Rolls-Royce</b></p>		

Table-A II-5 Grouping of tasks "Seated Upright"

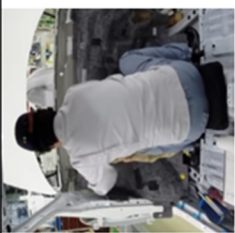
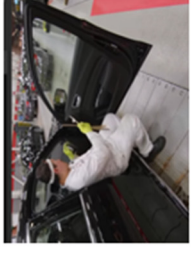
<b>Seating Upright</b>			
			
<b>Toyota Mirai</b>	<b>Toyota Corolla</b>	<b>Honda Accord 2019</b>	<b>Honda Accord 2019</b>
			
			<b>Honda Odyssey</b>

Table-A II-6 Grouping of tasks "Seated Bent"

<b>Seating Bent</b>	
	
<b>Toyota Mirai</b>	<b>Toyota Corolla</b>

Table-A II-7 Grouping of tasks "Kneeling Upright"

<b>Kneeling Upright</b>		
 <p><b>Toyota Mirai</b></p>	 <p><b>Toyota Corolla</b></p>	 <p><b>Volkswagen Golf 2017</b></p>

Table-A II-8 Grouping of tasks "Kneeling Bent"

<b>Kneeling Bent</b>			
 <p><b>Toyota Mirai</b></p>	 <p><b>Volkswagen Touareg 2017</b></p>	 <p><b>Volkswagen Touareg 2017</b></p>	 <p><b>Mercedes Actros</b></p>
 <p><b>Rolls-Royce</b></p>	 <p><b>Rolls-Royce</b></p>	 <p><b>Rolls-Royce</b></p>	

Table-A II-9 Grouping of tasks " Kneeling Above the head"

<b>Kneeling Above the head</b>	
	
<b>Volkswagen Golf 2017</b>	<b>Volkswagen Touareg 2017</b>



## LIST OF REFERENCES

- Abdel-Malek, K., Yang, J., Kim, J.H., Marler, T., Beck, S., Swan, C., Frey-Law, L., Mathai, A., Murphy, C., Rahmatallah, S. & Arora, J. (2007). Development of the Virtual-Human Santos™. In V.G. Duffy (Eds.), *Digital Human Modeling: 1<sup>st</sup> International Conference, ICDHM 2007, Beijing, China, July 22-27, 2007*, (Vol. 4561, pp. 490-499). Heidelberg, Berlin, Germany: Springer-Verlag.
- AnyBody Technology. (2020). The AnyBody Modeling System. Retrieved from <https://www.anybodytech.com/software/>
- Ay, H., Sommerich, C.M. & Luscher, A.F. (2013). Linear modeling of human hand-arm dynamics relevant to right-angle torque tool interaction. *Human Factors*, 55(5), 893-910. DOI: 10.1177/0018720813485977
- Badler, N.I., Phillips, C.B. & Webber, B.L. (1993). Behavioral control. *Simulating humans: Computer graphics, animation, and control*. (pp. 101-136). New York, NY: Oxford University Press.
- Baerlocher, P. (2001). *Inverse kinematics techniques of the interactive posture control of articulated figures*. (Doctoral thesis, École Polytechnique Fédérale de Lausanne, Lausanne, France).
- Baril-Gingras, G. & Lortie, M. (1995). The handling of objects other than boxes: Univariate analysis of handling techniques in a large transport company. *Ergonomics*, 38(5), 905-925. DOI: 10.1080/00140139508925159
- Berlin, C. & Adams, C. (2017). Digital human modeling. *Production ergonomics: Designing work systems to support optimal human performance* (pp. 161-174). London, England: Ubiquity Press. DOI: 10.5334/bbe.i
- Bubb, H., Engstler, F., Fritzsche, F., Mergl, C., Sabbah, O., Schaefer, P. & Zacher, I. (2006). The development of RAMSIS in past and future as an example for the cooperation between industry and university. *International Journal of Human Factors Modelling and Simulation*, 1(1), 140-157. DOI: 10.1504/IJHFMS.2006.011686
- Charland, J. (2019). Virtual Ergonomics by Dassault Systèmes. In S. Scataglini & G. Paul (Eds.), *DHM and Posturography* (pp. 97-103). Cambridge, MA: Academic Press.
- Chaffin, D.B. (2008). Digital human modeling for workspace design. *Reviews of Human Factors and Ergonomics*, 4(1), 41-74. DOI: 10.1518/155723408X342844

- Clauser, C.E., McConville, J.T. & Young, J.W. (1969). *Weight, volume, and center of mass of segments of the human body* (Report No. TR-69-70). Wright-Patterson Air Force Base, Ohio: Aerospace Medical Research Laboratory.
- Dassault Systèmes. (2020). DELMIA 3DEXPERIENCE. Retrieved from <https://www.3ds.com/products-services/delmia/products/delmia-3dexperience/>
- Delfs, N., Bohlin, R., Hanson, L., Högberg, D. & Carlson, J.S. (2013). *Introducing stability of forces to the automatic creation of digital human postures*. Paper presented at the 2<sup>nd</sup> International Digital Human Modeling Symposium (DHM2013). Retrieved from [http://mreed.umtri.umich.edu/DHM2013Proceedings/Individual\\_Papers/](http://mreed.umtri.umich.edu/DHM2013Proceedings/Individual_Papers/)
- De Looze, M.P., Van Greuningen, K., Rebel, J., Kingma, I. & Kuijer, P.P. (2000). Force direction and physical load in dynamic pushing and pulling. *Ergonomics*, 43(3), 377-390. DOI: 10.1080/001401300184477
- Dempster, W.T. (1955). *Space requirements of the seated operator* (Report No. TR-55-159). Wright-Patterson Air Force Base, Ohio: Wright Air Development Center.
- Dijkstra, E.J. & Gutierrez-Farewik, E.M. (2015). Computation of ground reaction force using zero moment point. *Journal of Biomechanics*, 48(14), 3776-3781. DOI: 10.1016/j.jbiomech.2015.08.027
- Faraway, J.J. (2003). *Data-based motion prediction* (Report No. 2003-01-2229). Warrendale, PA: SAE International.
- Forde, M.S. & Buchholz, B. (2004). Task content and physical ergonomic risk factors in construction ironwork. *International Journal of Industrial Ergonomics*, 34(4), 319-333. DOI: 10.1016/j.ergon.2004.04.011
- Gordon, C.C., Blackwell, C.L., Bradtmiller, B., Parham, J.L., Barrientos, P., Paquette, S.P., Corner, B.D., Carson, J., Venezia, J.C., Rockwell, B.M., Mucher, M. & Kristensen, S. (2014). *2012 Anthropometric survey of u.s. army personnel: methods and summary statistics* (Report No. NATICK/TR-15/007). Natick, MA: U.S. Army Natick Soldier Research, Development and Engineering Center.
- Granata, K.P. & Bennett, B.C. (2005). Low-back biomechanics and static stability during isometric pushing. *Human Factors*, 47(3), 536-549. DOI: 10.1518/001872005774859962
- Haslegrave, C.M., Tracy, M.F. & Corlett, E.N. (1997). Force exertion in awkward working postures-strength capability while twisting or working overhead. *Ergonomics*, 40(12), 1335-1362. DOI: 10.1080/001401397187405

- Hanson, L., Högberg, D. & Söderholm, M. (2012). Digital test assembly of truck parts with the IMMA-tool-- an illustrative case. *Work*, 41(1), 2248-2252. doi: 10.3233/WOR-2012-0447-2248
- Hanson, L., Högberg, D., Carlson, J. S., Bohlin, R., Brodin, E., Delfs, N., Mårdberg, P., Gustafsson, S., Keyvani, A. & Rhen, I.-M. (2014). *Imma - Intelligently moving manikins in automotive applications*. Presented at the 3<sup>rd</sup> International Summit of Human Simulation, ISHS2014, Tokyo, Japan.
- Hoffman, S.G., Reed, M.P. & Chaffin, D.B. (2007a). The relationship between hand force direction and posture during two-handed pushing tasks. *Proceedings of the Human Factors and Ergonomics Society Annual Meeting*, 51(15), 928-932. DOI: 10.1177/154193120705101513
- Hoffman, S.G., Reed, M.P. & Chaffin, D.B. (2007b). *Predicting force-exertion postures from task variables* (Report No. 2007-01-2480). Warrendale, PA: SAE International.
- Hoffman, S.G., Reed, M.P. & Chaffin, D.B. (2008). Postural behaviors during one-hand force exertions. *SAE International Journal of passenger cars*, 1(1), 1136-1142. DOI: 10.4271/2008-01-1915
- Hoffman, S.G., Reed, M.P. & Chaffin, D.B. (2010). A study of the difference between nominal and actual hand forces in two-handed sagittal plane whole-body exertions. *Ergonomics*, 54(1), 47-59. DOI: 10.1080/00140139.2010.535021
- Holbein, M.A. & Redfern, M.S. (1997). Functional stability limits while holding loads in various positions. *International Journal of Industrial Ergonomics*, 19(5), 387-395. DOI: 10.1016/s0169-8141(96)00023-6
- Holbein-Jenny, M.A., McDermott, K., Shaw, C. & Demchak, J. (2007). Validity of functional stability limits as a measure of balance in adults aged 23–73 years. *Ergonomics*, 50(5), 631-646. DOI: 10.1080/00140130601154814
- Horak, F.B. & Nashner, L.M. (1986). Central programming of postural movements: adaptation to altered support-surface configurations. *Journal of Neurophysiology*, 55(6), 1369-1381. DOI: 10.1152/jn.1986.55.6.1369
- Howard, B., Yang, J. & Ozsoy, B. (2014). Optimal posture and supporting hand force prediction for common automotive assembly one-handed tasks. *Journal of Mechanisms and Robotics*, 6(2), 1-10. DOI: 10.1115/1.4025749
- Human Solutions. (2020). RAMSIS General. Retrieved from <https://www.human-solutions.com/en/products/ramsisis-general/index.html>

- Jones, M.L.H., Reed, M.P. & Chaffin, D.B. (2013). The effect of bracing availability on one-hand isometric force exertion capability. *Ergonomics*, 56(4), 667-681. DOI: 10.1080/00140139.2013.765601
- Kong, Y.-K., Lowe, B.D., Lee, S.-J. & Krieg, E.F. (2007). Evaluation of handle design characteristics in a maximum screwdriving torque task. *Ergonomics*, 50(9), 1404-1418. DOI: 10.1080/00140130701393775
- Latour, F., Zeighami, A., Hagemester, N., Charland, J. & Aissaoui, R. (2020). Experimental evaluation of postural stability using stepping strategies during industrial tasks. In L. Hason, D. Högberg & E. Brodin (Eds.), *Proceedings of the 6<sup>th</sup> International Digital Human Modeling Symposium (DHM2020)*, Skövde, Sweden, August 31-September 2, 2020, (Vol. 11, pp. 156-165). Amsterdam, Netherlands: IOS Press.
- Lemieux, P.O., Barré, A., Hagemester, N. & Aissaoui, R. (2017). Degrees of freedom coupling adapted to the upper limb of a digital human model. *IJHFMS*, 5(4), 314-337. DOI: 10.1504/IJHFMS.2017.087015
- Lemieux, P.O., Barré, A., Aissaoui, R. & Hagemester, N. (2020). *United States patent n° 10,621,384 B2*. Waltham, MA (US): Dassault Systemes Americas Corp.
- Lucy, S.D & Hayes, K.C. (1985). Postural sway profiles: Normal subjects and subjects with cerebellar ataxia. *Physio Canada*, 37, 140-148.
- Marchand, D. & Giguère, D. (2010). *Les risques de troubles musculo-squelettiques aux membres supérieurs dans le secteur des services à l'automobile* (Report No. R-645). Montreal, Canada: IRSST.
- Marchand, D. & Giguère, D. (2012). *Contraintes biomécaniques exercées aux membres supérieurs lors de l'utilisation de petits outils dans le secteur des services à l'automobile* (Report No. R-726). Montreal, Canada: IRSST.
- Marler, T., Knake, L. & Johnson, R. (2011). Optimization-based posture prediction for analysis of box lifting tasks. In V.G. Duffy (Eds.), *Digital Human Modeling: 3<sup>rd</sup> International Conference, ICDHM 2011, Orlando, Florida, July 9-14, 2011*, (Vol. 6777, pp. 151-160). Heidelberg, Berlin, Germany: Springer-Verlag.
- Marshall, R., Case, K., Porter, M., Summerskill, S., Gyi, D., Davis, P. & Sims, R. (2010). HADRIAN: a virtual approach to design for all. *Journal of Engineering Design*, 21(2-3), 253-273. DOI: 10.1080/09544820903317019
- McGorry, R.W. & Lin, J.-H. (2007). Power grip strength as a function of tool handle orientation and location. *Ergonomics*, 50(9), 1392-1403. DOI: 10.1080/00140130701340115

- Mochimaru, M., Kouchi, M. & Dohi, M. (2000). Analysis of 3-D human foot forms using the free form deformation method and its application in grading shoe lasts. *Ergonomics*, 43(9), 1301-1313. DOI: 10.1080/001401300421752
- Pai, Y-C. & Patton, J. (1997). Center of mass velocity-position predictions for balance control. *J Biomech.*, 30(4), 347-354. DOI: 10.1016/s0021-9290(96)00165-0
- Pai, Y-C., Rogers, M.W., Patton, J., Cain, T.D. & Hanke, T.A. (1998). Static versus dynamic predictions of protective stepping following waist-pull perturbations in young and older adults. *J Biomech.*, 31(12), 1111-1118. DOI: 10.1016/s0021-9290(98)00124-9
- Phan, G.-H., Kana, S. & Campolo, D. (2017, November). *Instrumentation of a grinding tool for capturing dynamic interactions with the workpiece*. Presented at 8<sup>th</sup> IEEE International Conference on Cybernetics and Intelligent Systems and IEEE Conference on Robotics, Automation and Mechatronics, Ningbo, Chine (pp. 551-555). DOI: 10.1109/ICCIS.2017.8274836
- Popovic, M.R., Pappas, I.P.I., Nakazawa, K., Keller, T., Morari, M. & Dietz, V. (2000). Stability criterion for controlling standing in able-bodied subjects. *J Biomech.*, 33(11), 1359-1368. DOI: 10.1016/S0021-9290(00)00123-8
- Rakheja, S., Marcotte, P., Kalra, M., Adewusi, S. & Dewangan, K. (2016). *A laboratory study of a low-cost system for measuring coupling forces* (Report No. R-923). Montreal, Canada: IRSST.
- Reed, M.P., Faraway, J., Chaffin, D.B. & Martin, B.J. (2006). *The HUMOSIM ergonomics framework: A new approach to digital human simulation for ergonomic analysis* (Report No. 2006-01-2365). Warrendale, PA: SAE International.
- Reed, M.P. & Wagner, D.W. (2007). *An integrated model of gait and transition stepping for simulation of industrial workcell tasks* (Report No. 2007-01-2478). Warrendale, PA: SAE International.
- Santos Human inc. (2020). Products for Human-Centric Design. Retrieved from <https://www.santoshumaninc.com/products/>
- Scataglini, S. & Paul, G. (2019). *DHM and posturography*. Cambridge, MA: Academic Press.
- Seitz, T, Recluta, D, Zimmermann, D & Wirsching, H.J. (2005). *FOCOPP - An approach for a human posture prediction model using internal/external forces and discomfort* (Report No. 2005-01-2694). Warrendale, PA: SAE International.
- Siemens. (2020). Process Simulate Human. Retrieved from <https://www.dex.siemens.com/plm/tecnomatix/process-simulate-human>

- Singh, J. & Khan, A.A. (2010). Effect of feed force and duration on discomfort level using a hand drill machine. *Noise & Vibration Worldwide*, 41(8), 30-37. DOI: 10.1260/0957-4565.41.8.30
- Stapley, P., Pozzo, T., Grishin, A. & Papaxanthis, C. (2000). Investigating centre of mass stabilisation as the goal of posture and movement coordination during human whole body reaching. *Biological Cybernetics*, 82, 161-172. DOI: 10.1007/s004220050016
- Tyan, M., Espinoza-Cuadros, F., Pozo, R.F., Toledano, D., Gonzalo, E.L., Ramirez, J.D.A. & Gomez, L.A.H. (2017). Obstructive sleep apnea in women: study of speech and craniofacial characteristics. *JMIR Mhealth Uhealth*, 5(11), 1-18. DOI: 10.2196/mhealth.8238
- van Rijn, R.M., Huisstede, B.M., Koes, B.W. & Burdorf, A. (2010). Associations between work-related factors and specific disorders of the shoulder-a systematic review of the literature. *Scandinavian Journal of Work, Environment & Health*, 36(3), 189-201. DOI: 10.5271/sjweh.2895
- van der Molen, H.F., Foresti, C., Daams, J.G., Frings-Dresen, M.H.W. & Kuijper, P.P.F.M. (2017). Work-related risk factors for specific shoulder disorders: a systematic review and meta-analysis. *Occup Environ Med.*, 74(10), 745-755. DOI: 10.1136/oemed-2017-104339
- Vaughan, C.L., Davis, B.L. & O'Connor, J.C. (1999). The three dimensional and cyclic nature of gait. In C.L. Vaughan (Ed.), *Dynamics of human gait* (2<sup>nd</sup> ed., pp. 11-12). Cape Town, South Africa: Kiboho.
- Vukobratović, M. & Borovac, B. (2004). Zero-moment point - thirty five years of its life. *International Journal of Humanoid Robotics*, 1(1), 157-173. DOI: 10.1142/S0219843604000083
- Wagner, D.W., Reed, M.P. & Chaffin, D.B. (2005). *Predicting foot positions for manual materials handling tasks* (Report No. 2005-01-2681). Warrendale, PA: SAE International.
- Wagner, D.W., Reed, M.P. & Chaffin, D.B. (2006). *A task-based stepping behavior model for digital human models* (Report No. 2006-01-2364). Warrendale, PA: SAE International.
- Wagner, D.W., Reed, M.P. & Chaffin, D.B. (2010). The development of a model to predict the effects of worker and task factors on foot placements in manual material handling tasks. *Ergonomics*, 53(11), 1368-1384. DOI: 10.1080/00140139.2010.523482

- Warwick, D., Novak, G., Schultz, A. & Berkson, M. (1980). Maximum voluntary strengths of male adults in some lifting, pushing and pulling activities. *Ergonomics*, 23(1), 49-54. DOI: 10.1080/00140138008924717
- Weston, E.B, Aurand, A., Dufour, J.S., Knapik, G.G. & Marras, W.S. (2018). Biomechanically determined hand force limits protecting the low back during occupational pushing and pulling tasks. *Ergonomics*, 61(6), 853-865. DOI: 10.1080/00140139.2017.1417643
- Wilkinson, A.T., Pinder, A.D.J. & Grieve, D.W. (1995). Relationships between one-handed force exertions in all directions and their associated postures. *Clinical Biomechanics*, 10(1), 21-28. DOI: 10.1016/0268-0033(95)90433-A
- Winter, D.A., Patla, A.E. & Frank, J.S. (1990). Assessment of balance control in humans. *Medical Progress through Technology*, 16(1-2), 31-51.
- Winter, D.A., Prince, F., Stergiou, P. & Powell, C. (1993). Medial-lateral and anterior-posterior motor responses associated with centre of pressure changes in quiet standing. *Neuroscience Research Communications*, 12(3), 141-148.
- Zeighami, A., Lemieux, P.O., Charland, J., Hagemester, N. & Aissaoui, R. (2019). *Stepping behavior for stability control of a digital human*. Presented at the International Society of Biomechanics (ISB2019), Calgary, Canada.



## BIBLIOGRAPHY

- Alpha SQUAD official. (2018, 25 December). *2019 Honda ACCORD Manufacturing - Honda ACCORD 2019 Production and Assembly* [Video file]. Retrieved from [https://www.youtube.com/watch?v=hhV\\_Rw8hyWI](https://www.youtube.com/watch?v=hhV_Rw8hyWI)
- Car TV. (2014, 10 January). *Ford Mustang Production* [Video file]. Retrieved from <https://www.youtube.com/watch?v=tjhDAPI2t2w>
- Car TV. (2015, 23 November). *Mercedes Actros Production* [Video file]. Retrieved from <https://www.youtube.com/watch?v=qKXDVk-Muh4>
- Car TV. (2016, 28 February). *Toyota Corolla Production* [Video file]. Retrieved from <https://www.youtube.com/watch?v=Zcnug6dY07c>
- Car TV. (2016, 12 November). *Honda Odyssey Production* [Video file]. Retrieved from <https://www.youtube.com/watch?v=Ehw5sMPx4Qk>
- Car & Performance TV. (2017, 9 September). *CAR FACTORY: VOLKSWAGEN Golf Production Line 2017 - HOW IT'S MADE* [Video file]. Retrieved from <https://www.youtube.com/watch?v=GlZ8BimtqOA>
- Car TV. (2017, 27 September). *Rolls-Royce Production - Awesome* [Video file]. Retrieved from [https://www.youtube.com/watch?v=XPUno4Lb\\_MI](https://www.youtube.com/watch?v=XPUno4Lb_MI)
- Car TV. (2018, 15 May). *2019 Ford Focus Production* [Video file]. Retrieved from <https://www.youtube.com/watch?v=IiounrP492U>
- For the love of life. (2011, 4 July). *How Its Made 18 wheeler - Discovery Channel* [Video file]. Retrieved from <https://www.youtube.com/watch?v=xSHxbBbzT7A>
- LylandTrucksLtd. (2015, 6 October). *Leyland Produced PACCAR Body* [Video file]. Retrieved from <https://www.youtube.com/watch?v=gAryObM5HQU>
- Make In India. (2015, 11 May). *Make in India - Volkswagen* [Video file]. Retrieved from <https://www.youtube.com/watch?v=YvaMEUsz2TA>
- Motor.TV. (2017, 30 January). *CAR FACTORY : 2017 VOLKSWAGEN TOUAREG PRODUCTION l Bratislava, Slovakia Plant* [Video file]. Retrieved from <https://www.youtube.com/watch?v=s097dA2QL-I>
- Motor.TV. (2017, 10 February). *CAR FACTORY : NEW 2017 TOYOTA PRIUS PRODUCTION l TSUTSUMI PLANT (JPN)* [Video file]. Retrieved from <https://www.youtube.com/watch?v=t0E66vaiXeg>

- Schaub, K., Wakula, J., Berg, K., Kaiser, B., Bruder, R., Glitsch, U. & Ellegast, R.P. (2015). The Assembly Specific Force Atlas. *Human Factors and Ergonomics in Manufacturing & Service Industries*, 25(3), 329-339. DOI: 10.1002/hfm.20545
- TestDriven. (2016, 21 September). *2017 Honda Civic Production* [Video file]. Retrieved from <https://www.youtube.com/watch?v=6BF35U2ea3A>
- TSC. (2017, 23 October). *Toyota Mirai FULL PRODUCTION in Japan* [Video file]. Retrieved from <https://www.youtube.com/watch?v=kCRa-5NJOoU>
- YOUCAR. (2019, 1 February). *2019 Ford Ranger - Production Line - American Car Factory* [Video file]. Retrieved from <https://www.youtube.com/watch?v=dzf6T3am6NI>